

AD



AD 668936

TECHNICAL REPORT ECOM-02464-F

VOLTAMMETRIC STUDIES OF NON-AQUEOUS SYSTEMS

FINAL REPORT

By

R.F. FOGLE, E.T. SEO, H.P. SILVERMAN

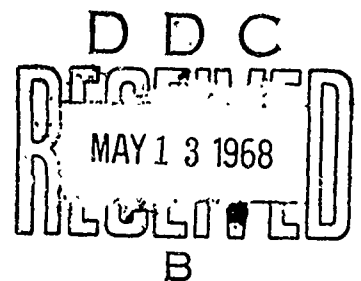
DECEMBER 1967

ECOM

UNITED STATES ARMY ELECTRONICS COMMAND • FORT MONMOUTH, N.J.

DISTRIBUTION OF THIS DOCUMENT IS UNLIMITED

CONTRACT DA-28-043-AMC-02464(E)
TRW SYSTEMS GROUP
ONE SPACE PARK
REDONDO BEACH, CALIFORNIA 90278



Reproduced by the
CLEARINGHOUSE
for Federal Scientific & Technical
Information, Springfield Va. 22151

122

TECHNICAL REPORT ECOM-02464-F

DECEMBER 1967

VOLTAMMETRIC STUDIES OF NON-AQUEOUS SYSTEMS

FINAL REPORT

1 JULY 1966 to 31 AUGUST 1967

Report No. 2

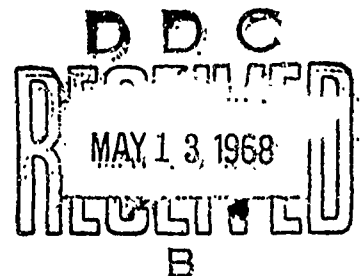
CONTRACT NO. DA-28-043-AMC-02464 (E)

DA PROJECT NO. IC014501A34A-00-09

Prepared by

R. F. FOGLE, E.T. SEO, H. P. SILVERMAN

TRW SYSTEMS GROUP
ONE SPACE PARK
REDONDO BEACH, CALIFORNIA 90278



For

U. S. ARMY ELECTRONICS COMMAND, FORT MONMOUTH, N. J. 07703

ABSTRACT

Voltammetric studies of the reduction of organic compounds in organic solvents were undertaken as part of a program to develop high-energy-density organic electrolyte batteries. Cyclic voltammetry has been used as a major diagnostic tool for evaluating organic oxidizing agents as possible high-energy-density cathode materials, and to elucidate the mechanisms of a heterogeneous electron transfer and any homogeneous follow-up chemical reactions.

This report covers the study of various nitroaromatic compounds; cyclic voltammetric current-potential curves and their interpretation have been presented for a number of selected nitroaromatic compounds. The effects of methyl-, halo-, and hydroxy-groups on the electroreduction process have been demonstrated. Compounds studied included *m*- and *p*-dinitrobenzene, 2, 5-dinitrophenol, *m*-dinitrotoluene, 1-chloro-2, 6-dinitrobenzene, and nitroalkanes. The addition of lithium ions has been shown to have a beneficial effect on organic reductions under selected conditions.

Polarization and capacity data were obtained at the plate level through constant-current and fixed-load discharge of cells comprising *m*-dinitrobenzene as the electroactive cathode material, a lithium anode, and a lithium perchlorate-propylene carbonate electrolyte solution. Cathodes were prepared in both pressed and paste forms. Various cathode compositions and fabrication procedures were evaluated.

Polarization studies showed that among the several binder materials tested, Canada balsam and an acrylic molding compound imparted the desired structural integrity to the cathode and provided a reasonable shelf life for the cell. Capacity data indicated that paste cathodes were superior to pressed cathodes. Energy densities ranged from 16 to 133 W-hr/lb. Results showed that the lithium anode limited cell performance.

TABLE OF CONTENTS

Abstract.	ii
List of Tables	v
List of Figures	vi
1. Introduction.	1
2. Experimental.	3
2.1 Voltammetric Studies	3
2.1.1 Instrumentation	3
2.1.2 Electrochemical Cell and Solution Preparation	3
2.1.3 Working Electrodes	3
2.2 Plate-Level Studies	6
2.2.1 Electrolyte System Preparation	6
2.2.2 Test Cell Design and Preparation	6
2.2.3 Electrode Fabrication.	9
2.2.4 Tests.	10
2.3 Reagents.	10
3. Voltammetric Study of Dinitrobenzenes	13
3.1 Introduction.	13
3.2 Studies in <u>N,N</u> -Dimethylformamide.	13
3.2.1 Dinitrocompounds.	13
3.2.1.1 <u>m</u> -Dinitrobenzene.	14
3.2.1.2 <u>p</u> -Dinitrobenzene	23
3.2.1.3 <u>m</u> -Dinitrotoluenes	23
3.2.1.4 1-Chloro-2, 6-dinitrobenzene	24
3.2.1.5 Dinitrophenols.	24
3.2.2 Acid Studies	26
3.2.3 Iodine Elimination Studies	26
3.2.4 Effect of Lithium Ion	31
3.3 Studies in Propylene Carbonate.	33
3.3.1 Nitrobenzene	33
3.3.2 <u>m</u> -Dinitrobenzene.	39

TABLE OF CONTENTS (Continued)

3.4	Discussion of Voltammetric Results	44
4.	Plate-Level Studies on <u>m</u> -Dinitrobenzene	55
4.1	Introduction.	55
4.2	Results of Discharge Tests on Lithium <u>m</u> -Dinitro- benzene Cells	55
4.3	Studies Monitoring Individual Electrode Potentials . .	95
4.4	Discharge Capacity Studies	104
4.5	Conclusions.	107
5.	References	109

LIST OF TABLES

3-1	Current-Integral Ratios for Iodine Elimination	31
3-2	Current-Potential Data for <u>m</u> -Dinitrobenzene in DMF Solutions Varying in Amounts of Lithium Ion at Scan Rate of 0.05 V/sec	38
4-1	Physical Data of Organic Cathodes Used in Cell Testing	55
4-2	Polarization and Impedance Data of Organic Cathode- Lithium Anode Cells	58
4-3	Visual Inspection of Cell Components	61
4-4	Discharge-Capacity Data	105
4-5	Cell Component Weights	105

LIST OF FIGURES

2-1	Block Diagram of Cyclic Voltammeter	4
2-2	Electrolysis Cell	5
2-3	Test Cell	7
2-4	Cell Arrangement for Measuring Electrode Potentials .	8
2-5	Constant-Current Circuit Diagram Using Regulated Power Supply.	11
3-1	I-E Curves of 1 <u>mF</u> Dinitrobenzenes in 0.2 <u>F</u> TPAP-DMF.	15
3-2	I-E Curves of 1 <u>mF</u> Dinitrobenzenes in 0.2 <u>F</u> TPAP-DMF	16
3-3	I-E Curves of 1 <u>mF</u> Dinitrobenzenes in 0.2 <u>F</u> TPAP-DMF Containing 1 <u>F</u> Water	17
3-4	I-E Curves of 1 <u>mF</u> Dinitrobenzenes in 0.2 <u>F</u> TPAP-DMF Containing 1 <u>F</u> Water.	18
3-5	I-E Curves of 1 <u>mF</u> Dinitrobenzenes in 0.1 <u>F</u> TPAP-DMF Containing 0.02 <u>F</u> Perchloric Acid.	19
3-6	I-E Curves of 1 <u>mF</u> Dinitrobenzenes in 0.1 <u>F</u> TPAP-DMF Containing 0.02 <u>F</u> Perchloric Acid.	20
3-7	Integrated Current <u>vs.</u> (Scan Rate) ^{-1/2} Curves for 1 <u>mF</u> <u>m</u> -Dinitrobenzene in 0.1 <u>F</u> TPAP-DMF	21
3-8	I-E Curve of 1 <u>mF</u> <u>m</u> -Dinitrobenzene in 0.2 <u>F</u> TPAP-DMF	22
3-9	I-E Curve of 1 <u>mF</u> 2, 6-Dinitrophenol in 0.2 <u>F</u> TPAP-DMF	25
3-10	Integrated Current <u>vs.</u> (Scan Rate) ^{-1/2} Curves for 1 <u>mF</u> 1-Iodo-4-nitrobenzene (NB-I) and 1 <u>mF</u> Nitrobenzene (NB) in 0.1 TPAP-DMF.	27
3-11	Integrated Current <u>vs.</u> (Scan Rate) ^{-1/2} Curves for 1 <u>mF</u> 2, 4-Dinitroiodobenzene (DNB) in 0.1 <u>F</u> TPAP-DMF	28
3-12	I-E Curves for 1 <u>mF</u> 1-Iodo-4-nitrobenzene in 0.1 <u>F</u> TPAP-DMF at Different Scan Rates	29
3-13	I-E Curves for 1 <u>mF</u> 2, 4-Dinitroiodobenzene in 0.1 <u>F</u> TPAP-DMF at Different Scan Rates.	30
3-14	I-E Curves for 0.1 <u>F</u> Lithium Perchlorate in 0.1 <u>F</u> TPAP-DMF.	32
3-15	I-E Curves of 1 <u>mF</u> <u>m</u> -Dinitrobenzene in 0.01 <u>F</u> Lithium Perchlorate-DMF.	34

LIST OF FIGURES (Continued)

3-16	I-E Curves of 1 <u>mF</u> <u>m</u> -Dinitrobenzene in 0.1 <u>F</u> Lithium Perchlorate-DMF.	35
3-17	I-E Curve of 1 <u>mF</u> <u>m</u> -Dinitrobenzene in 1 <u>F</u> Lithium Perchlorate-DMF.	36
3-18	Integrated Current <u>vs.</u> (Scan Rate) ^{-1/2} Curves for 1 <u>mF</u> <u>m</u> -Dinitrobenzene in DMF in Solutions Varying in Lithium Ion Concentration	37
3-19	Peak Current <u>vs.</u> (Scan Rate) ^{1/2} Curves for 1 <u>mF</u> Nitrobenzene in 0.2 <u>F</u> TPAP-DMF at Different Temperatures.	40
3-20	I-E Curves of 1 <u>mF</u> <u>m</u> -Dinitrobenzene in 0.2 <u>F</u> TPAP-PC at Different Temperatures.	41
3-21	I-E Curves of 1 <u>mF</u> <u>m</u> -Dinitrobenzene at Different Temperatures in 0.2 <u>F</u> TPAP-PC Containing 0.1 <u>F</u> Water.	42
3-22	Comparison of Peak-Current Variation with Temperature for Wet and Dry Solutions of 1 <u>mF</u> <u>m</u> -Dinitrobenzene in 0.2 <u>F</u> TPAP-PC	43
3-23	Peak Current/(Scan Rate) ^{1/2} <u>vs.</u> Scan Rate Curves for Wet and Dry Solutions of 1 <u>mF</u> <u>m</u> -Dinitrobenzene in 0.2 <u>F</u> TPAP-PC	45
3-24	I-E Curves of 1 <u>mF</u> <u>m</u> -Dinitrobenzene in 0.2 <u>F</u> TPAP-PC at Different Scan Rates at 26 °C	46
3-25	I-E Curves of 1 <u>mF</u> <u>m</u> -Dinitrobenzene in 0.2 <u>F</u> TPAP-PC Containing 0.1 <u>F</u> Water at 26 °C	47
3-26	I-E Curve of 1 <u>mF</u> <u>m</u> -Dinitrobenzene in 0.2 <u>F</u> TPAP-PC Containing 0.1 <u>F</u> Water at 26 °C	48
4-1	Polarization Data for Cell P-6.	63
4-2	Polarization Data for Cell P-7.	64
4-3	Polarization Data for Cell P-10	65
4-4	Polarization Data for Cell P-11	66
4-5	Polarization Data for Cell PP-2.	67
4-6	Polarization Data for Cell PP-3.	68
4-7	Polarization Data for Cell PP-4.	69
4-8	Polarization Data for Cell PP-5.	70
4-9	Polarization Data for Cell PP-6.	71
4-10	Polarization Data for Cell PP-7.	72

LIST OF FIGURES (Continued)

4-11	Polarization Data for Cell PP-8.	73
4-12	Polarization Data for Cell PP-10	74
4-13	Polarization Data for Cell PP-11	75
4-14	Polarization Data for Cell PP-12	76
4-15	Polarization Data for Cell PP-13	77
4-16	Polarization Data for Cell PP-14	78
4-17	Polarization Data for Cell PP-15	79
4-18	Polarization Data for Cell PP-18	80
4-19	Polarization Data for Cell PP-19	81
4-20	Polarization Data for Cell PP-20	82
4-21	Polarization Data for Cell PP-21	83
4-22	Polarization Data for Cell PP-22	84
4-23	Polarization Data for Cell PP-23	85
4-24	Polarization Data for Cell PP-24	86
4-25	Polarization Data for Cell PP-25	87
4-26	Polarization Data for Cell PP-26	88
4-27	Polarization Data for Cell PP-27	89
4-28	Polarization Data for Cell PP-28	90
4-29	Polarization Data for Cell PP-29	91
4-30	Polarization Data for Cell PP-30	92
4-31	Polarization Data for Cell PP-31	93
4-32	Individual Electrode Polarization Curves - Cell PP-28.	96
4-33	Individual Electrode Polarization Curves - Cell PP-29.	97
4-34	Fixed-Load Discharge Curves - Cell P-8.	98
4-35	Fixed-Load Discharge Curves - Cell P-9.	99
4-36	Fixed-Load Discharge Curves - Cell PP-16	100
4-37	Fixed-Load Discharge Curves - Cell PP-17	101
4-38	Fixed-Load Discharge Curves - Cell P-11	102
4-39	Fixed-Load Discharge Curves - Cell PP-18	103

1. INTRODUCTION

The high energy content of organic chemical oxidants makes them very attractive candidates for cathode materials in high-energy-density batteries. This report summarizes an investigation of organic chemical cathode materials in organic solvent electrolyte systems sponsored by the United States Army Electronics Command under Contract DA-28-043-AMC-02464. The objectives of the program were to:

- a. Relate the structure of the compound to its electrochemical behavior.
- b. Investigate the compatibility of organic cathode materials with organic solvents, various electrolytes, and lithium anodes.
- c. Develop procedures for incorporating organic oxidants into pressed electrode structures.

Inorganic cathode materials have received much more attention than organic chemical materials because of their less complicated overall reaction mechanisms and more favorable solubility characteristics. However, cathodes based on organic compounds potentially have larger energy densities than known inorganic cathode components, and the electrochemical reduction products of organic cathode materials are more compatible with organic solvent electrolyte systems.

The development of organic oxidant-organic electrolyte system batteries is a much more complex problem than the development of aqueous batteries (at the present) because of:

- a. The almost infinite variety of electroactive organic compounds from which to select
- b. The paucity of data on the behavior of most of these compounds in organic solvent electrolyte systems
- c. The absence of an adequate theoretical treatment of electro-organic chemical reactions

Despite this, organic batteries with energy densities exceeding 200 W-hr/lb have been built and reported.¹

To date, most of the effort reported on organic solvent electrolyte solution batteries have used inorganic cathode material plus inorganic electrolytes in organic solvents, and very little of the reported effort has been devoted to the study of the reduction of organic compounds in organic solvent electrolyte solutions. Much of the published work on the electrochemical and concomitant chemical reaction behavior of organic chemical systems has been reported by R. N. Adams

at The University of Kansas and T. Kuwana at Case Western Reserve University, and their students. They have applied modern electrochemical techniques requiring modern electronic circuitry in conjunction with optical and spectroscopic methods to electrochemical research. As a result of their use of controlled perturbations to complement steady-state measurements in the study of electro-organic chemical reactions, new insight has been developed on the effect of substituent groups and solvent properties on the mechanism of electro-organic chemical processes. Most of their published work, however, has been confined to organic oxidations.

This report presents the results of a study, using the approach of Adams and Kuwana, of the electrochemical reduction of dinitro-compounds and their derivatives. The effects of steric factors, electronegativity, and the localization or delocalization of electrons are considered.

Modern electrochemical techniques, including cyclic voltammetry, were used to rapidly evaluate the effects of various organic solvents and supporting electrolytes on the reduction of the dinitro-benzenes. As a result, the important role of lithium ion in improving the reducibility of the organic chemical oxidants in battery systems was ascertained.

The results of these studies were tested by constructing laboratory model cells with cathodes containing organic compounds. Cathodes with *m*-dinitrobenzene as the electrochemically reducible organic chemical component were tested in cells with a lithium anode and a lithium perchlorate-propylene carbonate electrolyte solution. One objective of the cell investigations was to test methods for formulating cathodes with structural integrity, long shelf-life, and high capacity. Cell behavior was characterized by polarization studies; a reference electrode in the operating cell was used to measure the polarization of the individual electrodes. As a result of these preliminary investigations, several cells were built that had lifetimes in excess of 12 days (the limit of our test program) and discharge efficiencies of 75%.

Obviously, many problems have to be solved before organic oxidant-organic electrolyte solution batteries become functional. These problems are clearly stated by Braeuer and Harvey.¹ However, the broad spectrum of new systems presented by the consideration of organic chemical systems with their potential high cell voltages and high energy densities makes this a most rewarding area of research.

2. EXPERIMENTAL

2.1 Voltammetric Studies

2.1.1 Instrumentation. The cyclic voltammetry unit used in this study (block diagram—Figure 2-1) consisted of a potentiostat, programmed with a ramp generator with voltage-level detectors for switching, and a current integrator, all based on conventional operational amplifier circuits. For slow scan rates, the output current-potential signals were recorded on Moseley Models 7001AM and 7035AM and Varian Model F-80A X-Y Recorders. For scan rates greater than 0.25 V/sec, the signal was displayed on a Tektronix Type 564 storage oscilloscope. The current-potential displays were recorded with a Tektronix Type C-27 oscilloscope camera.

The basic circuits used in the cyclic voltammeter have been described and discussed by Lauer.² All the amplifiers are Philbrick solid-state units powered by a Philbrick Model PR-300 power supply. Input and feedback impedance components are 1% throughout. The sweep unit comprises: (a) a bistable multivibrator [(B), P45AU amplifier] with its output voltage swing clipped by a pair of Zener diodes; (b) a ramp generator (C) consisting of a voltage divider, a voltage follower (P65AU amplifier), and an integrator (P25AU amplifier); and (c) a limit switch containing two amplifiers (P65AU) used as simple voltage-level detectors with an external reference voltage.

The potentiostat (F) and the current-to-voltage transducer (G) are both P45AU amplifiers, and the voltage follower (H) and the current integrator (I) are both P25AU amplifiers.

2.1.2 Electrochemical Cell and Solution Preparation. The electrochemical studies were carried out in a one-compartment cell (Leeds and Northrup Coulometric Titration Cell 7961) consisting of a 100-ml beaker and a polyethylene cover (Figure 2-2). A double-junction saturated calomel reference electrode (sce) was separated from the bulk solution with a Luggin capillary or a fritted-glass bridge tube. A platinum wire served as auxiliary electrode and was spatially removed far enough from the working electrode to avoid mixing of electrolysis products.

Solution volumes were 50 to 75 ml. Degassing of the solutions was accomplished by bubbling with ultra high purity grade argon gas (Air Products Inc.) for 15 min. In general, all solutions for the electrochemical studies were prepared and used on the same day to avoid chemical changes or contamination. The supporting electrolyte was 0.1 or 0.2 F tetra-n-propylammonium perchlorate (TPAP).

2.1.3 Working Electrodes. Mercury-film and platinum button electrodes were used as working electrodes. The mercury-film electrodes were amalgamated Beckman (No. 39273) platinum-button

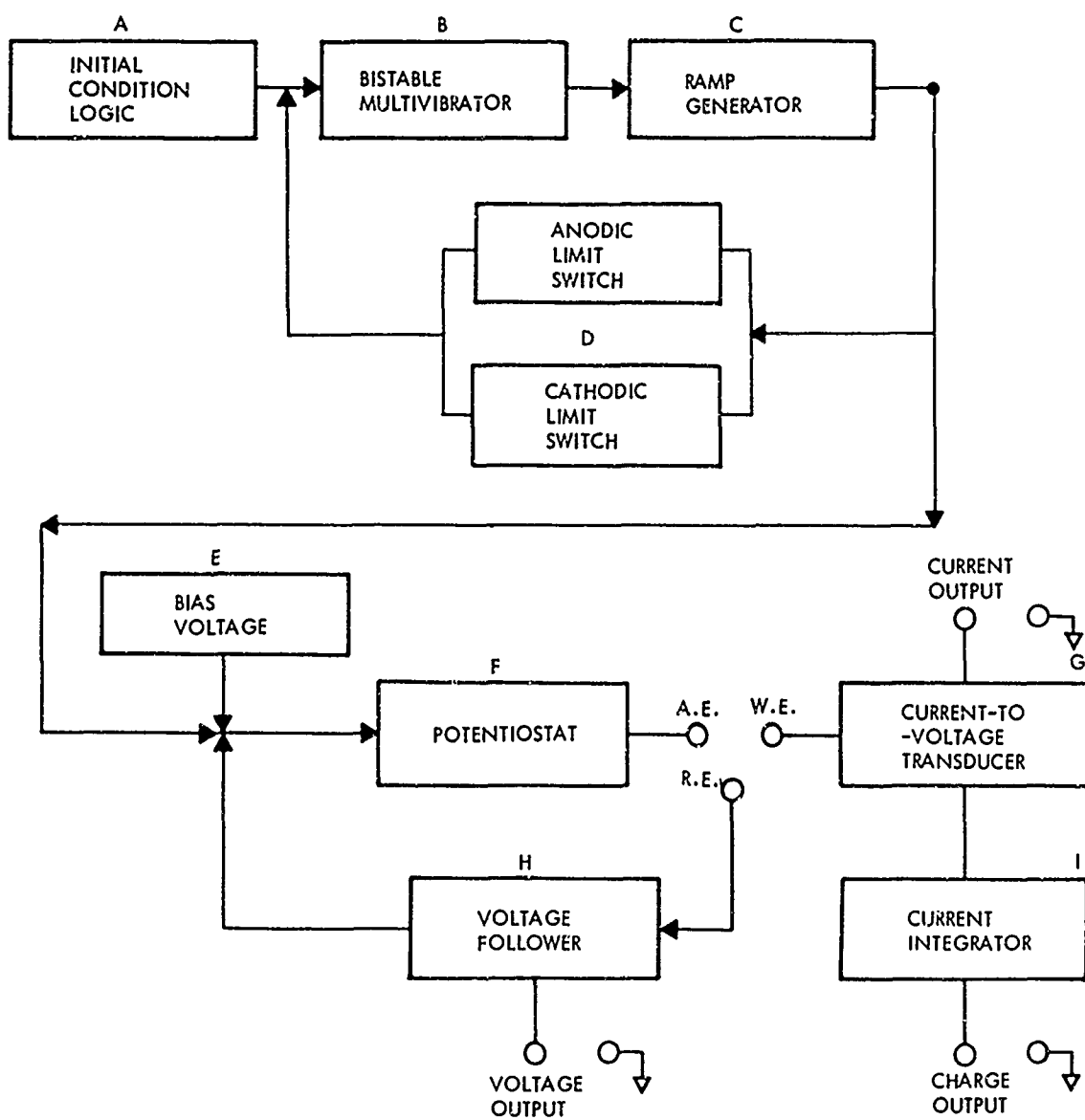


Figure 2-1. Block Diagram of Cyclic Voltammeter

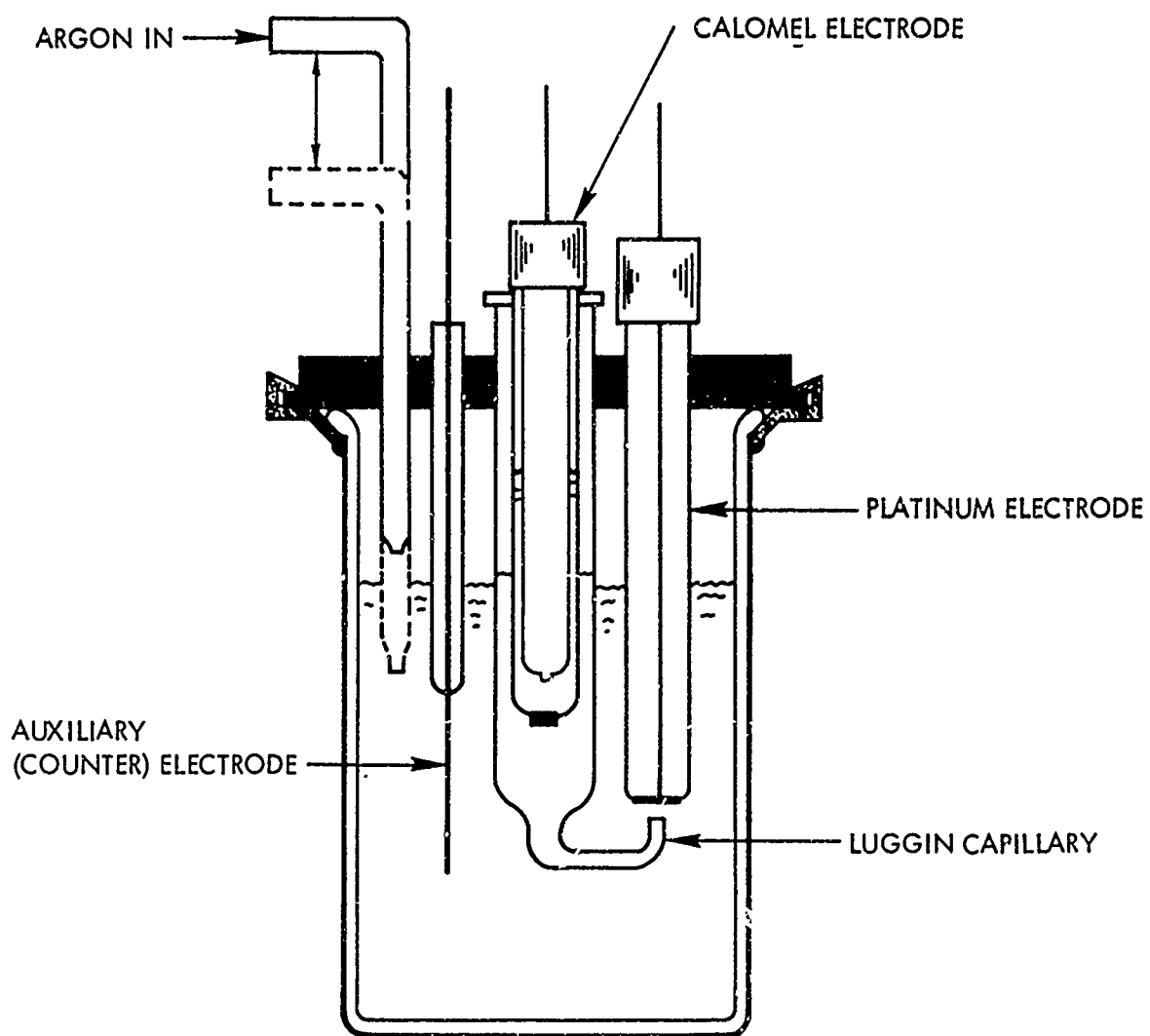


Figure 2-2. Electrolysis Cell

electrodes prepared in an electrolysis cell with a mercury-pool counter electrode and a dilute sulfuric acid electrolyte. The polarity of the platinum button and mercury pool was cycled several times. On the last cycle, the platinum electrode was held cathodic and immersed in a separated nonpolarized mercury pool in the same solution. The background current on this electrode showed a usable region to -2.7 V vs. sce in N,N-dimethylformamide containing 0.2 F tetra-n-propylammonium perchlorate. The cathodic limit for the platinum-button electrode was -1.8 V in this same solution.

2.2 Plate-Level Studies

2.2.1 Electrolyte System Preparation. The propylene carbonate (PC)-lithium perchlorate (LiClO_4) electrolyte system was prepared by adding 70 g of LiClO_4 (anhydrous, G. F. Smith) to 200 ml of vacuum-distilled PC with continuous stirring. After filtration to remove excess lithium perchlorate, the solution was diluted 1:4 with PC to give a final concentration of approximately 1.6 F.

The tetra-n-propylammonium perchlorate electrolyte system was prepared by adding 105 g of TPAP to 350 ml of vacuum distilled PC and stirring the mixture overnight.

2.2.2 Test Cell Design and Preparation. A diagram of the test cell used in the polarization studies is shown in Figure 2-3. Both the cell body and end plugs were fabricated out of polypropylene. A silver disc (0.005 in. thickness, 1.75 in. diameter), with a connecting wire soldered on, served as the cathode current collector. The electrical contact between the cathode and current collector was maintained by pressure. The connecting wires for both cathode and anode passed through a hole in the center of the end plugs. Rubber serum caps were used to seal the electrical leads to the end plugs. Three layers of fiberglass paper (0.015 in. thickness, 1.75 in. diameter) were used as separators.

The test cell was assembled in a dry box as follows: (a) the cathode (paste or pressed plate) was placed on the current collector; (b) the separators, saturated with electrolyte solution, were placed on top of the cathode; and (c) with the cathode and separators in the cell, the anode was screwed into place. The reference electrode plug was removed during the operation to allow excess electrolyte solution to escape from the cell. The various leads and holes were sealed and the cell removed from the dry box for polarization measurements.

For studies in which the anode and cathode potentials were monitored, the cell was modified as shown in Figure 2-4. The reference electrode, saturated calomel or silver-silver perchlorate (0.1 F in propylene carbonate), was isolated from the cell with a double junction comprising a glass-frit and a cracked-glass tube.

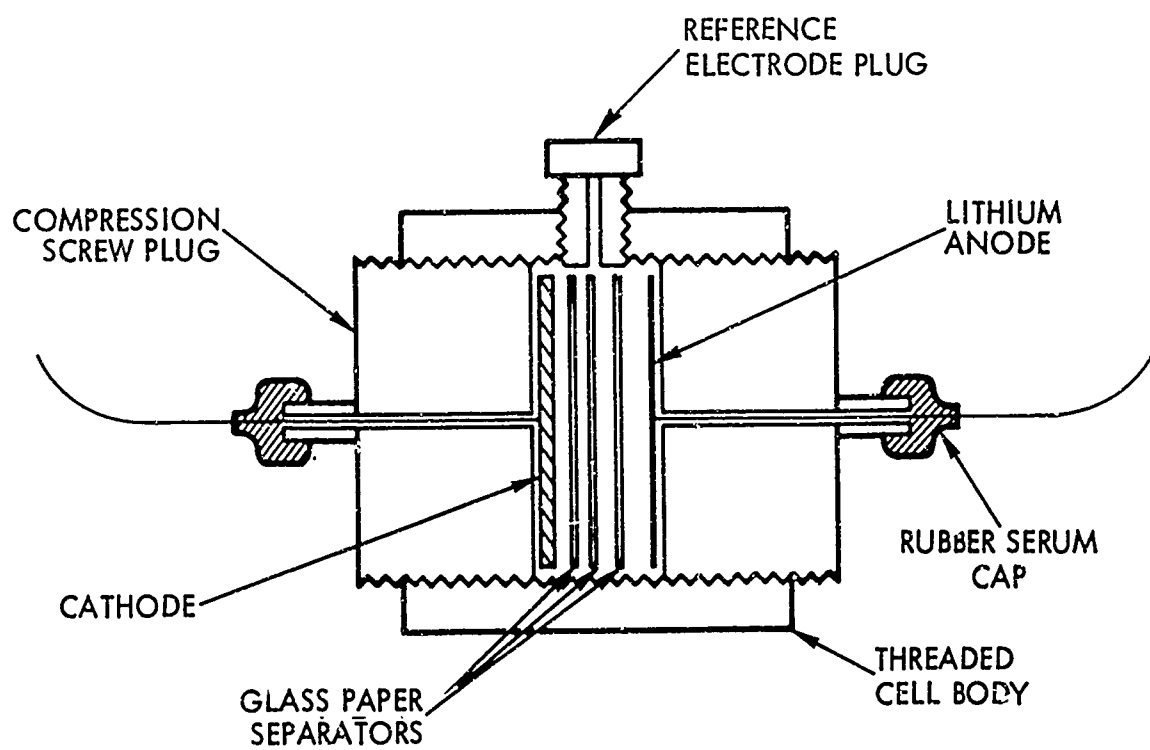


Figure 2-3. Test Cell

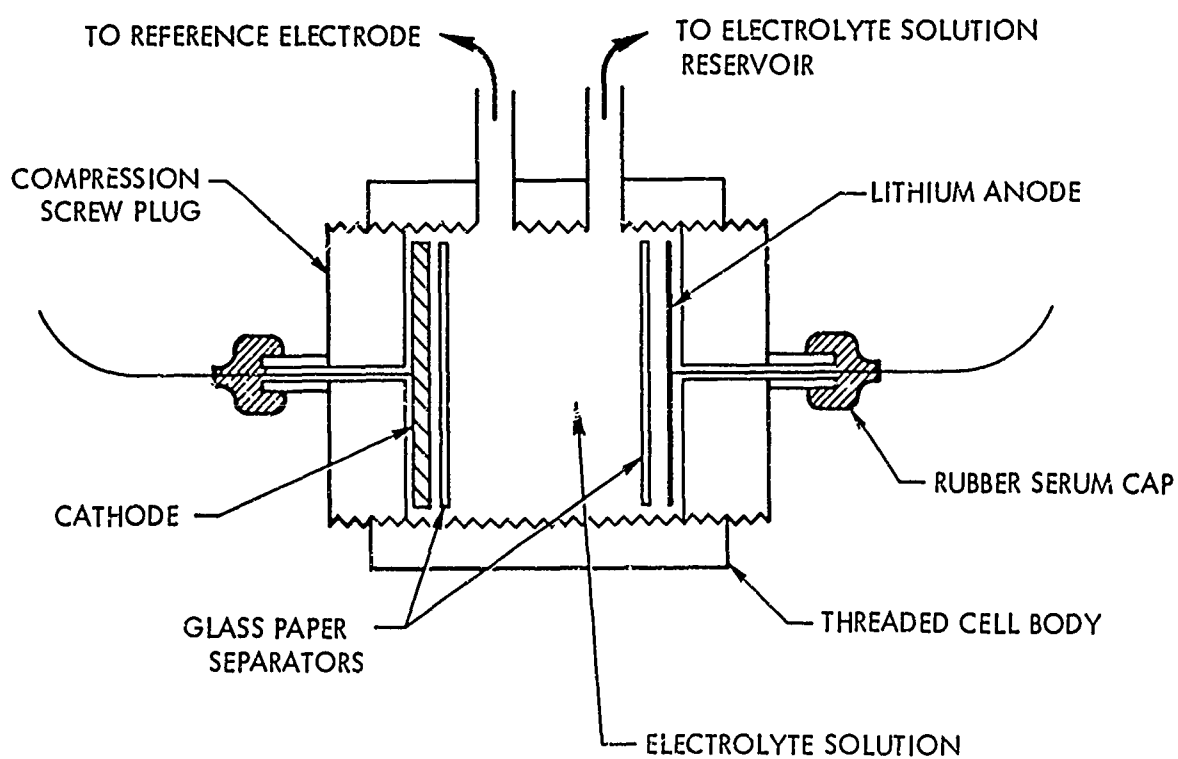


Figure 2-4. Cell Arrangement for Measuring Electrode Potentials

2.2.3 Electrode Fabrication. Cathodes were prepared in both the paste and pressed manner. For the paste cathodes, 1.5 g each of carbon (Cabot XC-72R) and m-dinitrobenzene (m-DNB) were thoroughly mixed. The dry mixture was placed in the dry box and 10 ml of the electrolyte was added to form a paste. Two paste cathodes, one using PC-LiClO₄ and the other PC-TPAP, were fabricated. The polarization studies on these two paste cathodes served as a reference for polarization studies on pressed, solid cathodes. A pressed cathode was composed of m-DNB, carbon powder to serve as the electronic conductor, and a binder material to impart physical integrity to the cathode.

The ratio of carbon powder to m-DNB was maintained constant. Acrylic and natural occurring resins were used as binders for all the cathodes fabricated. Plexiglass VS-1000 acrylic (Rohm and Haas), which is only slightly soluble in the PC-LiClO₄ electrolyte system, was chosen as the first binder material. The cathodes fabricated with the natural resins were compared with the acrylic binder cathodes.

To ensure the uniform distribution of the binder in the cathode, the binder was incorporated into the cathode mixture by means of a volatile solvent, dichloromethane. Three acrylic-dichloromethane solutions were prepared containing 5%, 2.5%, and 1% by weight of acrylic. No data is presented for the 1% acrylic because cathodes fabricated with this solution had no physical integrity and fell apart.

A mixture containing 1.5 g each of carbon powder and m-DNB was transferred to the dry box and to it was added 10 ml of the desired acrylic solution. After stirring to a paste consistency, the solvent was removed from the resulting mixture under reduced pressure at room temperature. The material was then ground, resubjected to reduced pressure, and size graded by pressing the dried mixture through a 40-mesh sieve. The particles which passed through the mesh were pressed in a 1.75 in. diameter die at 10,000 psi pressure with a Carver hydraulic laboratory press. The cathode thickness was varied by using 1, 2, and 3 g of the material. The fabricated electrodes were placed in plastic bags and stored in the dry box until they were incorporated in a cell.

Lithium discs were used as anodes and were formed from lithium rod (A.D. Mackay). A cleaned rod, approximately 1 in. long and 0.5 in. in diameter was sandwiched between two pieces of FEP Teflon film and pressed at 3000 psi into a flat disc approximately 1/16 in. thick. The FEP film was then removed from one face of the disc, and a disc of expanded silver metal (Exmet Corp. 5 Ag7-4/0) with a silver connecting wire soldered to it was imbedded in the lithium surface by means of a hydraulic press. The completed anode was then immersed in clean 1, 1, 1-trichloroethane and stored in a dry box.

2.2.4 Tests. Polarization studies were made by discharging a test cell at selected current densities using a constant-current source. The cell voltage was continuously monitored on a potentiometric strip-chart recorder and was also periodically checked with a high-impedance digital voltmeter. The current was applied for 2 min at each current density and the voltage at the end of the 2 min-period was plotted to obtain current-voltage curves. Depending on the final performance of the individual cells, the voltage change at the end of 2 min varied from several millivolts per minute to approximately 25 mV/min at the low current densities and from 50 mV/min to several hundred millivolts/minute at the high current densities. Figure 2-5 is a diagram of the circuit used in the polarization studies. Electrode potential measurements on individual electrodes using reference electrodes were made in a manner similar to that used for the polarization studies.

The impedance of the pressed cathodes, as well as that of the assembled cells was measured using a 60-Hz impedance bridge. The impedance measurements on the pressed cathodes were made by placing the cathode between two platinum discs, having the same diameter as the cathode and backed with plexiglass plates. A constant pressure was applied to the sandwiched cathode by placing a fixed weight on the top plastic plate. The impedance of the assembled cells was measured immediately before and after each polarization test.

Cells subjected to discharge studies were discharged to 0V using a fixed 67-ohm load. The cell voltage was continuously monitored on a potentiometric strip chart recorder and was also periodically checked with a high-impedance digital voltmeter.

2.3 Reagents. N,N-Dimethylformamide (Mallinckrodt reagent grade) was shaken with 50 g/liter of neutral, chromatographic grade alumina (Merck). The mixture was allowed to settle and the DMF decanted from the alumina. The DMF was distilled at 25 Torr from fresh alumina with a maximum pot temperature of 60 to 61 °C. The solvent was distilled through a 90-cm, helices-packed, vacuum-jacketed and silvered column after refluxing for 30 min prior to collection. A reflux ratio of 1:1 and distillation rate of 3 to 6 ml/min was maintained during the distillation. The middle fraction was retained for use.

Propylene carbonate (Aldrich) was distilled at 3 to 4 Torr using a 90-cm, helices-packed column. The sample was refluxed for 1 hr prior to collection. The distillation rate was maintained at 5 to 6 ml/min with a maximum pot temperature of 120 °C and 1:1 reflux ratio. The middle fraction was retained for use. The effectiveness of the purification procedures was monitored by vapor-phase chromatography and Karl Fischer analysis of the distillate fractions. Impurity levels were estimated from vapor phase chromatograms using methylethyl ketone as an internal reference.

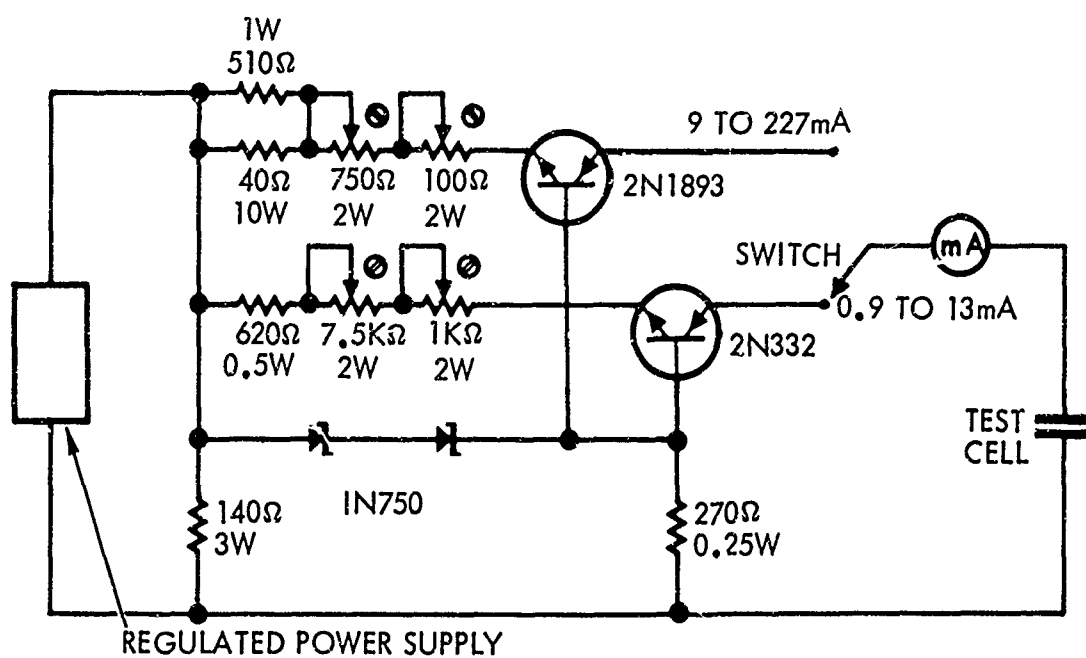


Figure 2-5. Constant-Current Circuit Diagram Using Regulated Power Supply

An Aerograph Autoprep Model 700 instrument with thermal conductivity detector was used in the vapor-phase chromatography studies. A 120-mesh, Porapak Q column (1/4 in. by 6 ft) was used with helium as the carrier gas. The sample volume used was 50 μ liters in each case. The sensitivity as estimated from the peak height of the internal reference was roughly 0.002% by volume.

For propylene carbonate, the middle fraction of a second distillation produced a sample with essentially no impurity peaks except for small amounts of carbon dioxide and water.

The vapor phase chromatograms for DMF showed that except for trace amounts of water, the impurity levels were reduced by distillation. The impurity level was estimated at about 0.01% by volume by comparison with the peak for methylethyl ketone used as internal standard.

Analysis for water in these solvents was performed by the Karl Fischer direct-titration method using the deadstop end point. Distillation decreased the water content generally from 0.06% to 0.02%. No analysis was performed on solvent-electrolyte mixtures.

Zone-refined m-dinitrobenzene (Aldrich) was used as received. All other nitro compounds were obtained from commercial sources and were purified by conventional methods including sublimation, column chromatography, and recrystallization.

Tetra-n-propylammonium perchlorate was prepared by neutralizing a 10% aqueous solution of tetra-n-propylammonium hydroxide (Eastman) with perchloric acid. The product was recrystallized three times from methanol and dried in vacuo at 80 °C.

3. VOLTAMMETRIC STUDY OF DINITROBENZENES

3.1 Introduction. A voltammetric study of substituted m-dinitrobenzenes and related compounds was made to determine the effect of substituent groups on the electroreduction process. Methyl-, chloro-, and hydroxy-substituted m-dinitrobenzenes were investigated. m-Dinitrobenzene was chosen as the parent compound, rather than o- or p-dinitrobenzene, because the later undergo nitro-group elimination. (A literature review on nitrobenzene reductions is presented in the semi-annual report.)

The dinitrotoluenes were studied to investigate the steric effects of ortho-substituents on the nitro group and also because the literature indicates that an ortho-methyl substituent can act as a proton source in the reduction of polynitroaromatic compounds.

A chlorodinitrobenzene was chosen to study the electron withdrawing effect of the chloro substituent on the nitro-group reduction and to investigate a possible halogen-elimination reaction which could increase the number of electrons involved in the overall reduction process.

The effect of a hydroxy substituent was studied because of reports that a six electron reduction is possible with mononitrophenols.

Experiments were also performed to test promising effects suggested by results in the literature. These experiments included studies on halogen-elimination reactions and lithium-ion effects, both of which are known to effectively enhance the reduction process for some mononitroaromatic compounds.

3.2 Studies in N, N-Dimethylformamide. The voltammetric studies were made in N, N-dimethylformamide (DMF) with 0.1 F tetra-n-propylammonium perchlorate (TPAP) as supporting electrolyte. The concentrations of the surveyed compounds were held constant to facilitate comparison of the salient features in the various sets of curves. In addition, the effects of the addition of water and perchloric acid to the electrolyte solution were also determined for certain compounds. The potential was scanned from 0 to -2.5 V vs. sce in neutral solution, except in acidic media where the meaningful voltage range was limited at -1.3 V, the potential at which the hydrogen-ion reduction current becomes significant.

3.2.1 Dinitrocompounds. From the current-potential (I-E) curves obtained by cyclic voltammetry, peak currents and peak reduction potentials are obtained in addition to a qualitative indication of the degree of reversibility and the presence of chemical reactions coupled to the charge-transfer step. Thus, a qualitative picture of the effect of the substituents or additives on the electrochemical process is easily obtained from examination of the I-E curves. The

relative effects of substituents can be derived by comparison of the I-E curves of *m*-dinitrobenzene and its derivatives. Effects favoring the reduction process show up as positive shifts in the peak reduction potentials and/or peak current enhancement.

Current-potential curves for several dinitroaromatic compounds dissolved in dry DMF and in DMF solutions containing 1 F water are shown for comparison in Figures 3-1 to 3-4. The curves obtained in DMF solutions containing 0.02 F perchloric acid are shown in Figures 3-5 and 3-6.

3.2.1.1 *m*-Dinitrobenzene. The I-E curves for the reduction of *m*-dinitrobenzene in DMF containing 0.2 F TPAP exhibit two reversible peaks, one at -0.80 V and another at -1.23 V (see Figure 3-1). An irreversible third peak is observed at -2.18 V. The quasi-reversibility of the first two peaks was shown by the 1:1 ratio of the anodic to cathodic peak currents and from the linearity of plots of the integrated current vs. (scan rate)^{-1/2} (Figures 3-7 and 3-8). The lines in Figure 3-7 intercept at 0 coulombs (within experimental error) indicating that complications due to adsorption and other nondiffusion-controlled processes are absent. Literature results show that the first peak corresponds to a one-electron reduction to the anion radical of *m*-dinitrobenzene.³ The similarity of the first two peaks indicates that the second peak also corresponds to a one-electron reduction producing the dianion of *m*-dinitrobenzene. The electrode process occurring at the third peak is not known.

Under similar conditions, electron spin resonance studies have detected a weak spectrum of the *m*-nitroaniline anion which is generated at potentials more negative than -2.2 V. The intensity of this spectrum is increased by the addition of small amounts of perchloric acid.⁴ This result suggests that during the reduction, the aniline may occur as a minor product of side reactions.

The reduction process can thus be assumed to proceed by consecutive one-electron steps followed by a complex, irreversible process in which the dianion is reduced by more than 2 electrons. The number of electrons involved in the third reduction process may be estimated by taking the 2/3 root of the ratio of the third peak current to the first peak current. This estimate yields 2.6 for the apparent value of *n* in this process, indicating that the overall process carried to -2.2 V requires four or more electrons, depending on the electrode reactions involved.

The addition of 1 F water to the solution causes little change in the reduction potentials of the first two peaks (Figure 3-3). The reversibility of the electron transfer for the first peak is unaffected by the water; that is, the peak current ratios of the anodic to the cathodic sweep remain essentially 1.0. However, the peak current ratio for the second peak is affected by the addition of water and the

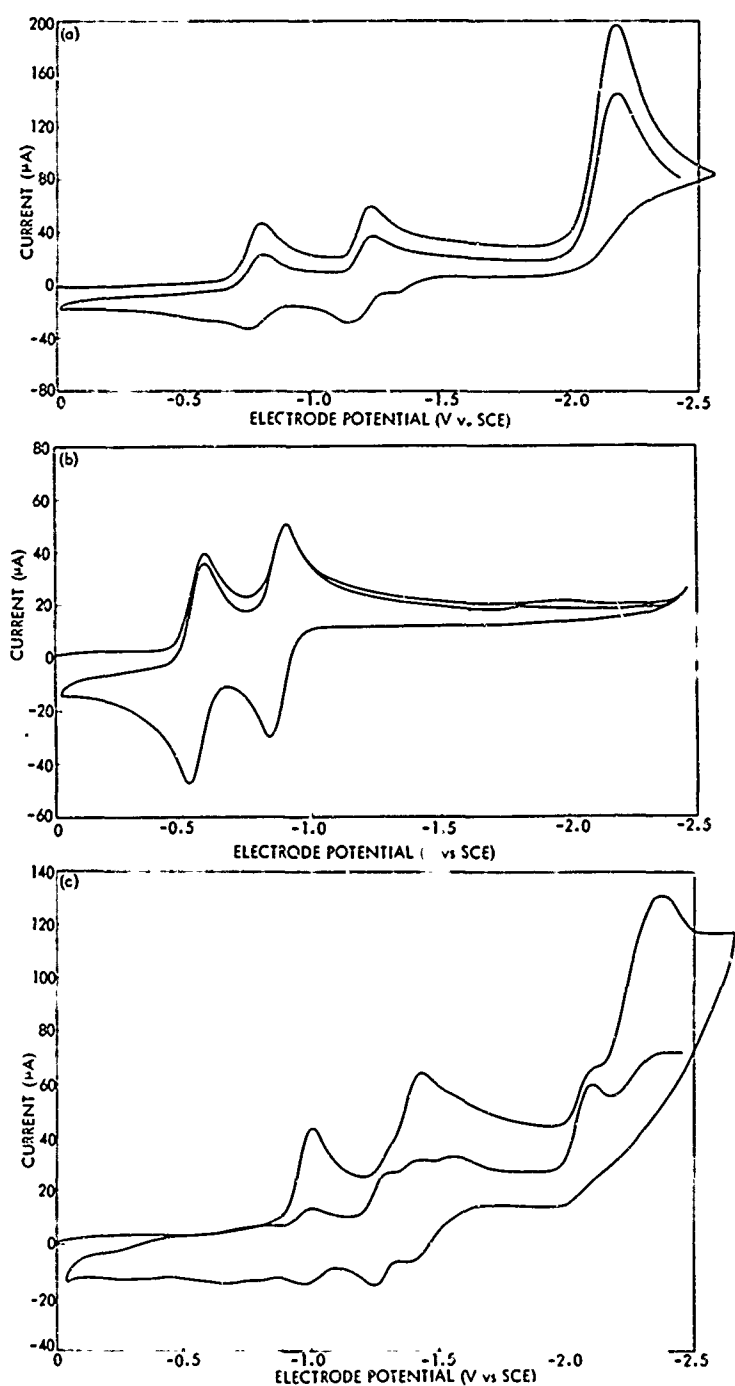


Figure 3-1. I-E Curves of 1 mF Dinitrobenzenes in 0.2 F TPAP-DMF. Curve (a) m-dinitrobenzene, (b) p-dinitrobenzene, (c) 2,6-dinitrotoluene. Mercury-film electrode, 0.22 cm². Scan rate, 0.05 V/sec.

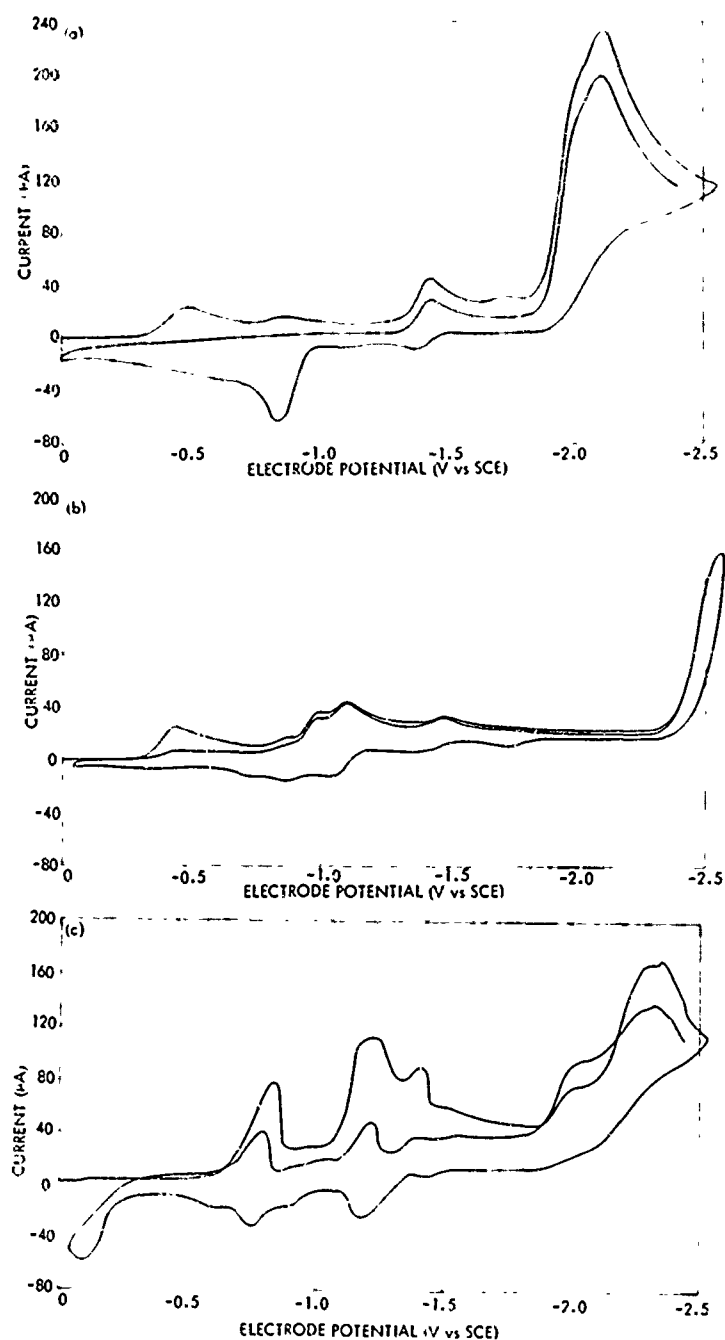


Figure 3-2. I-E Curves of 1 mF Dinitrobenzenes in 0.2 F TPAP-DMF. Curve (a) 2,6-dinitrophenol, (b) 2,5-dinitrophenol, (c) 1-chloro-2,6-dinitrobenzene. Mercury-film electrode, 0.22 cm². Scan rate, 0.05 V/sec.

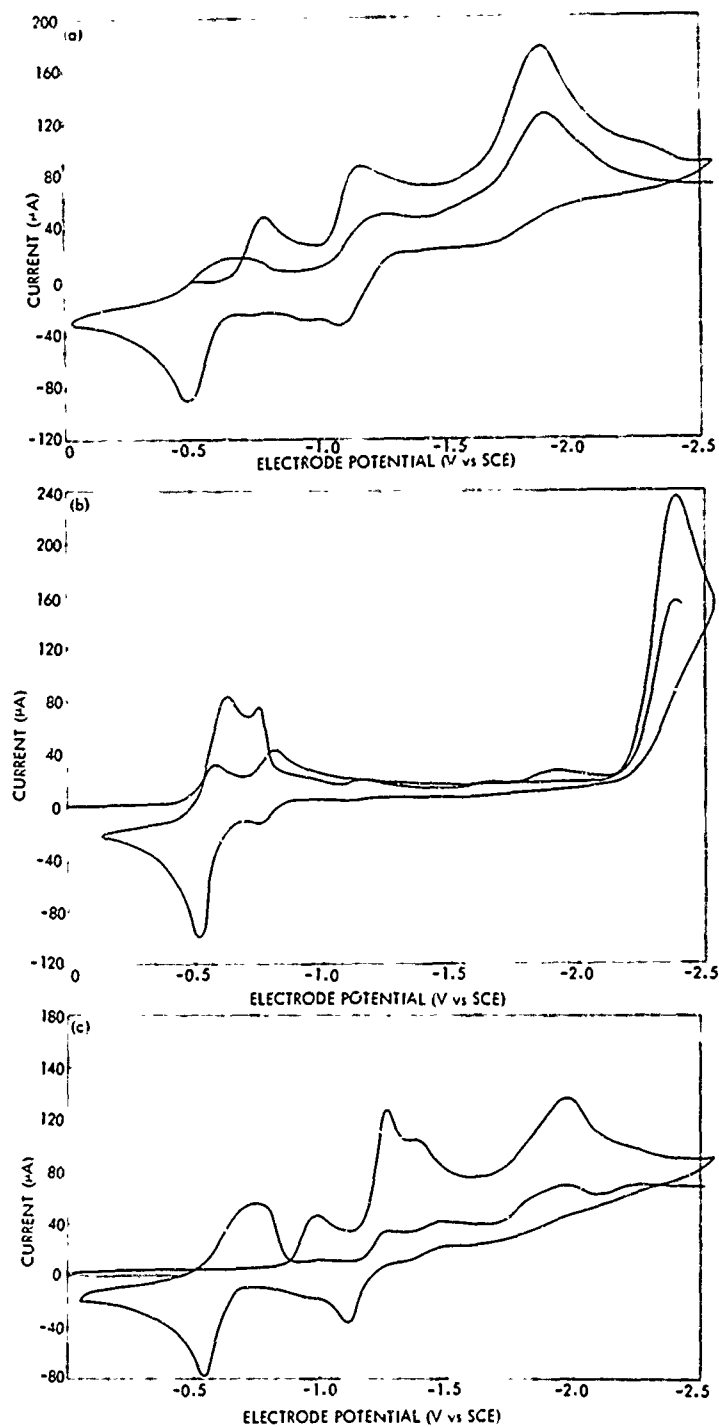


Figure 3-3. I-E Curves of 1 mF Dinitrobenzenes in 0.2 F TPAP-DMF Containing 1 F Water. Curve (a) m-dinitrobenzene, (b) p-dinitrobenzene, (c) 2,6-dinitrotoluene. Mercury-film electrode, 0.22 cm². Scan rate, 0.05 V/sec.

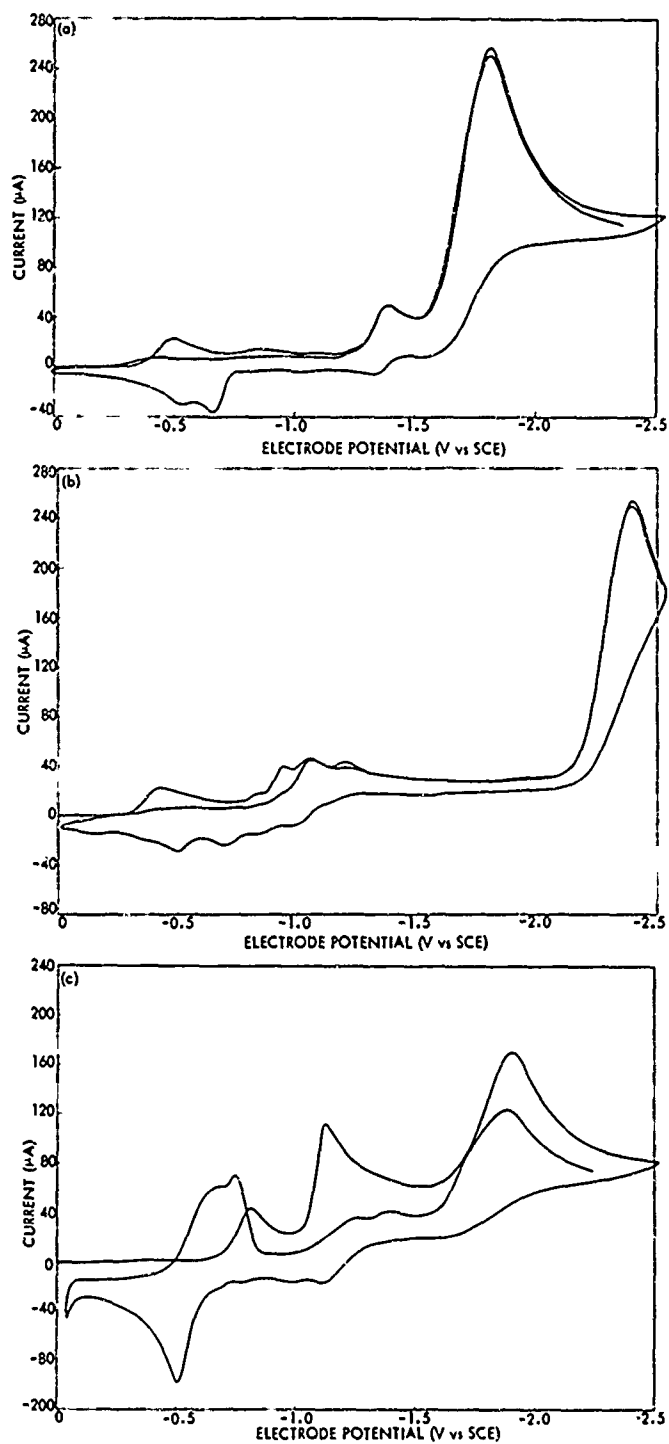


Figure 3-4. I-E Curves of 1 mF Dinitrobenzenes in 0.2 F. TPAP-DMF Containing 1 F Water. Curve (a) 2,6-dinitrophenol, (b) 2,5-dinitrobenzene, (c) 1-chloro-2,6-dinitrobenzene. Mercury-film electrode, 0.22 cm². Scan rate, 0.05 V/sec.

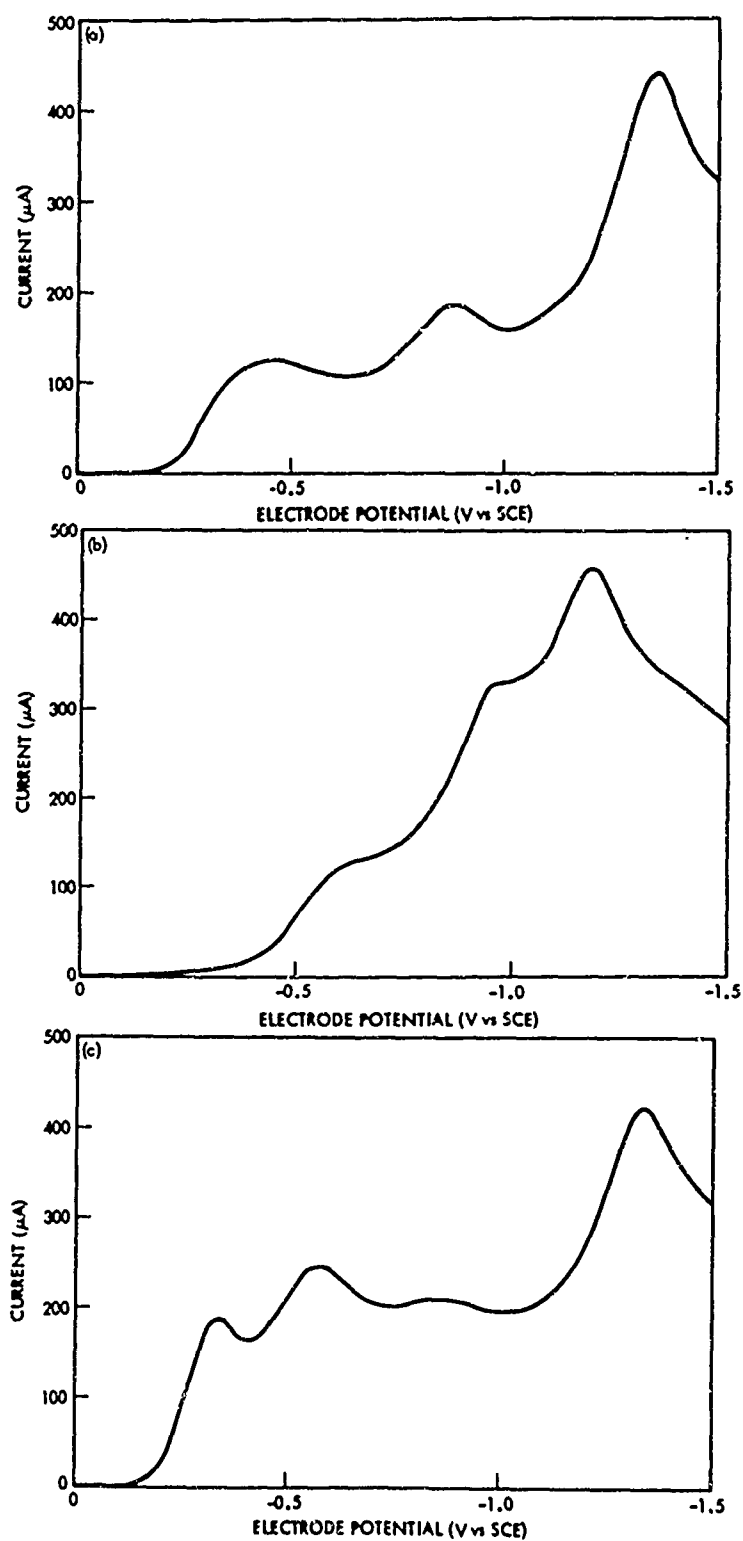


Figure 3-5. I-E Curves of 1 mF Dinitrobenzenes in 0.1 F TPAP-DMF Containing 0.02 F Perchloric Acid Curve (a) m-dinitrobenzene, (b) 2, 6-dinitrotoluene, (c) 2, 6-dinitrophenol. Mercury-film electrode, 0.22 cm². Scan rate, 0.05 V/sec.

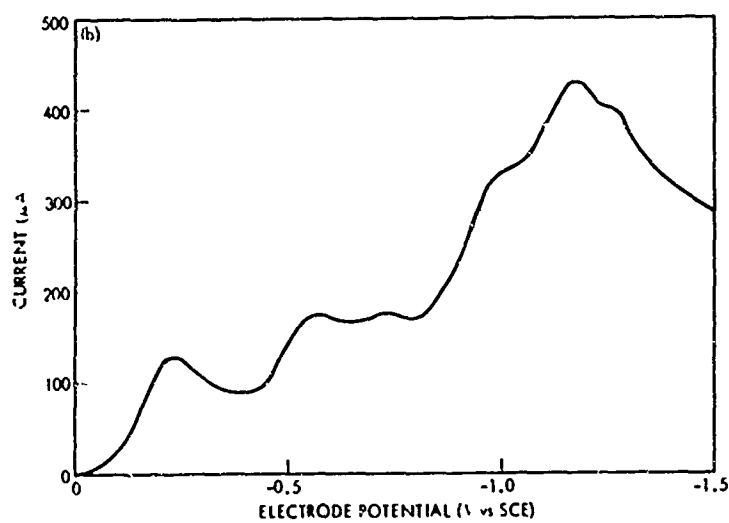
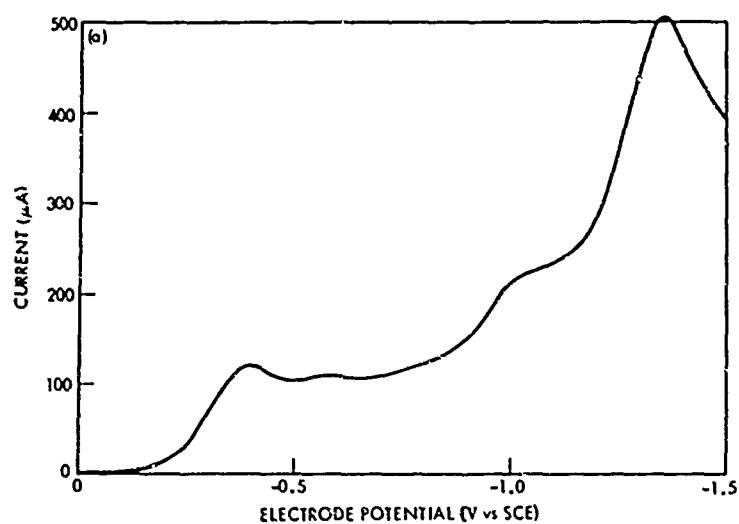


Figure 3-6. I-E Curves of 1 mF Dinitrobenzenes in 0.1 F TPAP-DMF Containing 0.02 F Perchloric Acid. Curve (a) 2,4-dinitrophenol, (b) 2,5-dinitrophenol. Mercury-film electrode, 0.22 cm². Scan rate, 0.05 V/sec.

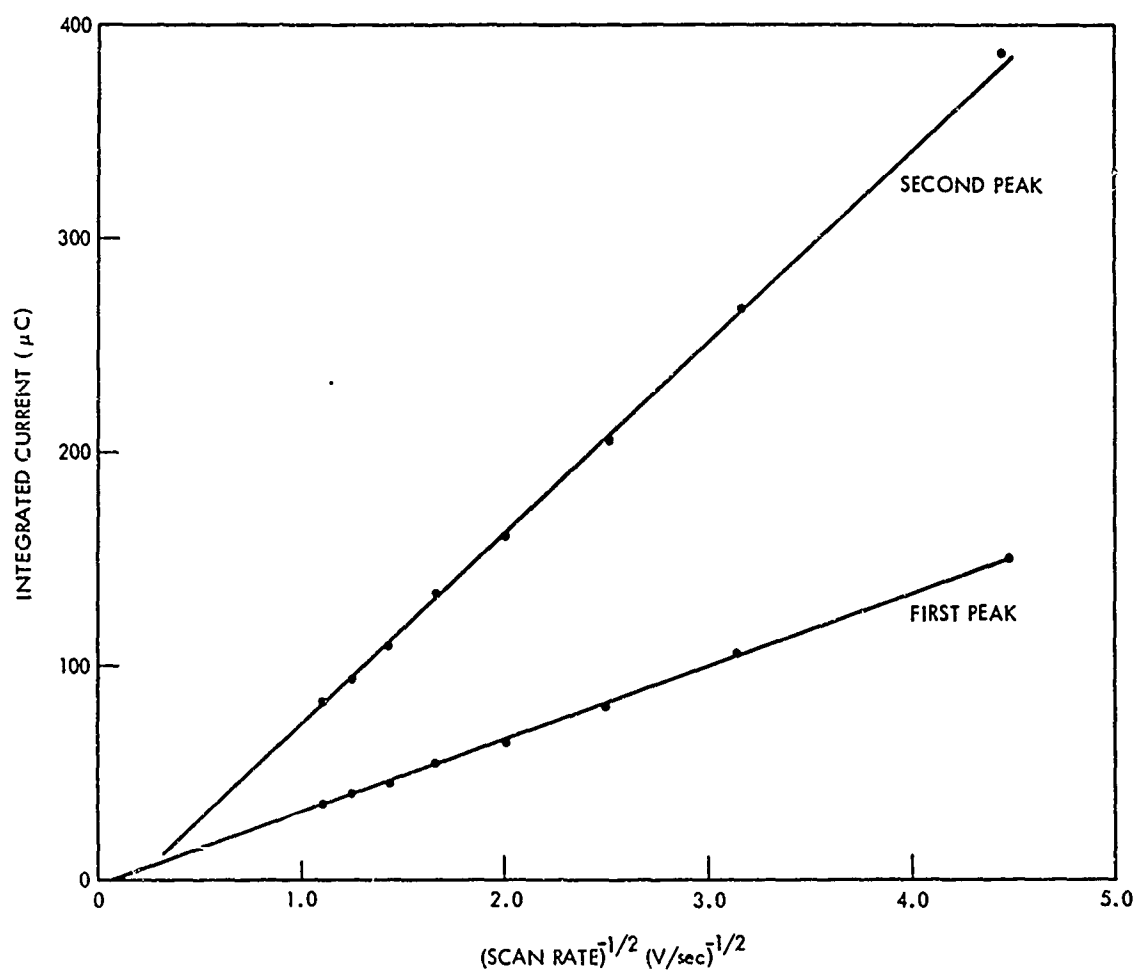


Figure 3-7. Integrated Current vs. (Scan Rate)^{-1/2} Curves for 1 mF m-Dinitrobenzene in 0.1 F TPAP-DMF. Platinum electrode, 0.21 cm². Integration limits, first peak -1.1 V, second peak -1.5 V.

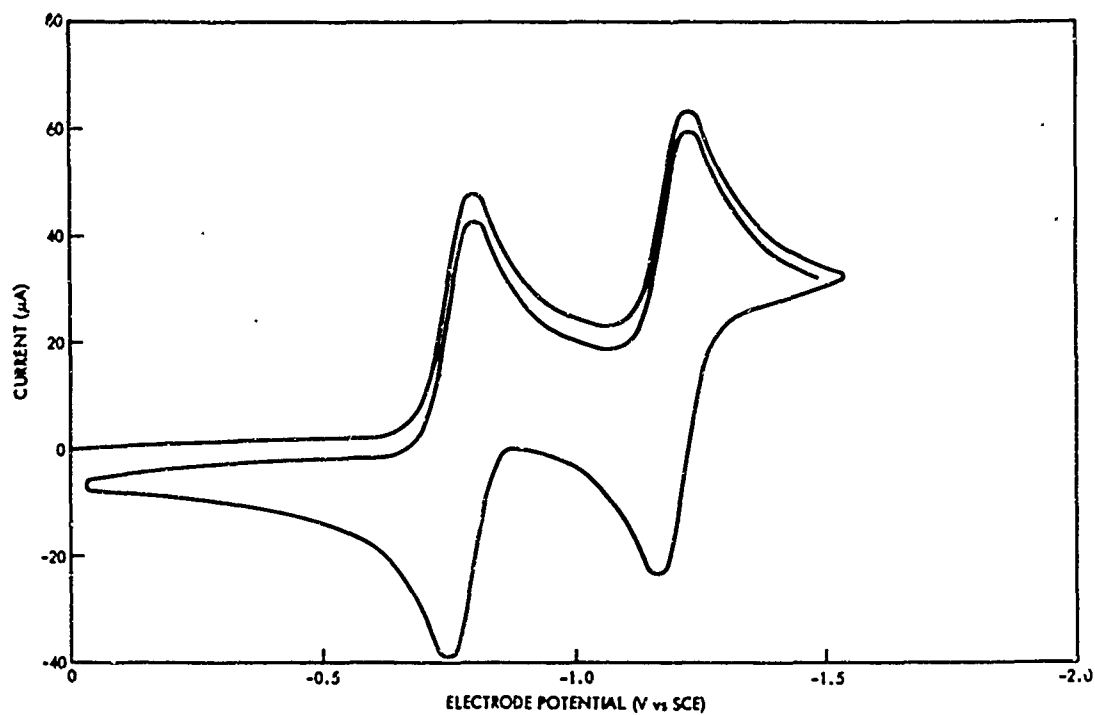


Figure 3-8. I-E Curve of 1 mF m-Dinitrobenzene in 0.2 F TPAP-DMF. Platinum electrode, 0.21 cm². Scan rate, 0.05 V/sec.

peak height is increased by about 25%, suggesting that additional reduction involving water occurs. The third reduction step shifts positive to -1.9 V where a broad peak is observed. A mechanism for the reduction of m-dinitrobenzene is discussed in Section 3.4.

3.2.1.2 p-Dinitrobenzene. The I-E curves for p-dinitrobenzene (Figures 3-1 and 3-3) are similar to those for m-dinitrobenzene, except that there is some shifting of the peak potentials. The two reversible peaks occur at more positive potentials than for the meta-isomer while the irreversible third peak occurs beyond -2.5 V. The large difference between the reduction potentials of the second and the third peaks is probably due to the stability of the p-dinitrobenzene dianion.⁵ The addition of water has little effect on the first two peaks, but the third peak is shifted to a more positive potential by about 0.2 V. The electrochemical reduction of p-dinitrobenzene in DMF with TPAP as the supporting electrolyte is reported to yield the anion of p-nitrophenol.⁶ The phenol is believed to form through a substitution reaction with trace hydroxide ions. The first two peaks have been shown to correspond to one-electron reversible reductions.

3.2.1.3 m-Dinitrotoluenes. The I-E curves for the m-dinitrotoluenes show differences in peak potentials and in peak currents when compared to the curves for m-dinitrobenzene (Figure 3-1). The first peak for 2,6-dinitrotoluene is similar in height and shape to the first peak of m-dinitrobenzene but it occurs at -1.02 V which is a negative shift of 0.2 V. While the first peak exhibits quasi-reversible character, suggesting a one-electron reduction to the radical anion, the second peak appears complicated with a shoulder at -1.3 V and a peak at -1.45 V.

Reversing the sweep direction past the second peak reveals anodic current peaks that result from the oxidation of electroactive products generated by the reduction process corresponding to the second peak. The third peak in the reduction sequence occurs at approximately the same potential as that for m-dinitrobenzene.

Similar results are obtained for 2,4-dinitrotoluene except that shifts in potential and changes in peak current are smaller.

The addition of 1 F water to the dry DMF solution shifts the reduction potentials to slightly more positive values with each succeeding peak being affected to a greater degree (Figure 3-3). The I-E curves for the wet solutions show a higher ratio of current of the second peak to the first than is obtained in dry solutions. This indicates that water is involved in the second reduction step possibly through follow-up chemical reactions of the dianion. This enhancement of the second peak current by water is greater for the dinitrotoluenes than for m-dinitrobenzene. No evidence of proton transfer from the methyl groups was observed.

3.2.1.4 1-Chloro-2,6-dinitrobenzene. The reduction of 1-chloro-2,6-dinitrobenzene shows effects of electrode filming or other surface complication in dry DMF (Figure 3-2). Addition of water removed these effects (Figure 3-4).

In solvent containing water, the reduction of 1-chloro-2,6-dinitrobenzene proceeds similarly to that of the dinitrotoluenes except that no significant shift in the reduction potentials is observed relative to m-dinitrobenzene. The first peak corresponds to a reversible one-electron step. Additional complications are observed for the second and third reduction processes and may be caused by halogen elimination reactions. A clear example of halogen elimination occurs with 1-iodo-4-nitrobenzene and 2,4-dinitroiodobenzene and is discussed in Section 3.2.3.

3.2.1.5 Dinitrophenols. The I-E curves for dinitrophenols show several features that are not observed in the reduction steps for m-dinitrobenzene (Figure 3-2). The I-E curve for the reduction of 2,6-dinitrophenol at a platinum electrode shows evidence of electrode filming or some other surface complication in dry DMF (Figure 3-9). Addition of water to the solution removes the complication. The curves show two or more overlapping peaks occurring between -0.4 V and -1.1 V with peak currents that are less than would be expected for a simple one-electron reduction process. Both the 2,6- and 2,4-dinitrophenols, however, show a peak exhibiting quasi-reversible character with a peak current corresponding to a one-electron reduction at -1.5 V. Further complicated irreversible reduction processes with large peak currents occur at -2 V. These peak currents are larger than those observed for m-dinitrobenzene and the dinitrotoluenes. The I-E curves for the 2,5-isomer show only poorly resolved overlapping peaks (Figure 3-2). For 2,5-dinitrophenol, the reduction step corresponding to the third step, generally observed for m-dinitrobenzene derivatives, occurs beyond -2.5 V.

Addition of water to the dinitrophenol solutions does not appreciably change the initial reduction steps but does affect the subsequent reduction processes at the more negative potentials, causing the peaks to shift to more positive potentials by about 0.2 V (Figure 3-4). The third reduction step peak current for 2,6-dinitrophenol is the largest of any obtained in this survey.

The reduction of 2,6-dinitrophenol is reported to yield 2,6-dinitrophenolate dianion radical at -1.5 V.⁷ No other electron spin resonance signals are detected at more positive potentials where other reduction processes occur. Rieger and coworkers⁷ explain the results by suggesting phenolic-hydrogen elimination as a reduction step to yield 2,6-dinitrophenolate anion as an intermediate.

Results for both 2,6- and 2,4-dinitrophenol are similar in that both indicate a one-electron reduction occurring at -1.45 V. The

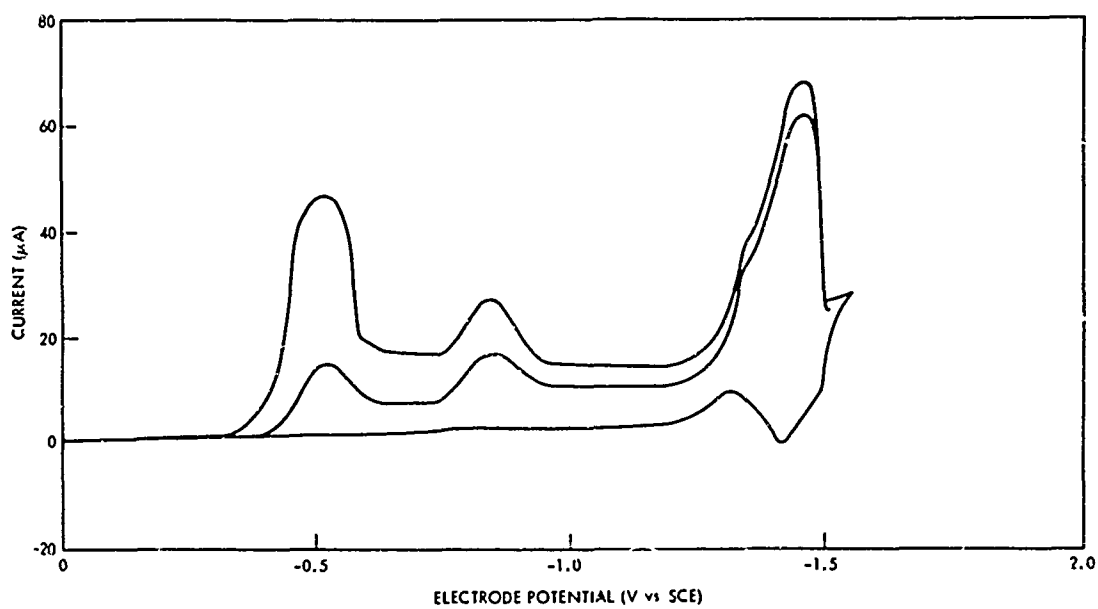


Figure 3-9. I-E Curve of 1 mF 2,6-Dinitrophenol in 0.2 F TPAP-DMF. Platinum electrode, 0.21 cm². Scan rate, 0.05 V/sec.

smaller peaks observed at less negative potentials might involve a complex equilibrium process between phenol and phenolate anions of the parent compound and/or phenolic hydrogen elimination as mentioned above.

3.2.2 Acid Studies. Some studies were made on the effect of adding acid to the solutions of the dinitroaromatic compounds. The I-E curves were obtained with DMF solutions containing 0.02 F perchloric acid, 0.1 F TPAP, and 0.1 F water. A background (blank) I-E curve obtained at a mercury-film electrode showed a proton-reduction peak at -1.5 V. The voltammetric data in acid solutions is meaningful in the 0 to 1.3 V range.

The addition of acid to the TPAP-DMF solutions results in a significant change in the overall reduction process. The I-E curves in Figures 3-5 and 3-6 show substantially higher peak currents and more positive reduction potentials than those obtained in TPAP-DMF solutions free of acid. The effects are significant and indicate that multiple-electron reduction steps occur more readily in the presence of acid. Peak heights suggest overall reductions involving six or more electrons.

3.2.3 Iodine Elimination Studies. The elimination of an iodine atom has been reported to occur during the reduction of iodonitrobenzene isomers in DMF.^{8, 9, 10} The overall reduction is reported to involve three electrons, two for the halogen-elimination step and one for the nitrobenzene reduction to the radical anion. The possibility of enhanced faradaic capacity indicated by these results prompted a study of halogen-elimination effects in dinitrobenzene reduction.

Voltammetric and current integration data were obtained for the reduction of 1-iodo-4-nitrobenzene, 2,4-dinitroiodobenzene, nitrobenzene, and *m*-dinitrobenzene in 0.1 F TPAP, DMF solution. Scan rates were varied from 0.05 to 5 V/sec, and current-integral values were obtained with scan rates from 0.05 to 1.0 V/sec. The integral values plotted as a function of (scan rate)^{-1/2} are shown in Figures 3-10 and 3-11, and the current-potential curves obtained with slow and fast scan rates are shown in Figures 3-12 and 3-13. The ratio of the current integrals of the halogen containing compound to the current integrals of the non-halogenated compound is shown in Table 3-1, with the integration limits being taken from 0 to -1.3 V for the mononitro compounds respectively. Figure 3-12 shows that, while one peak of 1-iodo-4-nitrobenzene disappears with increasing scan rate, the anodic current increases. This effect suggests that the reduction is approaching that of a one-electron reversible process and that the halogen-elimination reaction is suppressed at fast scan rates. The decrease in the integral ratio with increasing scan rates for the mononitro compounds supports this possibility. Likewise, the constancy of the integral ratios observed for the dinitro compounds

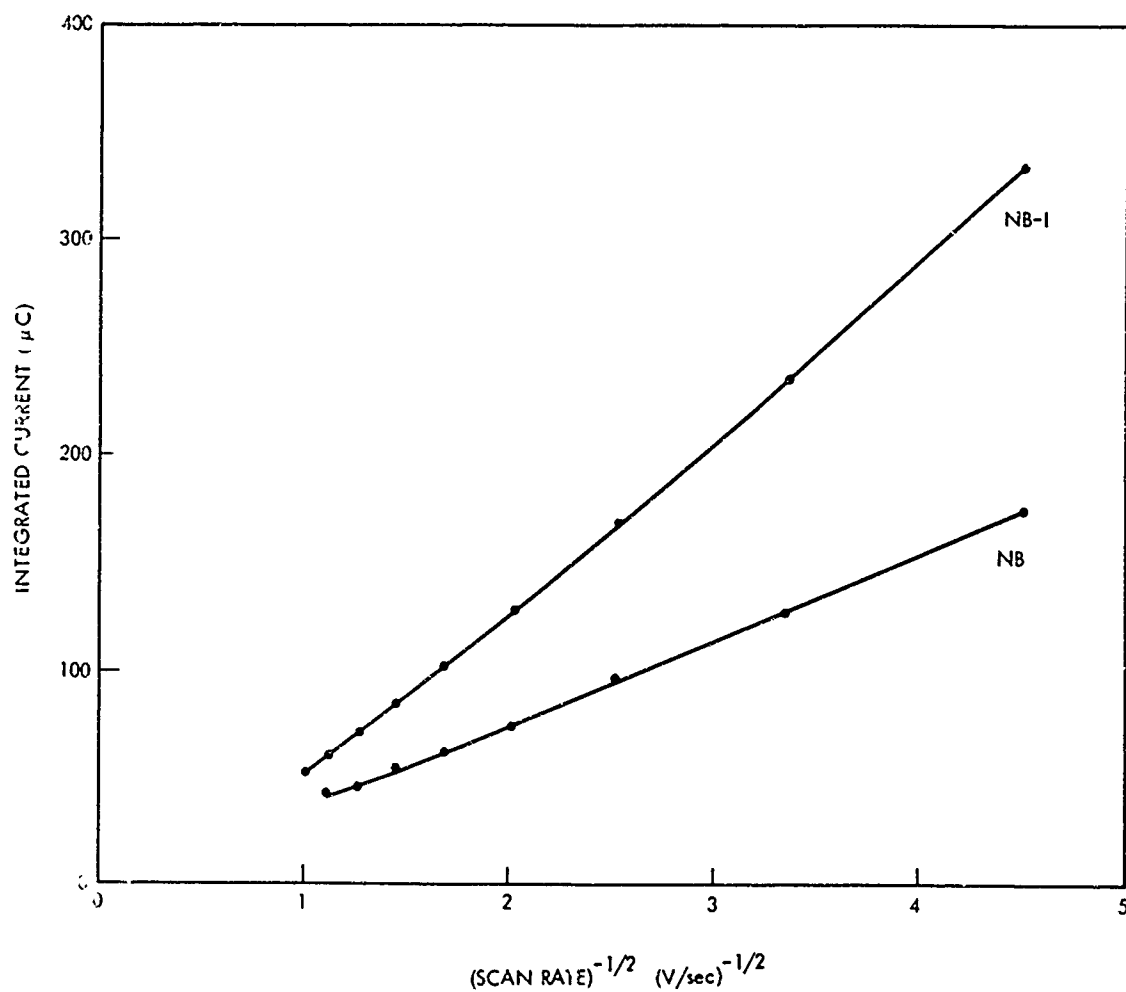


Figure 3-10. Integrated Current vs. (Scan Rate)^{-1/2} Curves for 1 mM 1-Iodo-4-nitrobenzene (NB-I) and 1 mF Nitrobenzene (NB) in 0.1 F TPAP-DMF. Platinum electrode, 0.20 cm².

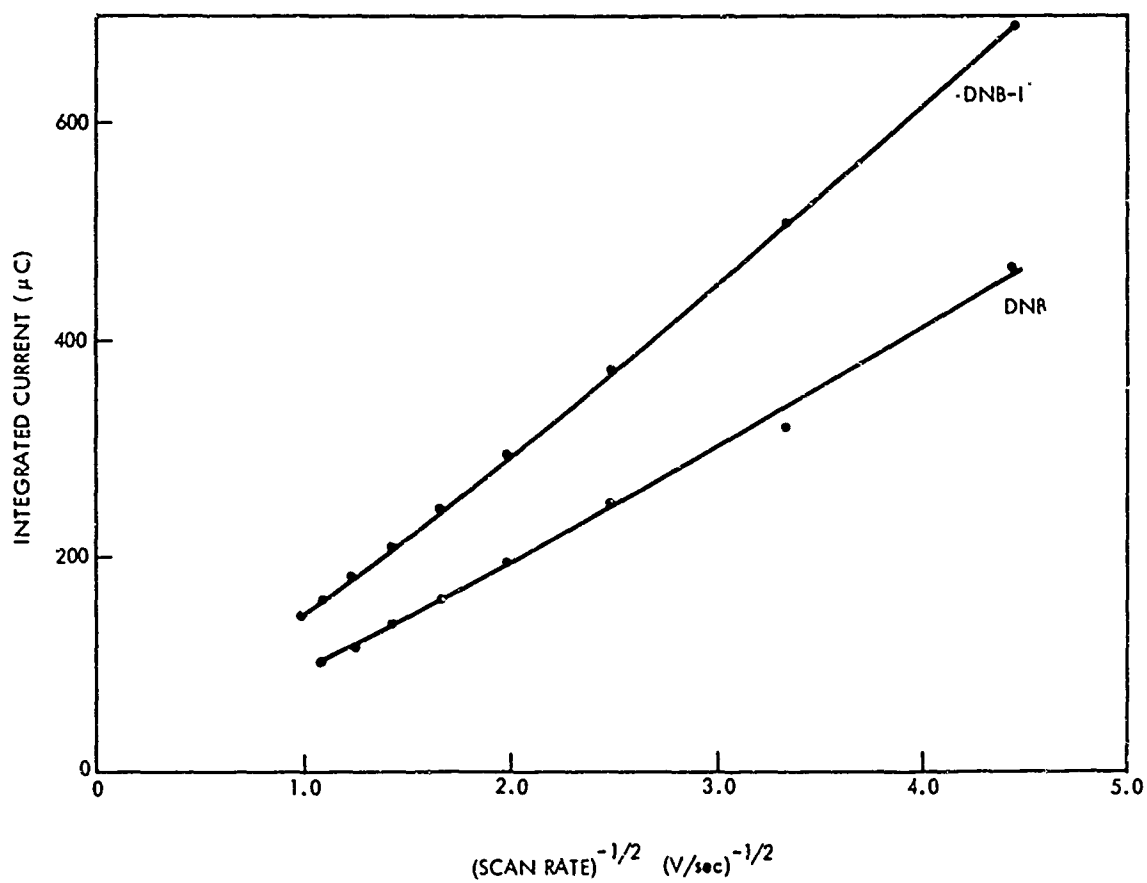


Figure 3-11. Integrated Current vs. (Scan Rate)^{-1/2} Curves for 1 mF 2,4-Dinitroiodobenzene (DNB-I) and 1 mF m-Dinitrobenzene (DNB) in 0.1 F TPAP-DMF. Platinum electrode, 0.20 cm².

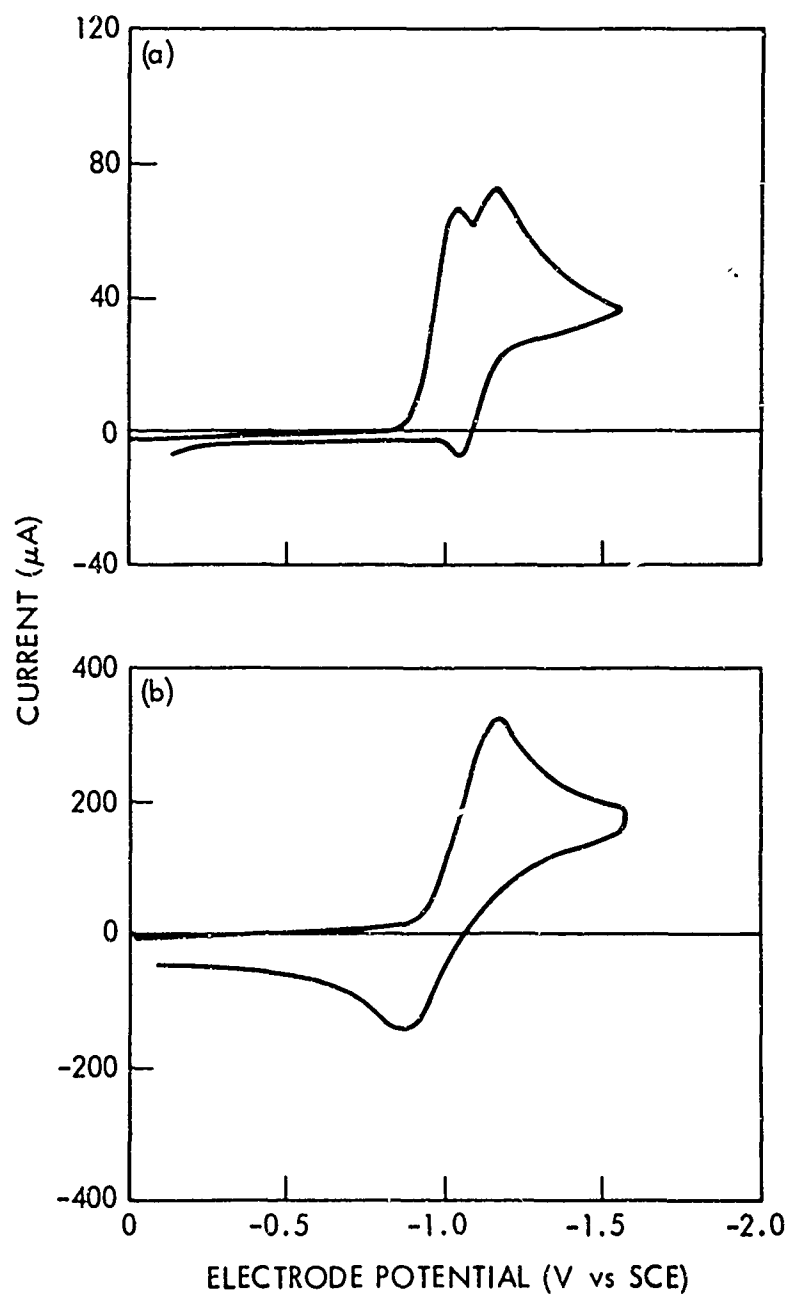


Figure 3-12. I-E Curves for 1 mF 1-iodo-4-nitrobenzene in 0.1 F TPAP-DMF at Different Scan Rates; (a) 0.10 V/sec, (b) 5.0 V/sec. Platinum electrode, 0.20 cm^2 .

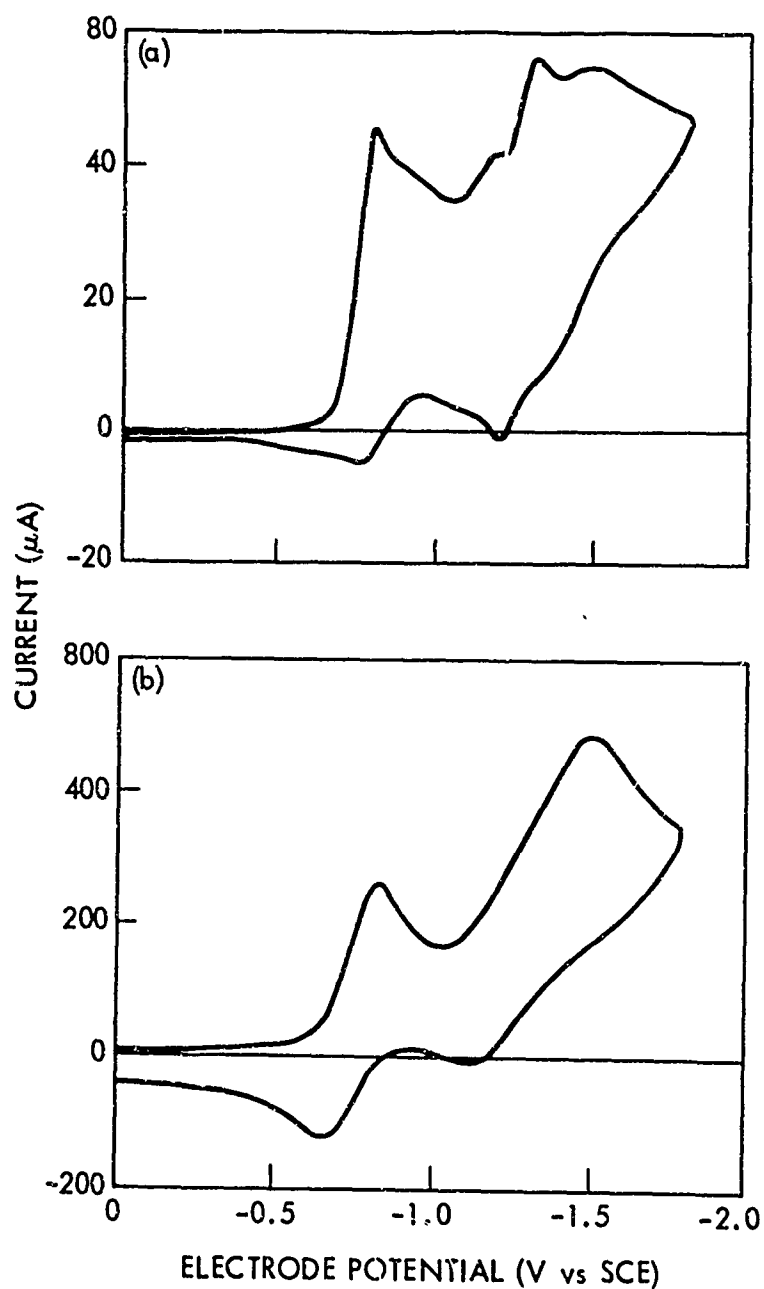


Figure 3-13. I-E Curves for 1 mF 2,4-Dinitroiodobenzene in 0.1 F TPAP-DMF at Different Scan Rates; (a) 0.05 V/sec, (b) 2.5 V/sec. Platinum electrode, 0.20 cm^2 .

TABLE 3-1
CURRENT-INTEGRAL RATIOS FOR IODINE ELIMINATION

Scan Rate V/sec	DNB-I/DNB	DNB-I/DNB	NB-I/NB
0.05	1.28	1.48	1.92
0.09	1.29	1.57	1.85
0.16	1.35	1.50	1.74
0.25	1.31	1.50	1.71
0.36	1.40	1.54	1.60
0.49	1.43	1.50	1.53
0.64	1.42	1.54	1.52
0.81	1.38	1.55	1.32

- (a) DNB-I = 2,4-dinitroiodobenzene
 DNB = m-dinitrobenzene
 NB-I = 1-iodo-4-nitrobenzene
 NB = nitrobenzene
- (b) All solutions are 1 mF electroactive material, 0.1 F TPAP in DMF.
- (c) The limits of integration for each column, from left to right, are -1.0 V, -1.5 V, and -1.3 V, respectively.

leads to the conclusion that halogen elimination occurs more readily for the dinitro compound than for the mononitro compound and that increasing scan rates do not suppress the wave. If halogen elimination is a general effect, it may be possible to obtain increased faradaic capacities with halogen-substituted dinitrobenzenes. The results, however, do not support the theory that two electrons are involved in the reduction of the halo-substituent.

3.2.4 Effect of Lithium Ion. Current-potential curves were obtained in solutions of lithium perchlorate in DMF to establish background currents and potential limits using a platinum electrode. The I-E curve for a solution of 0.1 F lithium perchlorate showed a broad impurity peak at -1.9 V with a peak current of 124 μ A at 0.05 V/sec (Figure 3-14a). A similar solution prepared using lithium perchlorate that had been dried overnight in vacuo at 220 °C also showed a broad impurity peak at -1.9 V, but the peak current was only 54 μ A at 0.05 V/sec (Figure 3-14b). These results indicate that the impurity is residual water.

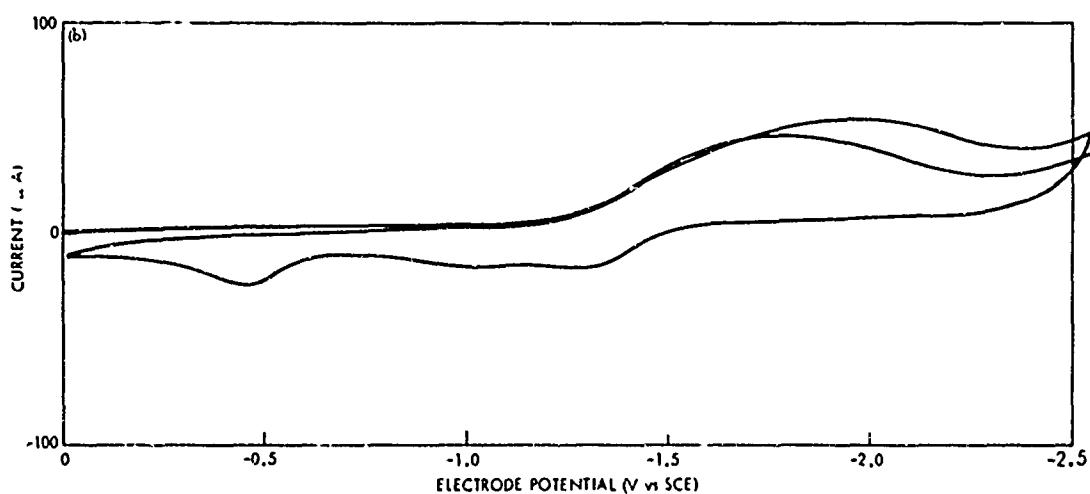
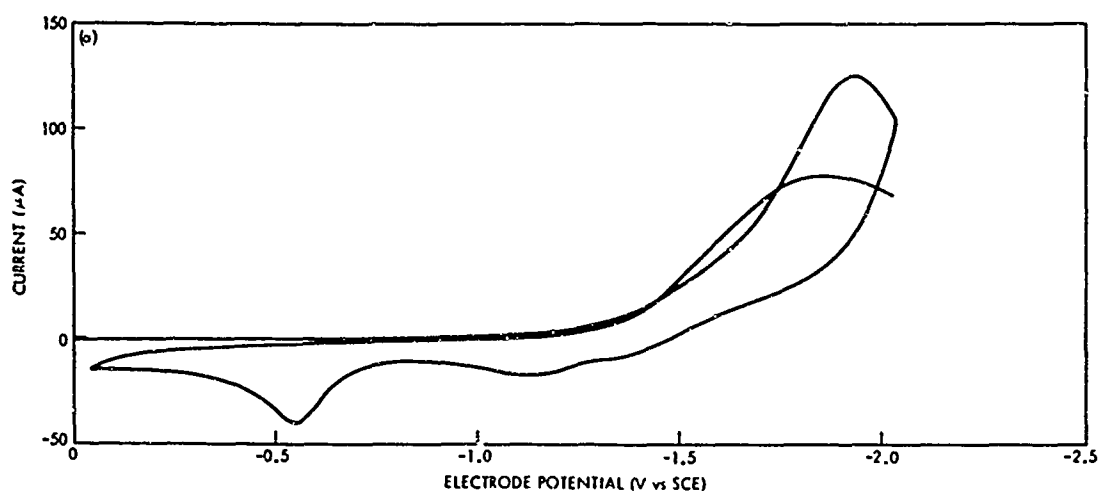


Figure 3-14. I-E Curves for 0.1 F Lithium Perchlorate in 0.1 F TPAP-DMF. Curve (a) lithium perchlorate used as received; (b) lithium perchlorate dried at 220 °C. Platinum electrode, 0.21 cm². Scan rate, 0.05 V/sec.

Preliminary voltammetric studies of the effect of lithium ion on the reduction of m-dinitrobenzene in DMF were performed. In these studies, the potential range was limited to -1.3 V in order to avoid the background peak. Integrated-current data was taken at -1.0 V, just past the first reduction peak for m-dinitrobenzene in DMF in the absence of lithium ion. Current-potential and current-integral data were obtained for solutions containing 0.01, 0.10, and 1.0 F lithium perchlorate.

The I-E curves of these solutions show a marked effect of lithium ion on the reduction process occurring at the second peak for m-dinitrobenzene (Figures 3-15 to 3-17). Both peaks shift toward more positive potentials; but the effect on the second peak is more pronounced with the two peaks almost merging into one at the higher lithium ion concentration. The first peak current remains almost constant while the second peak current increases by almost three times. The peak-current and current-integral results from data obtained at 0.05 V/sec are tabulated in Table 3-2, including the ratio of the second-peak current to the first-peak current. This ratio was calculated in order to minimize the effect of variations in concentration and changes in viscosity of the solutions. Current-integral data, as a function of the scan rate, were obtained only for the lowest and highest lithium perchlorate concentrations, and is plotted in Figure 3-18 as a function of the square root of the inverse scan rate. Integration data for m-dinitrobenzene, in the absence of lithium ion, is included in the figure for comparison. The current-integral values are in coulombs and, therefore, are related to the discharge capacity for the time span of the experiment at -1.0 V if the values are multiplied by the square root of the scan rate. The enhancement of the capacity by the addition of lithium ions is very clear from the data.

3.3 Studies in Propylene Carbonate. Voltammetric studies of nitrobenzene and m-dinitrobenzene were made in propylene carbonate (PC) to compare the results with those obtained in DMF. The studies were limited to the first reduction step of nitrobenzene and the first two steps of m-dinitrobenzene using a platinum electrode, and TPAP as the supporting electrolyte. Residual current measurements in both DMF and PC show a useable potential range out to -1.8 V on a platinum electrode and beyond -2.5 V on a mercury film electrode.

3.3.1 Nitrobenzene. Voltage scans of nitrobenzene at a mercury-film electrode showed a second peak at -2.0 V. This result corresponds to the second peak at -2.0 V in DMF using tetra-alkylammonium perchlorates as supporting electrolyte.⁸ No further studies were made on the second peak.

Two major effects were observed when the solvent was changed from DMF to PC for the reduction of m-dinitrobenzene. The first was a decrease in the peak height by a factor of about two for m-dinitrobenzene in 0.1 F TPAP, PC solution, and the second was a

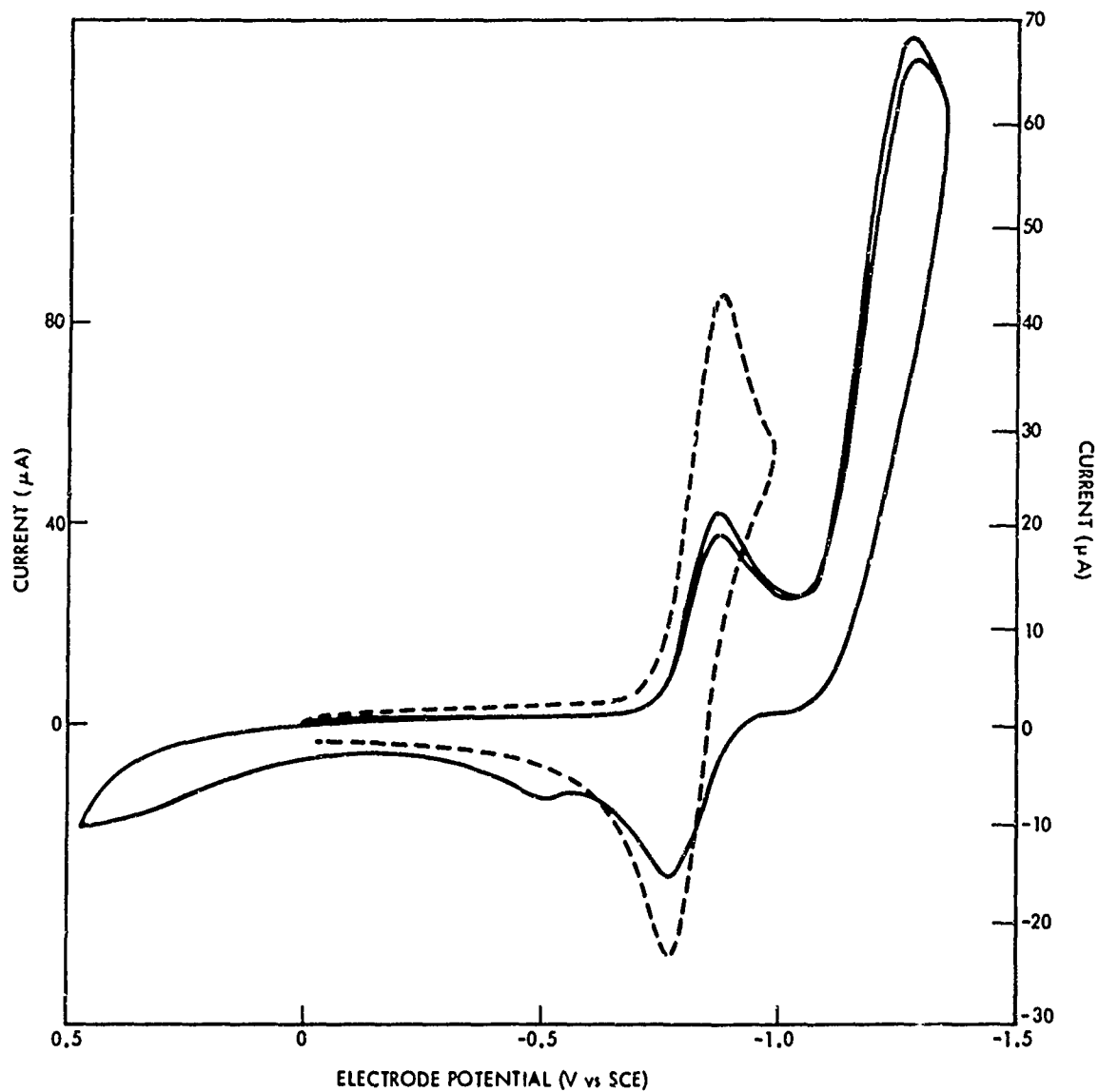


Figure 3-15. I-E Curves of 1 mF m-Dinitrobenzene in 0.01 F Lithium Perchlorate-DMF. Platinum electrode, 0.21 cm². Scan rate, 0.05 V/sec. Right-hand scale corresponds to broken line.

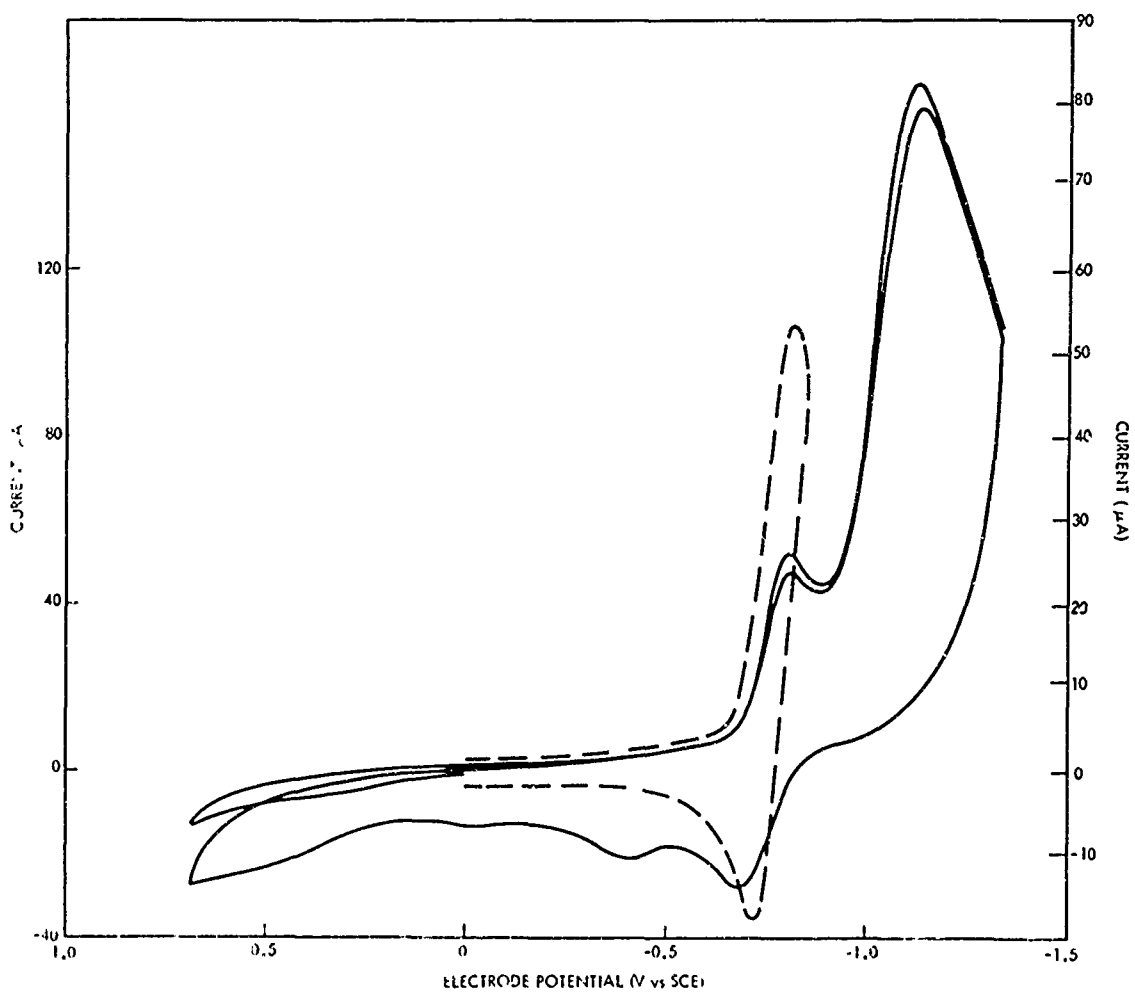


Figure 3-16. I-E Curves of 1 mF m-Dinitrobenzene in 0.1 F Lithium Perchlorate-DMF. Platinum electrode, 0.21 cm². Scan rate, 0.05 V/sec. Right-hand scale corresponds to broken line.

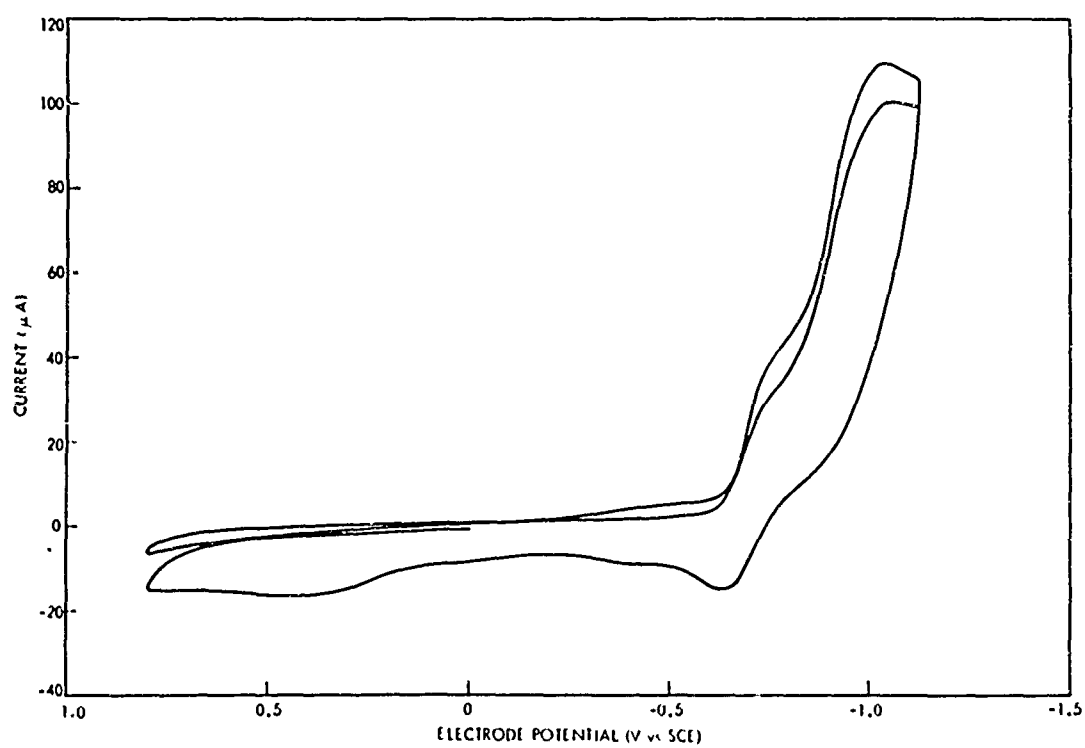


Figure 3-17. I-E Curve of 1 mF m-Dinitrobenzene in 1 F Lithium Perchlorate-DMF. Platinum electrode, 0.21 cm². Scan rate, 0.05 V/sec.

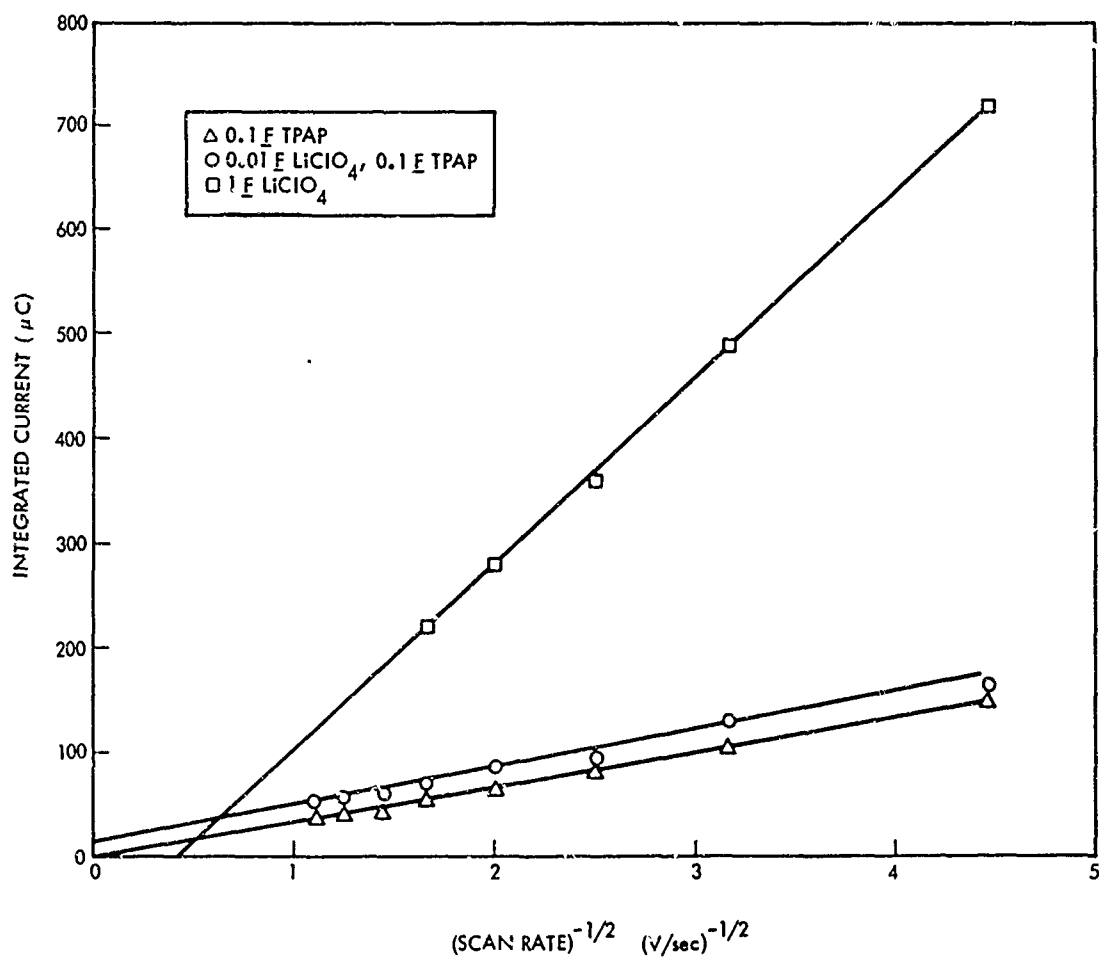


Figure 3-18. Integrated Current vs. (Scan Rate)^{-1/2} Curves for 1 mM m-Dinitrobenzene in DMF in Solutions Varying in Lithium Ion Concentration. Platinum electrode, 0.21 cm². Scan limit, -1.0 V vs. sce.

TABLE 3-2
CURRENT-POTENTIAL DATA FOR m-DINITROBENZENE IN DMF SOLUTIONS
VARYING IN AMOUNTS OF LITHIUM ION AT SCAN RATE OF 0.05 V/sec

Supporting Electrolyte	1st Peak		2nd Peak		Peak Current Ratio		Current-Integral (to -1 V) μC
	E_p V	I_p μA	E_p V	I_p μA	I_{P2}/I_{P1}		
0.1 F TPAP, -----	-0.87	52	-1.28	69	1.3		146
0.1 F TPAP, 0.01 F <u>F</u> LiClO ₄	-0.88	43	-1.29	135	3.1		165
0.1 F TPAP, 0.1 F <u>F</u> LiClO ₄	-0.82	57	-1.12	160	2.8		358
-----, 1.0 F <u>F</u> LiClO ₄	-0.75	37	-1.05	114	3.0		715

change in the character of the reduction process corresponding to the second peak from a quasi-reversible, one-electron transfer in DMF to a complicated process with a larger peak in PC. Therefore, experiments were made on nitrobenzene to examine these solvent effects on a simpler system.

The reduction of nitrobenzene in DMF containing 0.1 F TPAP occurs reversibly to yield the nitrobenzene radical anion.^{11,12} Cyclic voltammetric I-E curves of nitrobenzene in PC and DMF, obtained to compare the effects of the two solvents, showed that a reversible reduction takes place in both solvents. However, the curves also showed that the peak currents are approximately 1.7 times larger in DMF than in PC while the peak potentials remain the same. In addition, current integration shows a factor of 1.5 decrease on going from DMF to PC.

The differences in both the peak current and the integral values result from the difference in the diffusion coefficient of nitrobenzene in the two solvents. The peak current and integral values bear the same functional relation to the diffusion coefficient, and hence, are affected in an identical manner in the absence of complicating effects, and vary as the square root of the diffusion coefficients (which are proportional to the inverse of the viscosity).¹³ The viscosities of DMF and PC are 0.8 and 2.5 centipose, giving a square root ratio of 1.8. The experimental peak current and integral value ratios of 1.7 and 1.5 are in good agreement with the viscosity square root ratio.

3.3.2 m-Dinitrobenzene. A temperature study was made on solutions of nitrobenzene and m-dinitrobenzene in PC from room temperature to 80 °C. For both compounds, the peak currents increased with increasing temperature. The effect of temperature on the first peak of nitrobenzene was studied as a reference system. For nitrobenzene, plots of I_p vs. $v^{1/2}$ (square root of scan rate) at room temperature and 70 °C were found to be linear and with intercepts at the origin (Figure 3-19). Thus, the increase in peak current with temperature is by changes in viscosity with temperature rather than by changes in kinetics, turbulence, or some type of surface phenomenon.

Marked changes were observed in the I-E curves for the reduction of m-dinitrobenzene with increasing temperature (Figure 3-20). The first peak showed only a small increase in peak current with increasing temperature, but the second peak showed a rapid increase in current with temperature. A similar temperature effect was observed upon the addition of 0.1 F water (Figure 3-21). The peak currents as a function of temperature are shown for the wet and dry solutions in Figure 3-22. The first peak current which is not affected by water, increased from 25 μ A to 40 μ A over the temperature range 26 to 80 °C. This effect is similar to that for nitrobenzene and is probably caused by the decrease in the solvent viscosity. The second

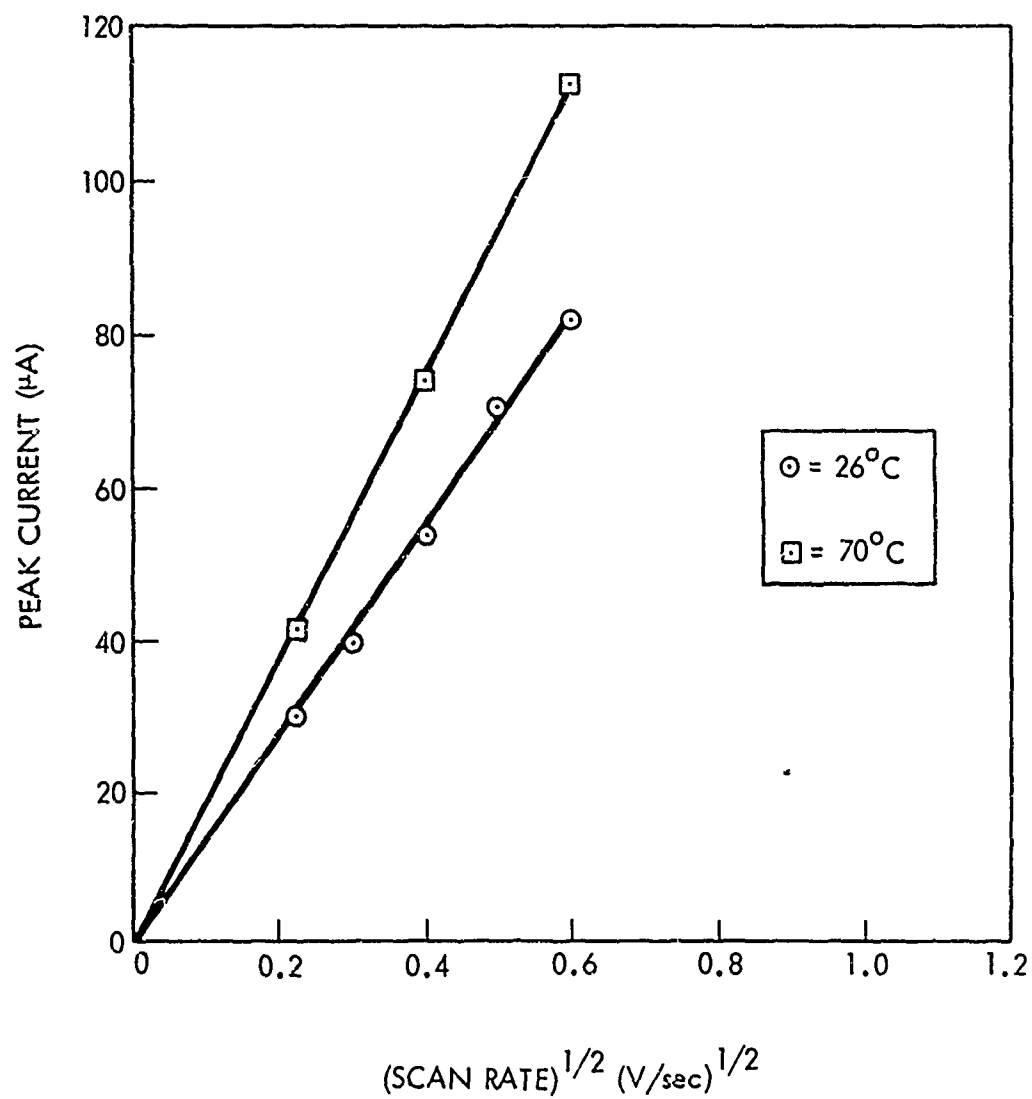


Figure 3-19. Peak Current vs. $(\text{Scan Rate})^{1/2}$ Curves for 1 mF Nitrobenzene in 0.2 F TPAP-PC at Different Temperatures. Platinum electrode, 0.21 cm^2 .

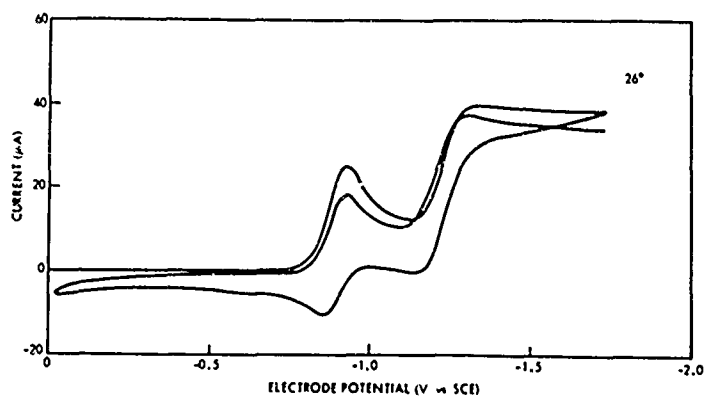
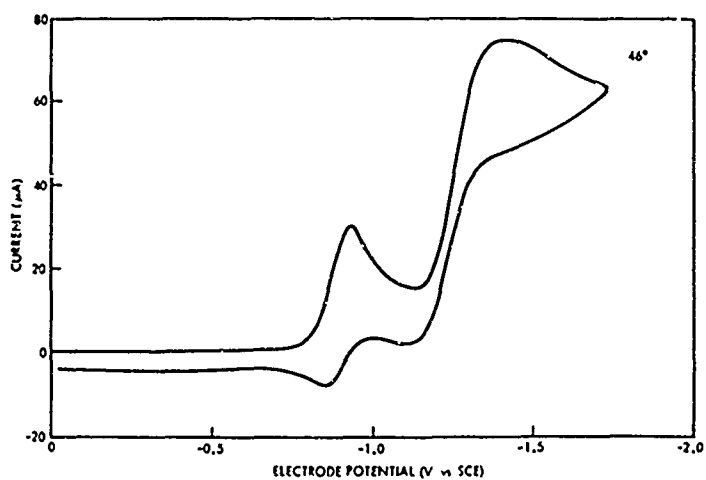
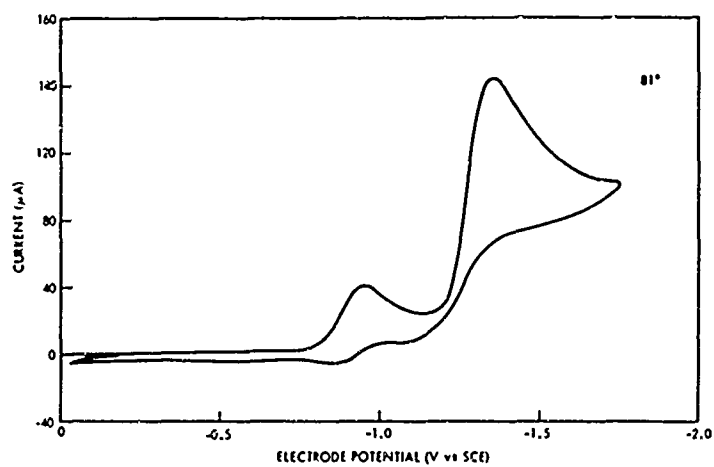


Figure 3-20. I-E Curves of 1 mF m-Dinitrobenzene in 0.2 F TPAP-PC at Different Temperatures. Platinum electrode, 0.21 cm². Scan rate, 0.05 V/sec.

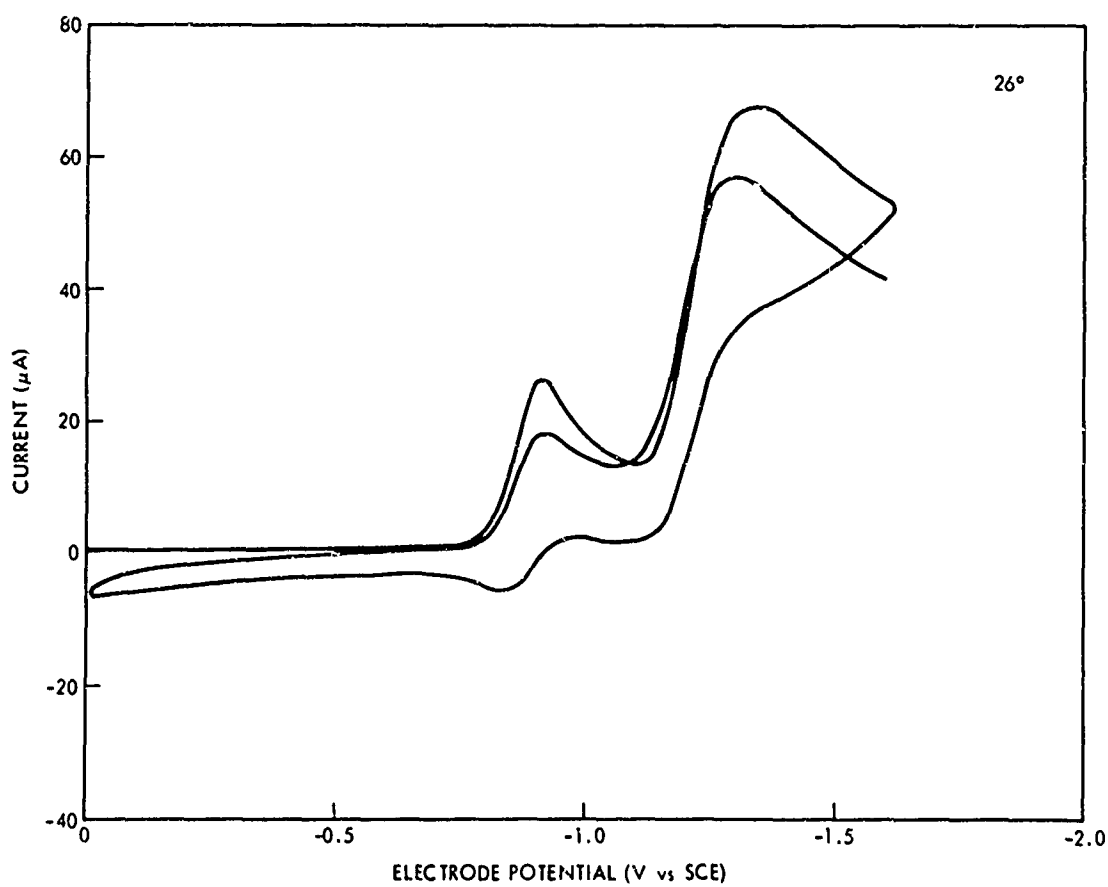
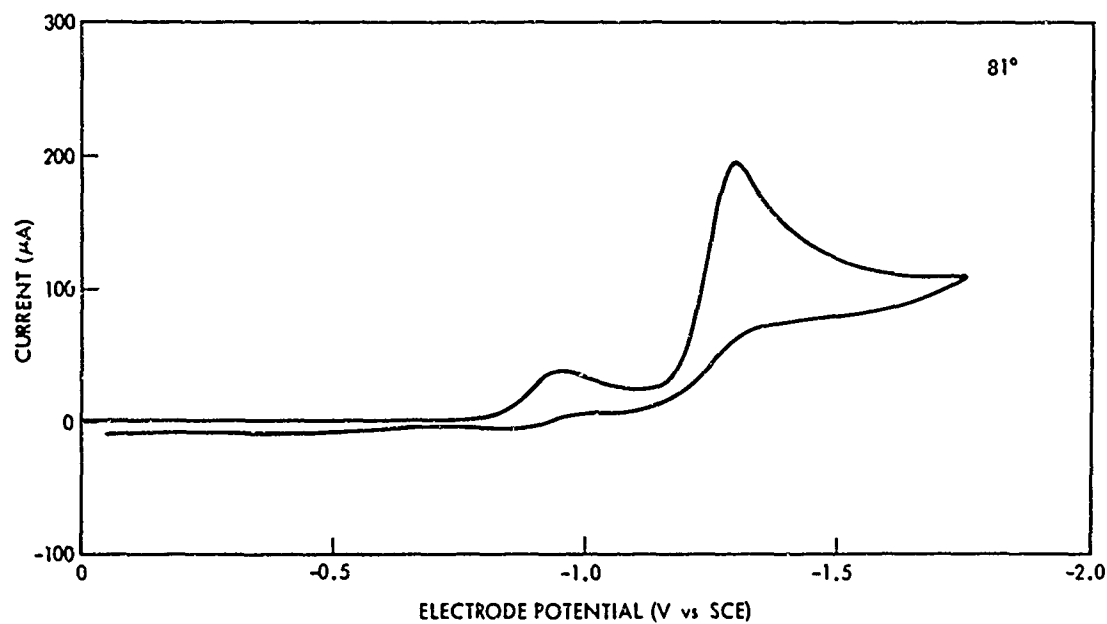


Figure 3-21. I-E Curves of 1 mF m-Dinitrobenzene at Different Temperatures in 0.2 F TPAP-PC Containing 0.1 F Water. Platinum electrode, 0.21 cm². Scan rate, 0.05 V/sec.

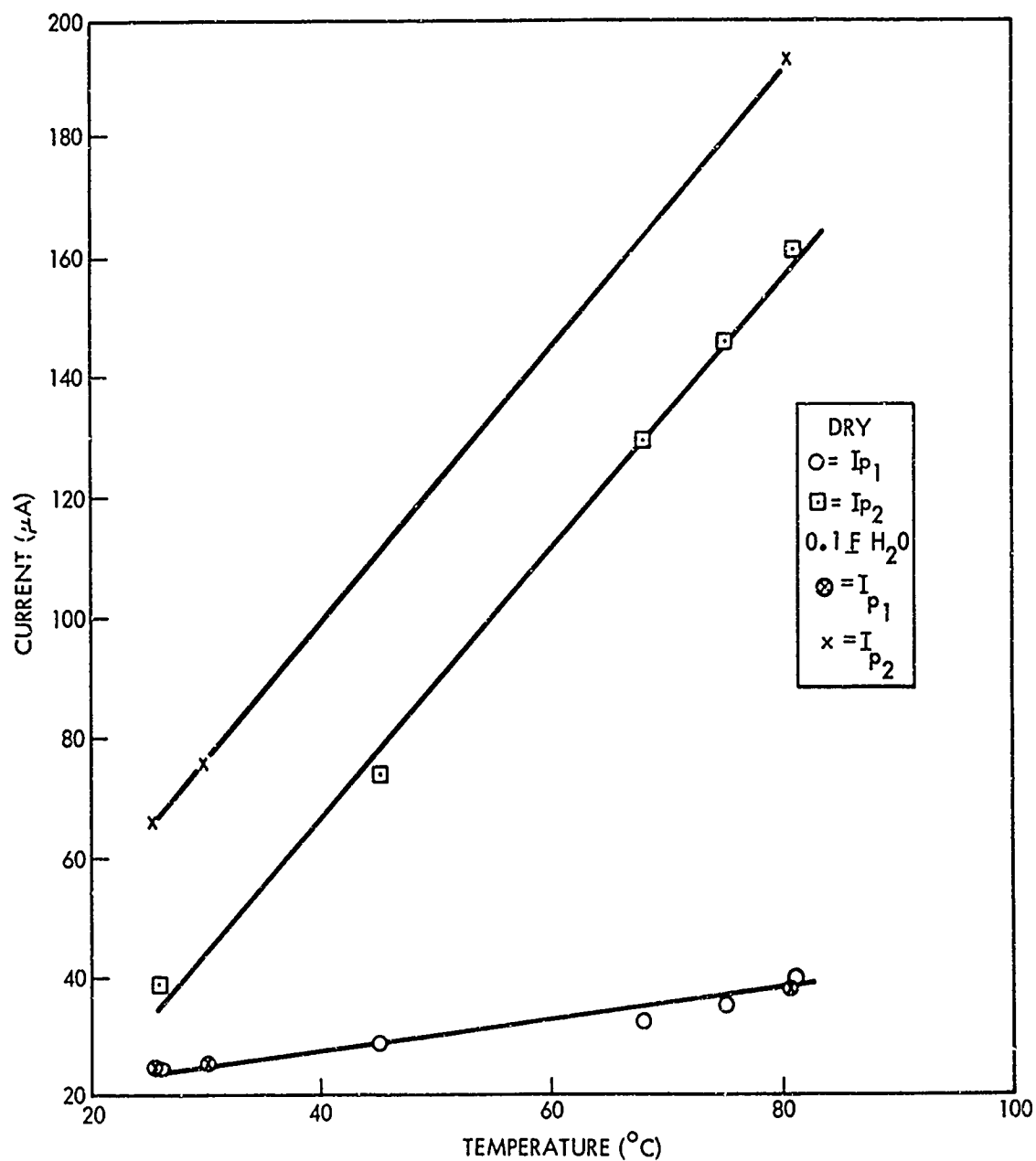


Figure 3-22. Comparison of Peak-Current Variation with Temperature for Wet and Dry Solutions of 1 mF m-Dinitrobenzene in 0.2 F TPAP-PC. Platinum electrode, 0.21 cm². Scan rate, 0.5 V/sec.

peak, which is affected by water, is broad at lower temperatures but narrows at higher temperatures. Figure 3-23 shows the results of a scan rate study performed at room temperature. In this figure, the function $I_p/v^{1/2}$ is plotted against scan rate in order to separate the effect of the scan rate on the diffusion process from its effect on the kinetic process. This function is independent of scan rate for non-complicated processes, and independent also at scan rates where the kinetic processes are either too fast or too slow to be observed.

The addition of water introduces another effect that can be seen by comparing I-E curves for the wet and dry solutions. At the lowest scan rate, the second peak in dry PC shows a flat plateau that gradually becomes a peak as the scan rate is increased from 0.05 to 0.25 V/sec (Figure 3-24). However, in wet PC, the slow scan rate yields a broad peak that becomes a plateau at intermediate scan rates and then becomes a peak at fast scan rates (Figures 3-25 and 3-26).

The scan rate also affects the second peak in other ways. At slow scan rates, the second peak shows no anodic current on the reverse sweep, while at fast scan rates an anodic peak does emerge. In addition, the effect of scan rate on the peak heights is linear for the first peak while for the second peak, the effect approaches linearity only at fast scan rates. In Figure 3-23, the constancy of the ratio $I_p/v^{1/2}$ for the second peak at fast scan rates is evident. At fast scan rates, the charge transfer behaves as if the electrode reaction is primarily diffusion controlled and takes on reversible character with a peak height comparable to that for a one-electron reduction.

The results in Figure 3-22 show that the electrode reaction occurring at the second peak has the same temperature dependence in both wet and dry solvent. This, plus the higher current in the wet solvent, shows that water affects the overall reaction at both the low and the high temperature.

The behavior of the function $I_p/v^{1/2}$ with scan rate for the second peak (Figure 3-23) is similar to that expected for an electrochemical-chemical-electrochemical (ece) process¹⁴ or a cyclic regeneration¹⁵ process. The current plateau observed in the I-E curves at slow scan rates also supports this conclusion because a plateau is usually observed when the regeneration process of electroactive species is fast compared to the scan rate or when regeneration is a simple catalytic reaction. Consequently, a plateau is favored by slower scan rates or by an increase in the regeneration rate.

3.4 Discussion of Voltammetric Results. The reduction processes of *m*-dinitrobenzene derivatives have been shown to be influenced by the substituents on the ring, by the addition of water to the solution, by addition of lithium perchlorate to the solution, and by the choice of solvent, e.g., DMF or PC. In DMF containing 0.2 F TPAP, the cyclic voltammetric current-potential curves

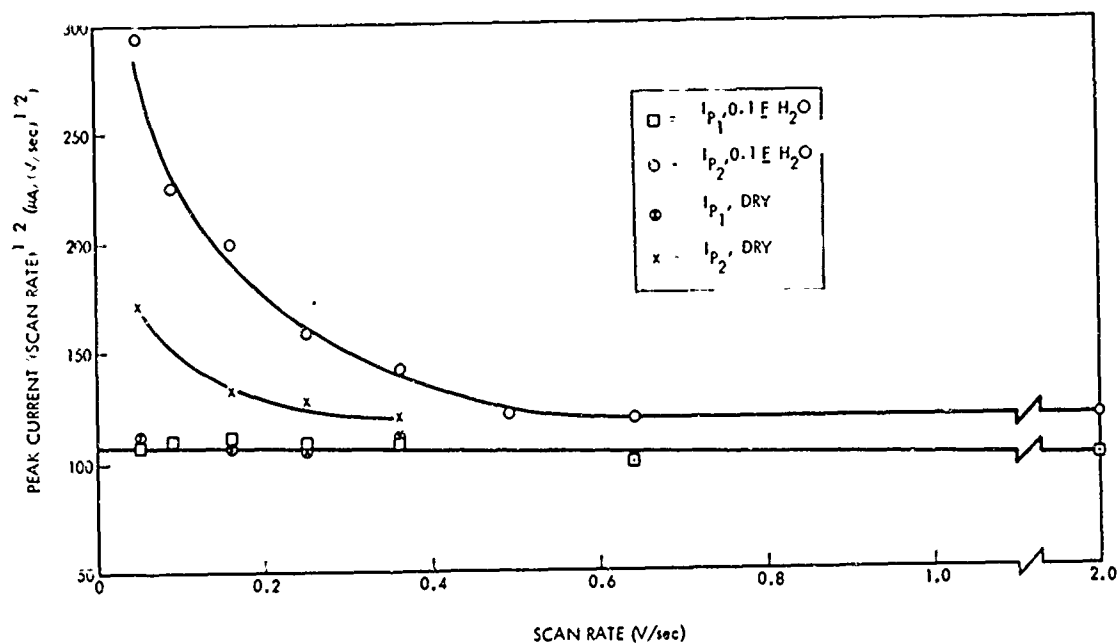


Figure 3-23. Peak Current/(Scan Rate)^{1/2} vs. Scan Rate Curves for Wet and Dry Solutions of 1 mF m-Dinitrobenzene in 0.2 F TPAP-PC. Platinum Electrode, 0.21 cm². I_{P1} and I_{P2} represent the first and second peaks, respectively.

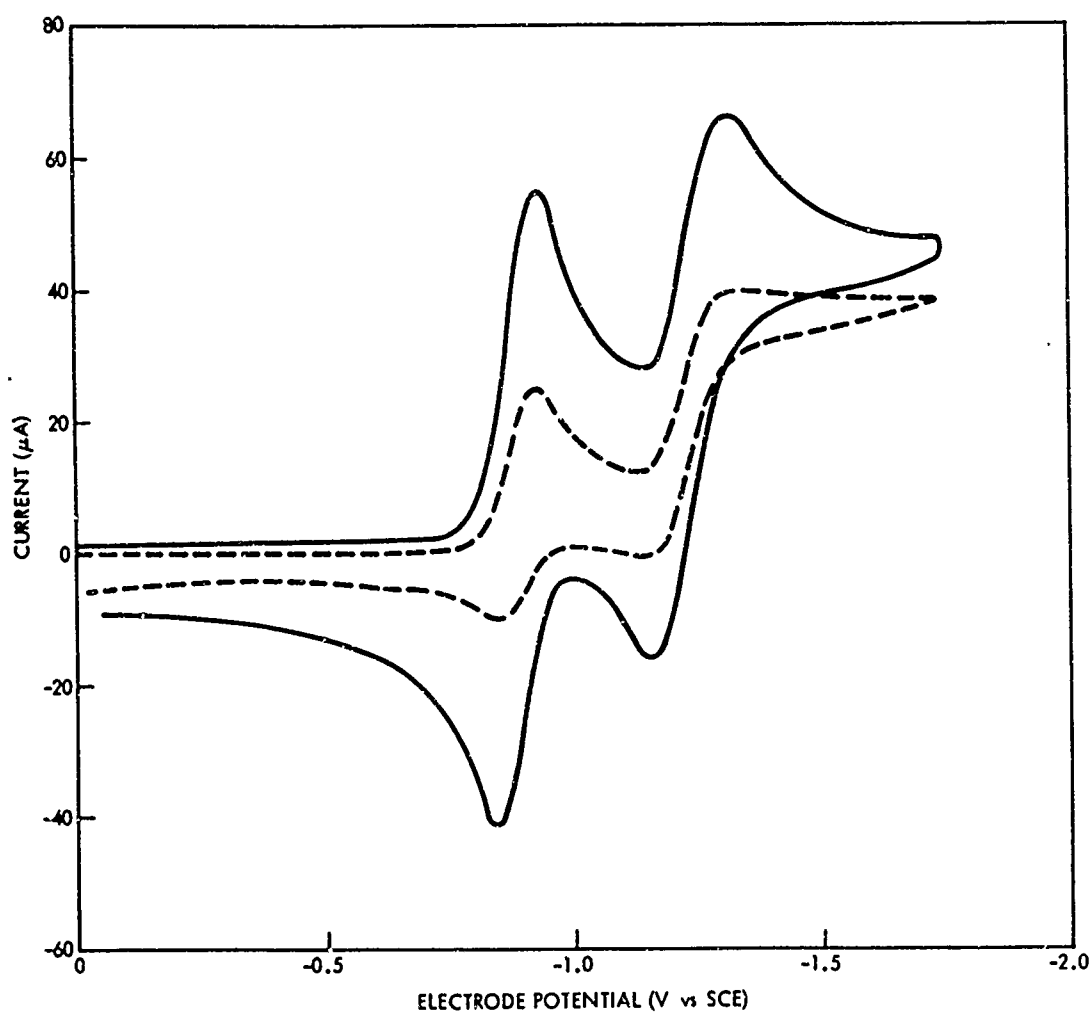


Figure 3-24. I-E Curves for 1 mF m-Dinitrobenzene in 0.2 F TPAP-PC at Different Scan Rates at 26 °C. Platinum electrode, 0.21 cm². Broken line, 0.05 V/sec; solid line, 0.25 V/sec.

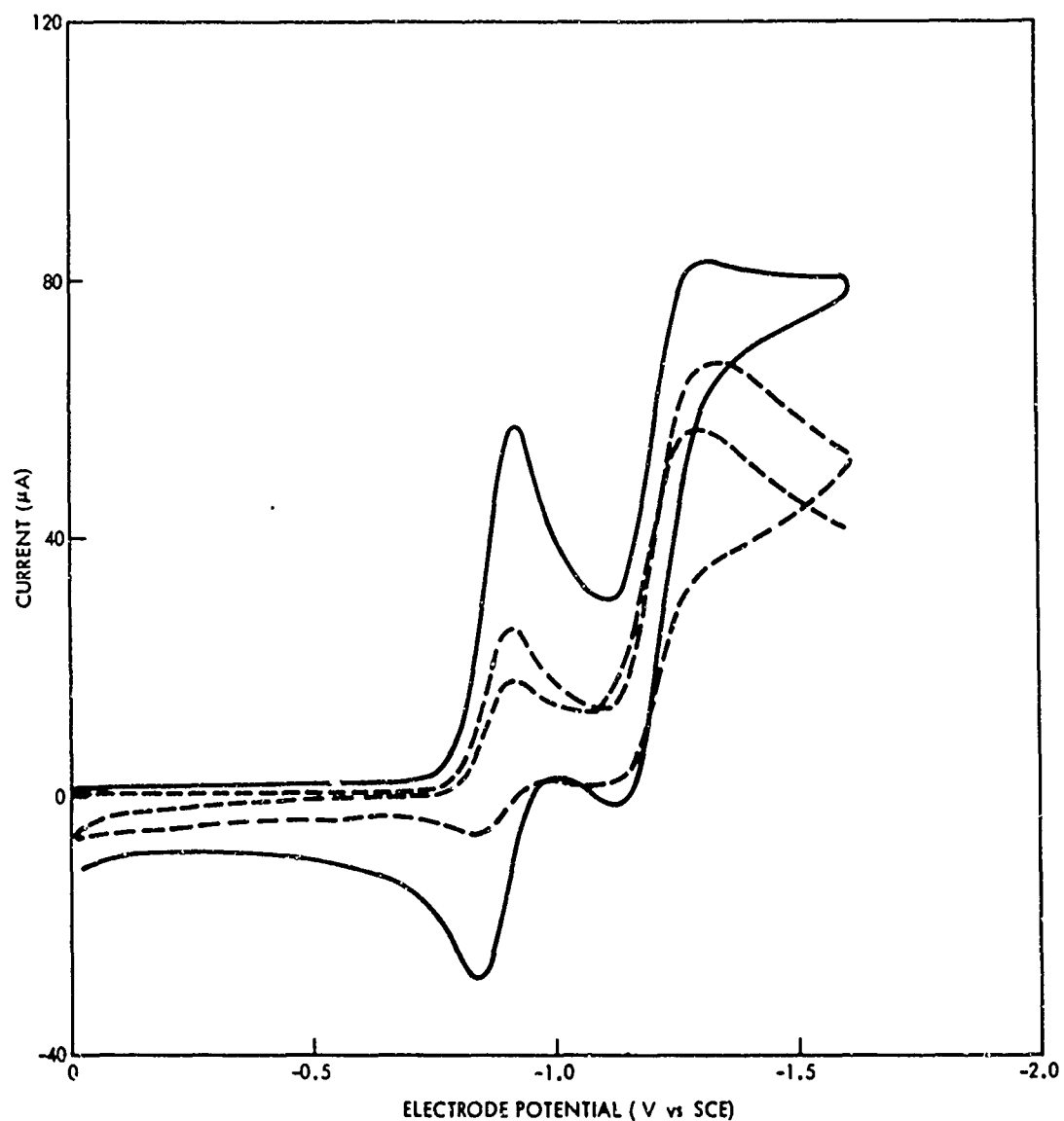


Figure 3-25. I-E Curves of 1 mF m-Dinitrobenzene in 0.2 F TPAP-PC Containing 0.1 F Water at 26 °C. Platinum electrode, 0.21 cm². Solid line, 0.25 V/sec; broken line, 0.05 V/sec.

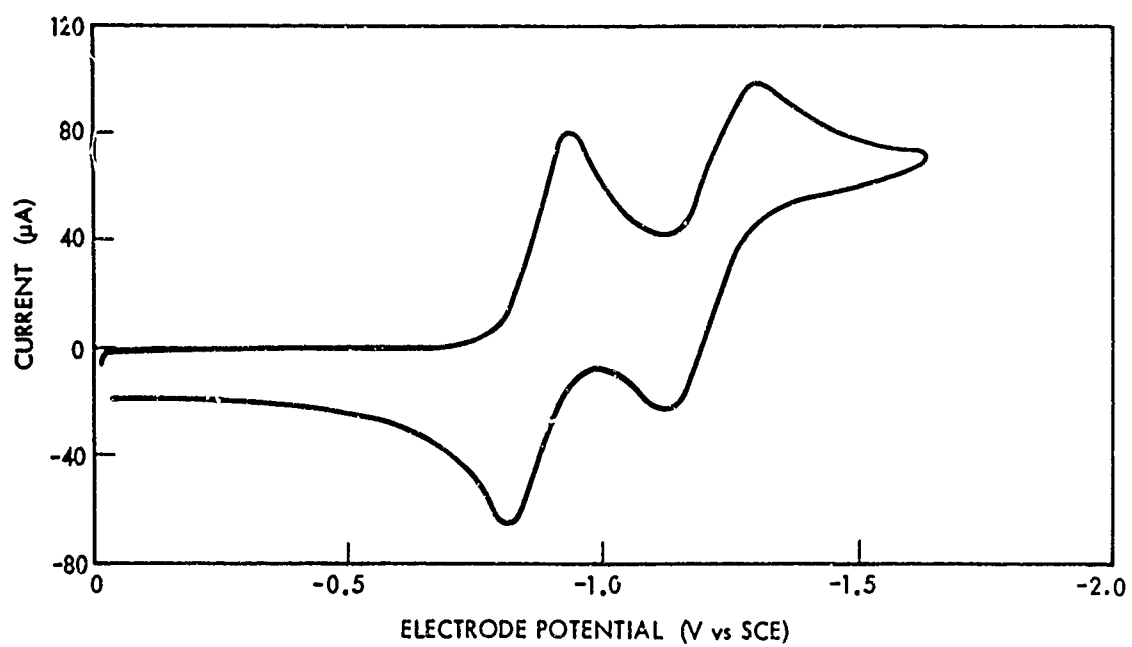
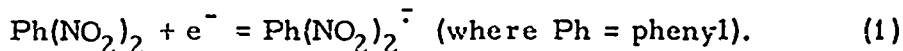
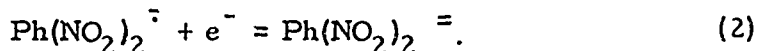


Figure 3-26. I-E Curve of 1 mF m-Dinitrobenzene in 0.2 F TPAP-PC Containing 0.1 F Water at 26 °C. Platinum electrode, 0.21 cm². Scan rate, 2.0 V/sec.

of m-dinitrobenzene derivatives clearly show that the reduction process generally proceeds through three reduction steps in the potential range 0 to -2.5 V, and that except for the dinitrophenols, the first reduction step involves a reversible, one-electron process yielding free radical anions:



The stability of this radical is dependent on the nature of the substituent groups and, except for the phenols and compounds with iodine substituents, the radical anion has been readily observed by electron spin resonance spectroscopy. In addition, it has been shown that the second reduction step results in another electron being reversibly added to the anion radical:



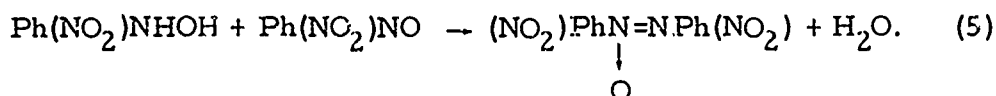
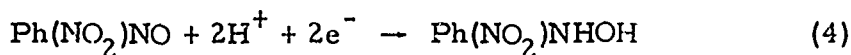
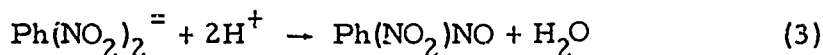
No attempt is made here to specify the charge distribution of the dianion or to imply stepwise reduction of the nitro groups. Further reduction after the second step is strongly influenced by molecular structure, the effect of substituents on the stability of the dianion, and the nature of the reduction media, e.g., the proton availability of the solvent.

For m-dinitrobenzene in dry DMF, each of the first two reduction peaks observed in cyclic voltammetric I-E curves corresponds to a one-electron process, while the process occurring at the third peak has not been defined. However, the characteristics of this third peak, its height, its lack of an anodic current minimum peak on sweep reversal, and its occurrence at high negative potentials indicate a reduction process involving the dianion in complex electrochemical reactions yielding possibly nitroso or hydroxylamine intermediates. The apparent n value for the third peak is 2.6, indicating that an overall process involving more than two electrons is occurring at the third peak. The apparent n value was estimated by taking the two-thirds root of the ratio of the third peak to the first peak (assuming n is one for the first peak) since theory indicates that the peak current is proportional to the three-halves power of the number of electrons involved in a simple case. When kinetic complications are present, a smaller peak current results, except for catalytic processes, and, as a result, the estimated n value is either equal to or less than the actual value of n.

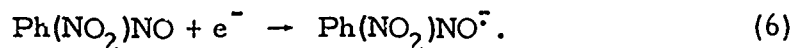
The reactions in dry DMF at the third peak are assumed to involve the addition of protons from an undetermined source and the elimination of water. The protons may be abstracted from the solvent by reactive intermediates generated electrochemically, but a more likely source is from trace contaminants, for example water, which may have a concentration as high as 0.01 F in the solvents used. A

detailed description would require much more work including the determination of the specific electrochemical process occurring at the third peak, product analysis, and coulometric data.

A set of reactions can be set forth that would be expected to occur in the presence of a proton source and would lead to the same products as the reduction of *m*-dinitrobenzene in aqueous media.¹⁶ The products of a four-electron reduction in aqueous solution are 3-nitrophenylhydroxylamine and 3,3'-dinitroazoxybenzene. Reduction of *m*-dinitrobenzene beyond the dianion to yield these products would then require reactions such as the following:



Reaction (4) may proceed through the reduction of the nitrosobenzene to its anion radical,



This type of mechanism has been postulated by Kemula and Sioda¹⁷ for the reduction of nitrosobenzene in DMF containing 0.2 F sodium nitrate. However, the anion radical $\text{PhNO}^{\cdot-}$ dimerizes to azoxybenzene¹⁸ and may account for the analogous radical not having been observed by electron spin resonance studies in the reduction of *m*-dinitrobenzene. These authors have also proposed that the dianion, PhNO^{2-} , formed by the two-electron reduction of nitrosobenzene may abstract protons from DMF. A similar proton abstraction process might occur in the reduction of *m*-nitronitrosobenzene yielding electroactive products that could be further reduced.

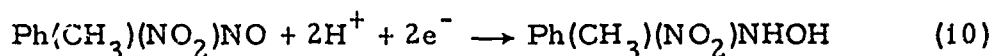
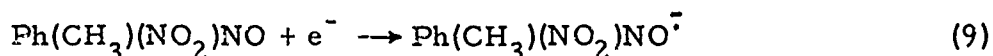
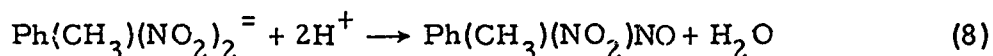
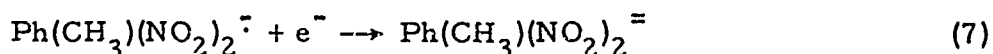
The major substituent effect on the reduction of the *m*-dinitrotoluenes is expected to arise from the steric effect of the *ortho*-methyl group. The results of polarographic and electron spin resonance experiments by Geske and co-workers¹⁹ on *ortho*-substituted nitrobenzenes indicate that the influence of *ortho*-substituent groups on nitroaromatic compounds is caused by the effect of steric displacement of the nitro group from coplanarity with the benzene ring. No assertions of the steric effect on the spatial disposition of the molecules in chemical and electrode reactions can be made. The displacement from coplanarity reduces the coupling between the π -electron systems of the benzene ring and of the nitro group and results in an increase of charge localization. Consequently, the effective charge of the reduced species tends to be localized on a nitro group. The loss of resonance energy causes a shift to more negative reduction

potentials, while the charge localization causes a positive shift by increasing the solvation energy relative to the planar molecule. Polarographic half-wave potentials of ortho-substituted nitrobenzenes are shifted negative relative to nitrobenzene itself, as would be expected because of the loss of resonance energy caused by steric displacement of the nitro group from planarity. On the other hand, the localization of charge should increase the rate of chemical reactions because of the interaction of the charged anions and a proton source.

The shifts in peak potential as well as the increase in the peak heights at the second peak which are observed in the I-E curves (Figures 3-1 and 3-3) for the m-dinitrotoluenes relative to those for m-dinitrobenzene are consistent with the foregoing description on the effect of methyl substituents in the ortho-position.

The reduction mechanism for the m-dinitrotoluenes can be discussed in terms of the model described for the reduction of m-dinitrobenzene. The first step in the reduction sequence corresponds to a one-electron reversible reduction and is equivalent to Reaction (1). The I-E curves of the second step show a complex peak shape whose height is increased by the addition of water (Figures 3-1 and 3-3).

For solutions containing 1 F water, the apparent n value, estimated by taking the ratio of peak currents of the second to the first peak, are 1.9 and 2.0 for 2,4- and 2,6-dinitrotoluene, respectively. These values indicate an overall process of two electrons or more at the second peak. The following reactions can explain the results:



The proton source in these reactions is either water or the solvent. The product of Reaction (8) is probably electroactive at the potential at which it is produced since the reduction of nitrosobenzene has been shown to occur earlier than that of nitrobenzene,¹⁷ and it is assumed that the reduction sequence is maintained for the nitronitrotoluenes and the dianion of the dinitrotoluenes.

The ortho-methyl groups could cause the kinetics of processes such as Reaction (8) to be faster for the dinitrotoluenes than for m-dinitrobenzene as a result of charge localization in a smaller effective

volume. Consequently, the apparent proton availability of the solvent would increase and provide an effective route between electrode processes such as those given by Reactions (7) and (9) or (10) above.

The increase in the peak current for the second reduction step of the m-dinitrotoluenes relative to that observed for m-dinitrobenzene may be accounted for by Reactions (8) and (9). If the proton source in Reaction (8) is water, the overall process at the second peak would then correspond to a two-electron or greater reduction in agreement with the results observed in solutions containing 1 F water.

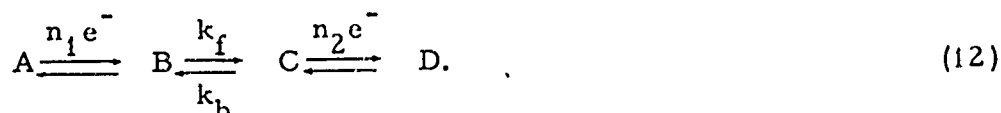
The reduction process at the third peak has not been identified although reactions similar to those discussed for m-dinitrobenzene are expected. In addition, proton abstraction from the methyl group, such as has been observed with trinitrotoluene,¹⁸ might also occur with the m-dinitrotoluenes.

The reduction of m-dinitrobenzene in PC exhibits a second reduction peak that is larger than that observed in DMF of comparable dryness. This enhanced current effect at the second peak is similar to that observed for the dinitrotoluenes in DMF and suggests that the apparent proton availability in PC is greater than in DMF. A tentative mechanism for the reduction of m-dinitrobenzene in PC containing 0.2 F TPAP as supporting electrolyte is discussed below.

As shown earlier, the first peak corresponds to a one-electron reversible reduction. This peak occurs at -0.92 V in PC and at -0.81 V in DMF. It is assumed, therefore, that in PC the radical anion of m-dinitrobenzene is the product at the first peak.



Scan rate studies indicate that the electrode process at the second peak corresponds to an ece (electrochemical-chemical-electrochemical) mechanism^{12,19} in which a chemical reaction is interposed between two charge-transfer reactions. The kinetics are represented by:

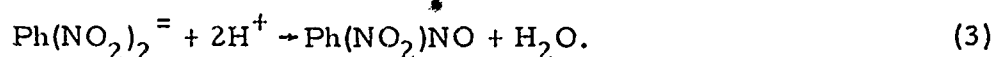


When C is more easily reduced than A, the peak current (at potentials corresponding to the reduction of A) is enhanced by the simultaneous reduction of a portion of C produced by the chemical reaction, with the enhancement being dependent on the scan rate and on the rate constants of the chemical reaction. Our results indicate that the first

step in this process is a one-electron reversible reduction. Hence, it is assumed that this first step occurring at -1.30 V in the PC-TPAP electrolyte solution corresponds to the production of B in the kinetic scheme and to the electrode reaction

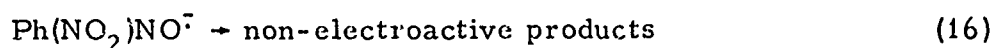
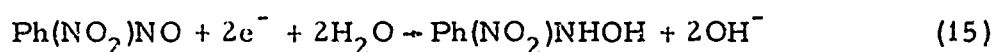


which in DMF-TPAP occurs at -1.23 V. The chemical step must be one that generates electroactive products which are readily reduced at potentials corresponding to the reduction of the $\text{Ph}(\text{NO}_2)_2^{\cdot-}$ radical anion. This chemical step is likely to be that shown earlier in Equation (3):



$\text{Ph}(\text{NO}_2)\text{NO}$ corresponds to C in the kinetic scheme.

The second electrochemical step can then correspond to the following set of reactions:



where the competition between Reactions (14), (15), and (16) are determined by the amount of water in the solvent. At room temperature, the rate of the chemical step is slow compared to Equations (14), (15), and (16) while at high temperatures this rate is fast. The experimental data support a model of this kind.

An apparent n value can be estimated from the two-third root of the ratio of the second peak to the first. At 80 °C, the apparent n values are 2.5 and 2.8 when the solution contains 0.02% and 0.2% water, respectively. Yet the rate of change of the peak height with temperature is independent on the amount of water in solution. Temperature appears to affect the proton availability in the solvent which, according to our mechanism, is involved in the conversion of the dianion to *m*-nitronitrosobenzene. A mechanism of this kind is indicated on the basis of our scan rate studies at room temperature. At high scan rates, a one-electron reduction presumably to the dianion is observed for both the wet and dry solutions (Figures 3-24, 3-25, and 3-26).

Reduction of the dianion $\text{Ph}(\text{NO}_2)_2^{2-}$ appears to be the limiting step in DMF with noncomplexing tetralkylammonium perchlorates as supporting electrolyte. While reduction to the dianion occurs at

-1.23 V, further reduction does not occur until potentials more negative by roughly 1 V are reached. However, the I-E curve (Figure 3-15) for reduction of m-dinitrobenzene in DMF containing as little as 0.01 F lithium perchlorate, with 0.1 F of the tetraalkylammonium perchlorate as supporting electrolyte, shows enhancement at the second peak which indicates strongly that reduction beyond the dianion occurs readily in the presence of lithium ion. Such a marked effect on the reduction at the second peak suggests the formation of an ion pair species which is more readily reduced than the dianion. Our data is not sufficiently complete to allow detailed interpretation, but, ion association between a dinitroaromatic anion and a lithium cation would be expected to occur as the electrostatic interaction is sufficiently great to rupture solvation shells.

4. PLATE-LEVEL STUDIES ON m-DINITROBENZENE

4.1 Introduction. Polarization, discharge capacity, and electrode potentials were measured for cells consisting of a lithium anode, a m-dinitrobenzene cathode, and a propylene carbonate-lithium perchlorate electrolyte solution. The objective for this work was to formulate and fabricate cathodes having good structural integrity and demonstrating a reasonable shelf life. Secondary objectives were to obtain capacity data on the most promising cathode, and to determine the electrochemical behavior of the individual electrodes.

4.2 Results of Discharge Tests on Lithium m-Dinitrobenzene Cells. The physical data (cathode thickness, pressing pressure, etc.) for the cathodes tested are presented in Table 4-1. In general, for each set of test parameters (thickness, percent binder, etc.), a dry and a wet cathode were tested. The cathodes were fabricated from a dry mixture of m-DNB, carbon, and acrylic. The dry cathodes were used without any further treatment; the wet cathodes were soaked for 15 min in the electrolyte solution prior to incorporation into the test cell. Paste cathodes, which were used as a reference for comparison, were fabricated from a mixture of the dry mix of the m-dinitrobenzene, carbon, and sufficient electrolyte to form a paste consistency. A summary of the polarization data is presented in Table 4-2. The polarization curves are shown in Figures 4-1 through 4-31. Polarization tests were performed immediately after assembly, after 5 days, after 12 days, and after 19 days. The results of a visual inspection of cathode physical integrity prior to incorporation into a cell and the visual appearance of cell components after testing are presented in Table 4-3.

TABLE 4-1
PHYSICAL DATA OF ORGANIC CATHODES USED IN CELL TESTING
(Cathode Mix - 1.5 g Carbon, 1.5 g m-DNB, 10 ml.
Binder Solution) (Cathode Weight = 3 g, except
when noted)

Cell No.	Binder Solution	Cathode Thickness (in)	Cathode Impedance (ohms)	Cathode Press Pressure (psi)	Cathode Test State
P-6	None	-	-	-	Paste
P-7 ^(b)	None	-	-	-	Paste
P-8	None	-	-	-	Paste
P-9	None	-	-	-	Paste
P-10	None	-	-	-	Paste
P-11	None	-	-	-	Paste

(a)

TABLE 4-1
 PHYSICAL DATA OF ORGANIC CATHODES USED IN CELL TESTING
 (Cathode Mix - 1.5 g Carbon, 1.5 g m-DNB, 10 ml.
 Binder Solution) (Cathode Weight = 3 g, except
 when noted) (Continued)

Cell No.	Binder Solution	Cathode Thickness (in)	Cathode Impedance (ohms)	Cathode Press Pressure (psi)	Cathode Test State
PP-2	5% Acrylic	0.082	0.338	10,000	Dry ^(c)
PP-3	2.5% Acrylic	0.080	0.235	10,000	Dry
PP-4 ^(d)	5% Acrylic	0.067	0.400	10,000	Dry
PP-5 ^(e)	5% Acrylic	0.026	0.600	10,000	Dry
PP-6	5% Acrylic	0.088	0.313	10,000	Wet ^(f)
PP-7	2.5% Acrylic	0.081	0.225	10,000	Wet
PP-8	5% Acrylic	0.070	0.400	10,000	Wet
PP-9 ^(e)	5% Acrylic	0.035	0.475	10,000	Wet
PP-10	5% Acrylic	0.107	0.425	5,000	Dry
PP-11	5% Acrylic	0.083	0.388	15,000	Dry
PP-12	5% Acrylic	0.104	0.425	5,000	Wet
PP-13	5% Acrylic	0.078	0.500	15,000	Wet
PP-14 ^(g)	5% Acrylic	0.087	0.225	10,000	Wet
PP-15	5% Acrylic	0.085	0.288	20,000	Wet
PP-16	2.5% Acrylic	0.082	0.100	10,000	Wet
PP-17	2.5% Acrylic	0.082	0.105	10,000	Wet
PP-18	5% Acrylic	0.089	0.250	10,000	Wet
PP-19	5% Acrylic	0.070	0.250	10,000	Wet
PP-20	2.5% Acrylic	0.092	0.140	10,000	Wet
PP-21	2.5% Acrylic	0.091	0.135	10,000	Wet
PP-22	5% Rosin	0.090	0.213	10,000	Wet
PP-23	5% Mastic Gum	0.088	0.155	10,000	Wet
PP-24	5% Benzoin Gum	0.081	0.263	10,000	Wet
PP-25	5% Dammar Gum	0.087	0.325	10,000	Wet

TABLE 4-1
PHYSICAL DATA OF ORGANIC CATHODES USED IN CELL TESTING
(Cathode Mix - 1.5 g Carbon, 1.5 g m-DNB, 10 ml.
Binder Solution) (Cathode Weight = 3 g, except
when noted) (Continued)

Cell No.	Binder Solution	Cathode Thickness (in)	Cathode Impedance (ohms)	Cathode Press Pressure (psi)	Cathode Test State
PP-26	5% Guaiac Gum	0.104	0.140	10,000	Wet
PP-27	5% Gum Arabic	0.090	0.090	10,000	Wet
PP-28	5% Acrylic	0.088	0.188	10,000	Dry ^(h)
PP-29	5% Acrylic	0.089	0.213	10,000	Dry ^(h)
PP-30	5% Canada Balsam	0.104	0.120	10,000	Wet
PP-31 ⁽ⁱ⁾	5% Acrylic	0.102	1.00	10,000	Wet

(a) The paste cathodes did not incorporate a binder; the electrolyte solution (LiClO_4 in propylene carbonate) was added to the carbon - m-DNB mix until a mixture having a pasty consistency was formed.

(b) The solvent-electrolyte combination for this cell was tetra-n-propylammonium perchlorate in propylene carbonate. The solvent-electrolyte combination for all other test cells was propylene carbonate - LiClO_4 .

(c) The pressed dry cathode was incorporated in the cell in the dry state.

(d) Cathode weight, 2 g.

(e) Cathode weight, 1 g.

(f) The pressed dry cathode was soaked 15 min in the solvent-electrolyte combination prior to assembly into the test cell.

(g) A new die for pressing was used on this and subsequent cells.

(h) Cathodes placed in cell dry, later flooded with electrolyte.

(i) Active organic cathode material was hexachloromelamine.

TABLE 4-2
POLARIZATION AND IMPEDANCE DATA OF ORGANIC CATHODE -
LITHIUM ANODE CELLS

Cell No.	Impedance (ohms)		Voltage (V)									
	Initial	Final	Unpolarized	1.0 mA/cm ²	2.0 mA/cm ²	3.0 mA/cm ²	4.0 mA/cm ²	5.0 mA/cm ²	6.0 mA/cm ²	7.0 mA/cm ²		
P-6	250	115	3.07	2.00								
P-7	75	70	3.07	2.17	1.44							
P-10	667	20	3.21	2.62	2.23	2.12	1.89	1.65				
P-11(a)	113	9	3.20	2.65	2.29	2.20	2.09	1.97	1.51	0.95		
PP-2	1000	24	3.07	2.02	1.82	1.58						
PP-3	525	200	3.05	1.74	1.31							
PP-4	500	180	3.06	1.91	1.58	0.86						
PP-5	256	60	3.16	2.31	2.26	2.20						
PP-6	180	14	3.14	2.37	2.25	2.20	2.13	1.97				
PP-7	87	9	3.18	2.44	2.26	2.21	2.16	2.08	1.91			
PP-8	350	150	3.13	3.12	1.96	1.47	0.11					
PP-10	500	4	3.18	2.39	2.28	2.20	1.99					
PP-11	475	190	3.11	2.23	2.15	1.67						
PP-12	1067	170	3.16	2.25	1.95	1.49	0.60					
PP-13	290	30	3.17	2.33	2.25	2.18	2.07	0.32				
PP-14	31	9	3.18	2.28	2.11	1.86	1.54					
PP-18	950	88	3.12	2.42	2.18	2.03	1.72	1.36	1.59			
PP-19	370	12	3.07	2.46	2.28	2.20	2.10	1.92				
PP-20	200	26	3.06	2.55	2.22	2.09	1.84	1.70	0.78			
PP-21(a)	155	11	3.16	3.60	2.24	2.13	2.02	1.87	1.32			
P-22(a)	238	20	3.11	2.57	2.37	2.19	1.96	1.68	0.35			
P-23	103	58	3.23	2.59	2.29	2.05	1.53	0.59				
PP-24	840	286	3.12	2.25	1.67							
PP-25	571	250	3.03	0.73								
PP-26	185	103	3.06									
PP-27	667	271	3.07	2.25	1.06							
PP-28(a,c)	525	250	3.18	2.24	1.54							
PP-29(a,c)	450	78	3.08	2.05	1.74	1.48	1.18					
PP-30	120	8	3.10	2.60	2.42	2.27	1.93	1.72	1.35			
PP-31	127	34	2.96	2.33	1.61	1.31						

TABLE 4-2
POLARIZATION AND IMPEDANCE DATA OF ORGANIC CATHODE -
LITHIUM ANODE CELLS (Continued)

Cell No.	Impedance (ohms)		Voltage (V)						
	Initial	Final	Unpolarized	1.0 mA/cm ²					
				2.0 mA/cm ²	3.0 mA/cm ²	4.0 mA/cm ²	5.0 mA/cm ²	6.0 mA/cm ²	7.0 mA/cm ²
				AFTER 5 DAYS					
P-6	12	13	2.82	2.27	2.09	1.72			
P-7	67	85	2.72						
P-10	550	220	2.89	1.54	0.81				
P-11(a)	1467	440	2.87	1.60	1.10	0.59			
PP-2	67	90	2.92	1.89					
PP-3	105	185	2.90	1.72					
PP-4	550	155	2.78	1.75	0.56				
PP-5	620	925	2.78	1.47					
PP-6	1000	300	2.83	1.82	1.59	1.17			
PP-7	950	90	2.85	1.84	1.47	0.38			
PP-10	2300	733	2.89	1.29	1.53				
PP-11	800	2000	2.88	1.85	1.13				
PP-12	667	73	2.90	1.76	1.17				
PP-13	667	83	2.93	1.82	1.00				
PP-14	8	14	2.93	2.30	2.15	1.99			
PP-15	10	18	2.90	2.21	2.02	1.69			
PP-18	350	73	2.90	1.99	1.50	1.05			
PP-19	2100	286	2.87	1.68	1.43	1.07	0.15		
PP-20	98	100	2.81	1.82					
PP-21(a)	314	210	2.90	2.00	1.40	0.97	0.44		
PP-22(a)	300	150	2.87	1.66	0.83				
PP-23	677	244	2.86	1.33					
PP-24	21	28	2.97	1.90					
PP-25	20	28	2.95	1.74					
PP-26	18	29	3.02	1.85					
PP-27	70	70	3.01	1.69					
PP-28(a,c)	3800	1900	2.35						
PP-29(a,c)	55	63	2.81	1.62	1.20	0.58			
PP-30(d)	583	220	2.775	1.90	1.67	1.34			
PP-31(a)	48	40	2.96	1.91	1.04				

TABLE 4-2
POLARIZATION AND IMPEDANCE DATA OF ORGANIC CATHODE -
LITHIUM ANODE CELLS (Continued)

Cell No.	Impedance (ohms)		Voltage (V)							
	Initial	Final	UnPolarized	1.0 mA/cm ²	2.0 mA/cm ²	3.0 mA/cm ²	4.0 mA/cm ²	5.0 mA/cm ²	6.0 mA/cm ²	7.0 mA/cm ²
<u>AFTER 12 DAYS</u>										
P-10	1050	200	2.91	1.55	0.79					
P-11(a)	1050	1300	2.90	1.70	1.26	0.84				
PP-18	2100	667	2.88	1.68	1.00					
PP-19	2000	1000	2.84	1.31						
PP-20	363	363	2.75							
PP-21(a)	950	463	2.87	1.68	1.26	0.89	0.45			
PP-22(a)	475	180	2.87	1.55	0.71					
PP-23	840	350	2.84	1.54	0.63					
PP-24	25	45	2.94	1.87						
PP-25	24	45	2.85	1.40						
PP-26	32	40	3.01	0.79						
PP-27	16	40	3.04	1.91						
<u>AFTER 19 DAYS</u>										
P-10	2000	500	2.91	1.55	0.82					
P-11(a)	2000	1000	2.89	1.64	1.13	0.55				
PP-14(b)	10	23	3.01	2.29	2.03	1.77				
PP-15(b)	17	27	2.94	2.08	1.58	0.48				
PP-18	4400	1050	2.89	1.35						
PP-19	2200	2100	2.86	1.34						
PP-20	629	325	2.81	1.82						
PP-21(a)	2200	667	1.66	1.23	0.84	0.23				
PP-22(a)	1050	400	2.83	1.29	0.23					
PP-23	925	463	2.83	1.57	0.82					
PP-24	62	189	2.92	1.87						
PP-25	38	47	2.82	1.41						
PP-26	38	53	3.00	0.53						

(a) 1,1,1-Trichloroethane was not used in the lithium anode cleaning process. (d) Tested after 3 days.
 (b) Tested at 18 instead of 19 days. (e) Tested after 1 day.
 (c) Individual electrode studies.
 NOTE: Cells P-8, P-9, PP-16, PP-17 were used for discharge test rather than polarization tests.
 Cell PP-9 was not run because the cathode degraded physically when soaked in the electrolyte solution.

TABLE 4-3
VISUAL INSPECTION OF CELL COMPONENTS

Cell No.	<u>Cathode Structural Integrity</u>	
	Initial	Final
P-6	Paste	Intact; moist
P-7	Paste	Intact; moist
P-8	Paste	Intact; moist
P-9	Paste	Intact; moist
P-10	Paste	Intact; moist
P-11	Paste	Contained cracks and crevices; relatively dry
PP-2	Good	Intact; moist
PP-3	Good	Intact; moist
PP-4	Good	Intact; moist
PP-5	Fragile	Intact; slightly moist
PP-6	Good	Intact; very slightly moist
PP-7	Good	Intact; moist
PP-8	Good	Intact; moist
PP-9	Fragile	Not run; disintegrated
PP-10	Good	Intact; moist
PP-11	Good	Intact; slightly moist
PP-12	Good	Intact; moist
PP-13	Good	Intact; moist
PP-14	Good	Intact; slightly moist
PP-15	Good	Intact; slightly moist
PP-16	Good	Intact; moist

TABLE 4-3
VISUAL INSPECTION OF CELL COMPONENTS (Continued)

Cell No.	<u>Cathode Structural Integrity</u>	
	Initial	Final
PP-17	Good	Intact; moist
PP-18	Good	Intact; moist
PP-19	Good	Intact; moist
PP-20	Good	Intact; very slightly moist
PP-21	Good	Intact; moist
PP-22	Good	Intact; very slightly moist
PP-23	Fair	Intact; slightly moist
PP-24	Good	Intact; moist
PP-25	Fair	Intact; moist
PP-26	Fair	Intact; moist
PP-27	Fair	Intact; moist
PP-28	Good	Intact; periphery moist center only slightly moist
PP-29	Good	Intact; moist
PP-30	Fragile	Intact; moist
PP-31	Good	Intact; slightly moist

Two paste cathodes were tested first, one in PC-LiClO₄ solution and the other in PC-TPAP solution. The results shown in Figures 4-1 and 4-2 respectively, indicate that the cathode in PC-LiClO₄ performed better both initially and after five days (Table 4-2). Therefore, screening was continued only with the PC-LiClO₄ electrolyte solution.

The data in Table 4-2 and Figures 4-5 through 4-15 (cells PP-2 through PP-13) definitely show that the wet cathodes out-perform the corresponding dry cathodes. This effect can partly be explained by the absorption of electrolyte solution by the dry cathodes from the separator which causes partial drying of the separator. Loss of electrolyte solution in the separators was observed when the cells were disassembled at the end of the test period. In general, separators in the dry cathode cells appeared to have lost more solution than those in cells with wet cathodes. The difference between the performance of wet and dry cathodes was not as evident for cathodes pressed at 5,000 psi (or 15,000 psi).

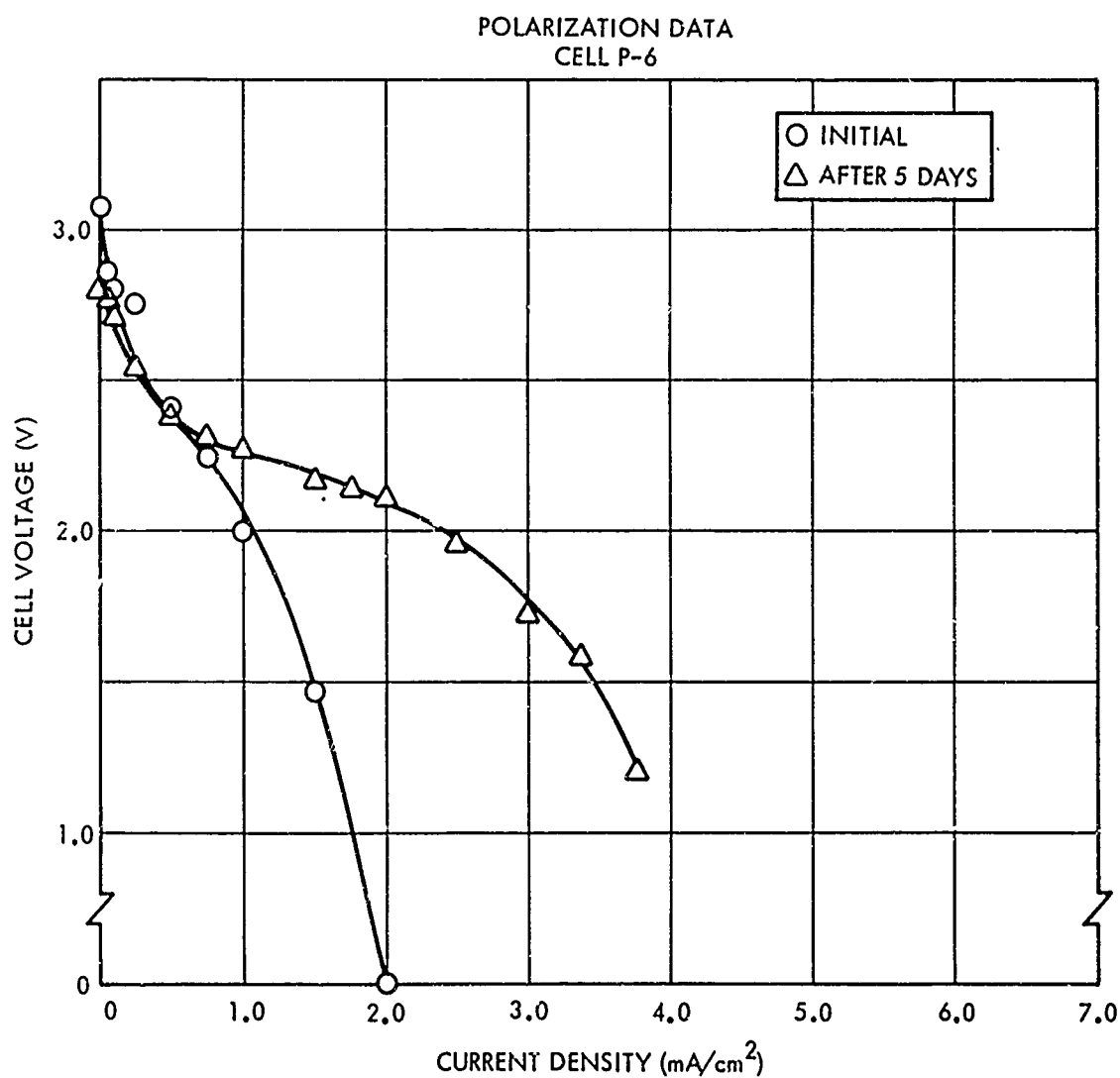


Figure 4-1. Polarization Data for Cell P-6. Paste cathode containing 1.5 g each of m-DNB and carbon.

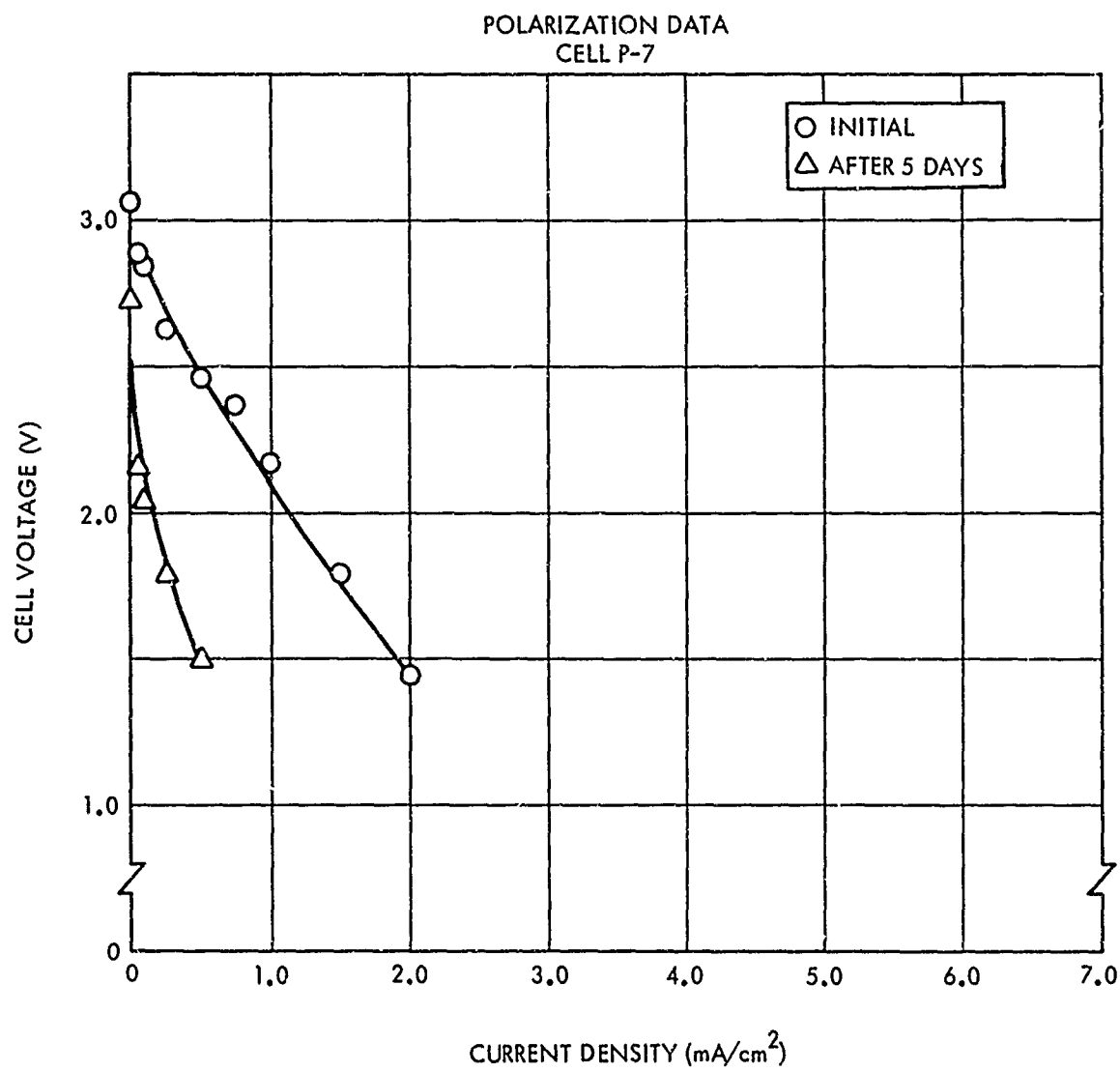


Figure 4-2. Polarization Data for Cell P-7. Paste cathode containing 1.5 g each of m-DNB and carbon.

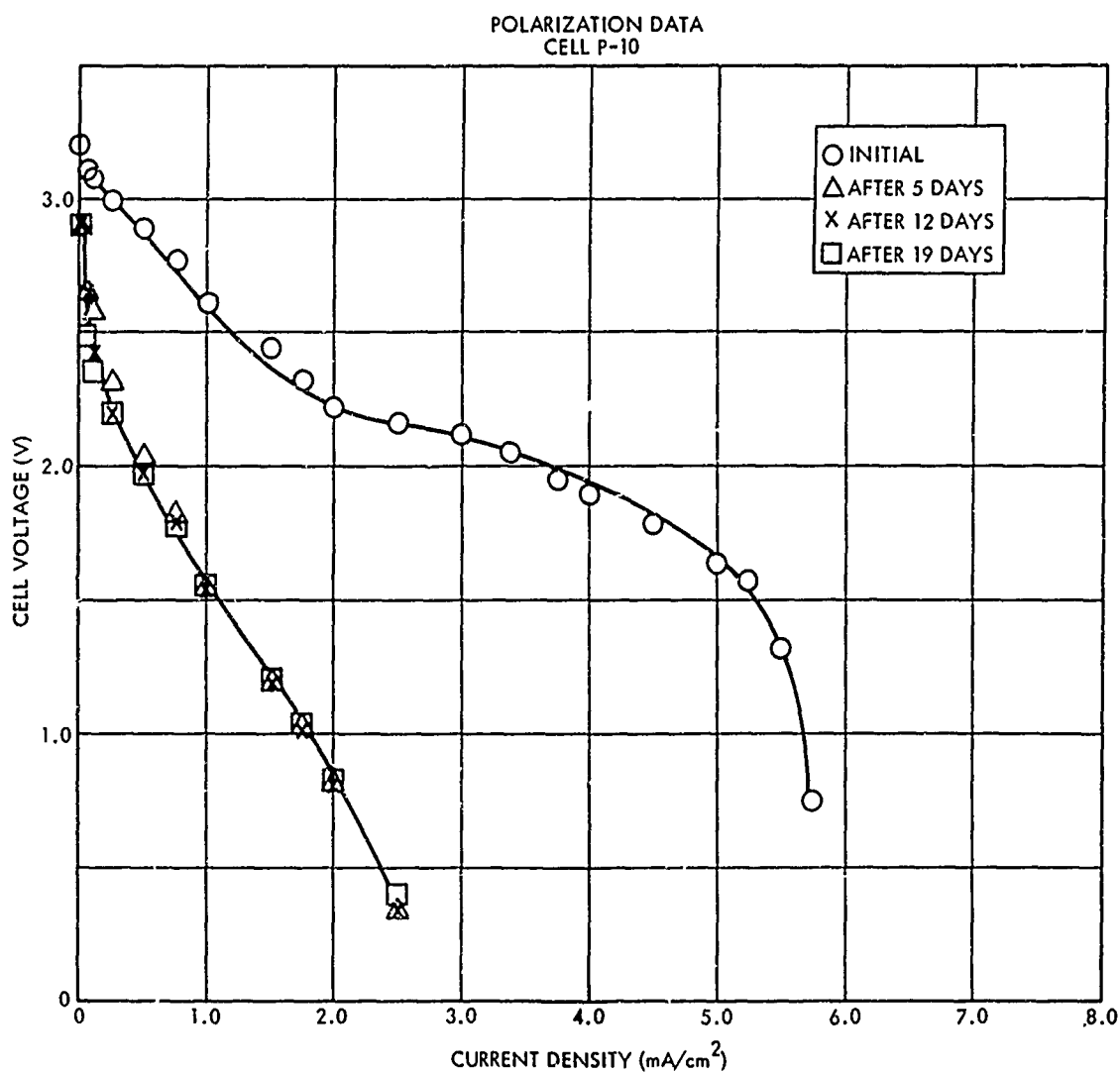


Figure 4-3. Polarization Data for Cell P-10. Paste cathode containing 1.5 g each of m-DNB and carbon.

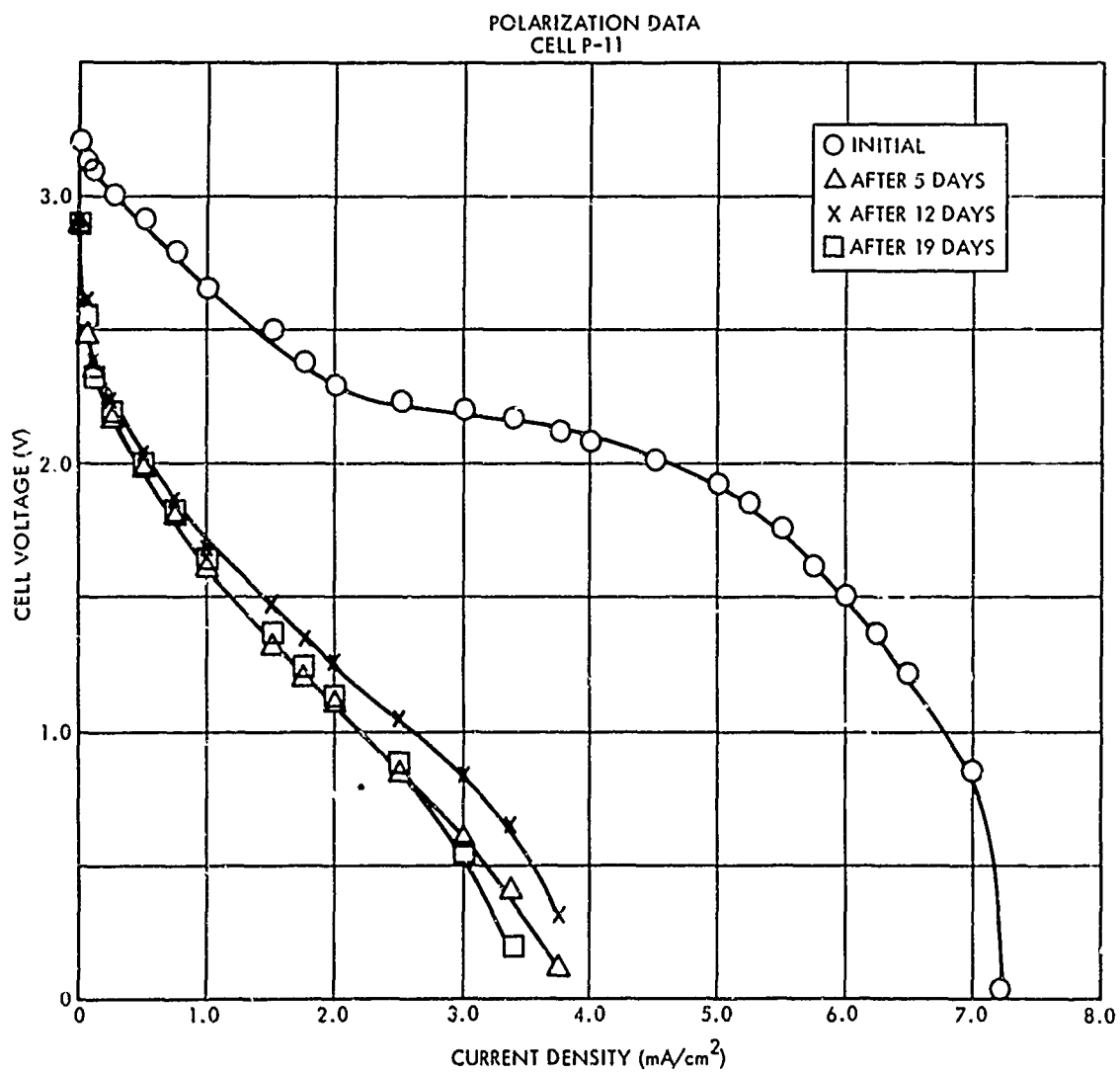


Figure 4-4. Polarization Data for Cell P-11. Paste cathode containing 1.5 g each of *m*-DNB, and carbon.

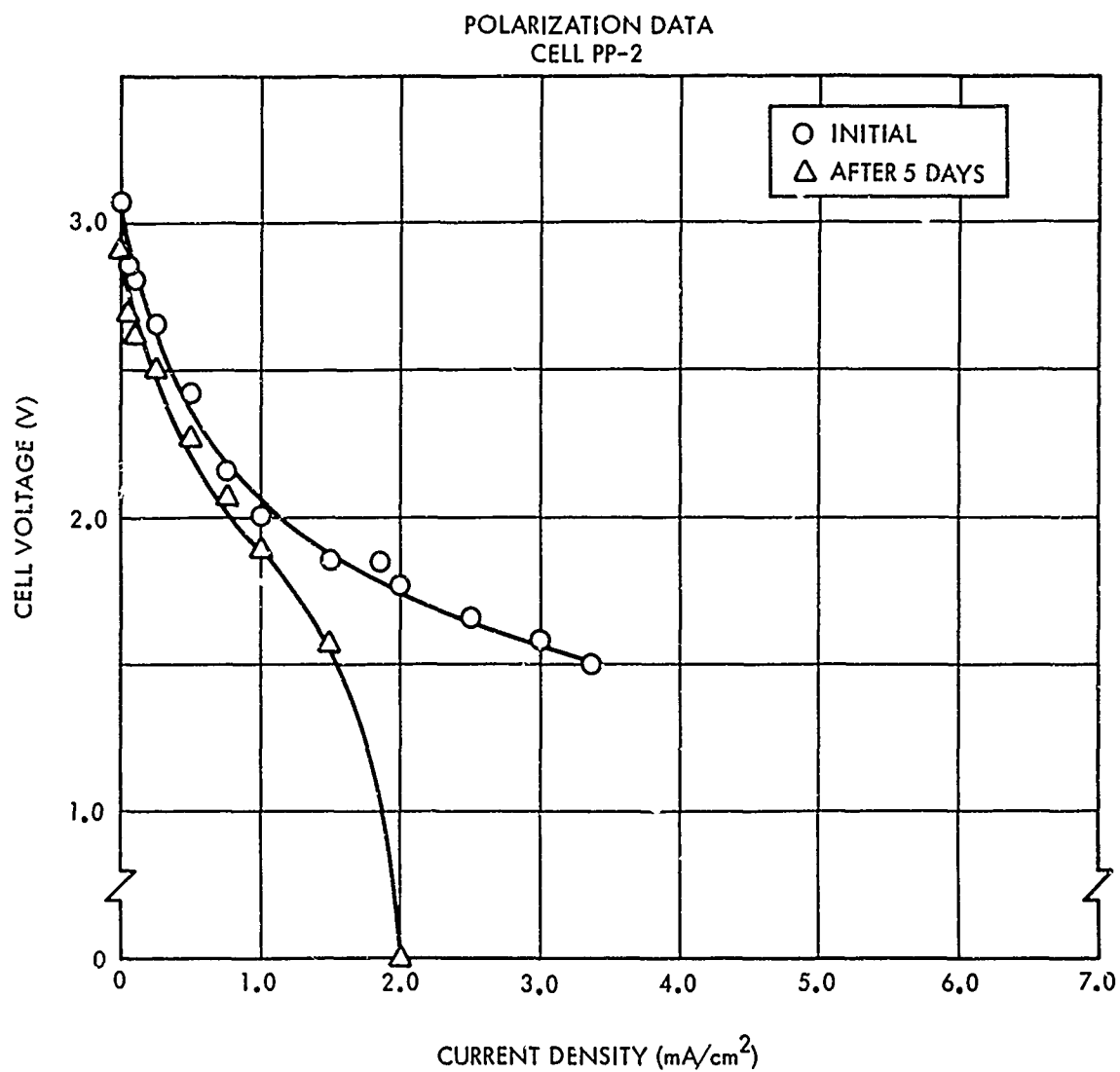


Figure 4-5. Polarization Data for Cell PP-2. Pressed cathode (10,000 psi) containing 1.5 g each of m-DNB and carbon and 5% acrylic and tested in the dry state.

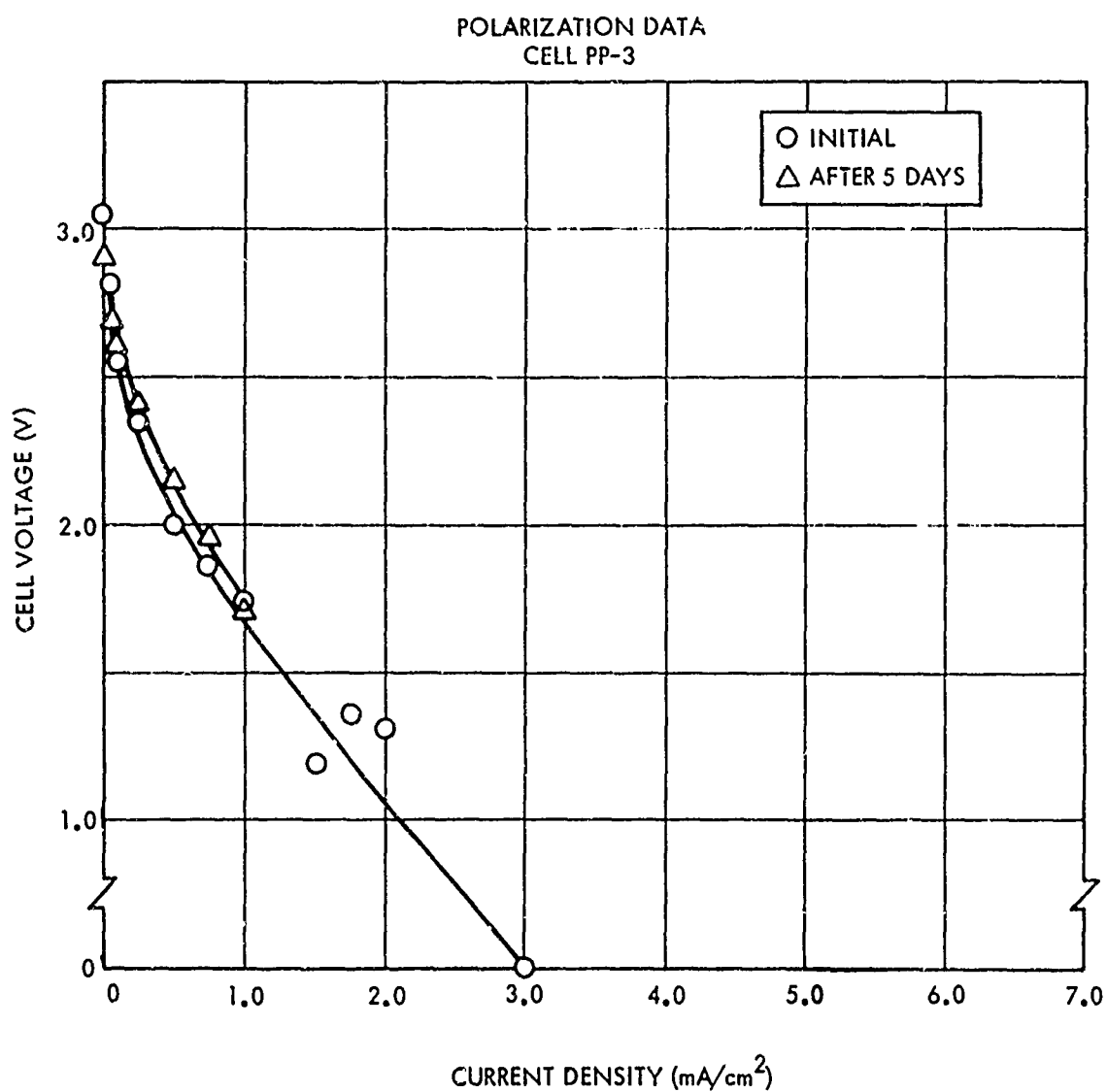


Figure 4-6. Polarization Data for Cell PP-3. Pressed cathode (10,000 psi) containing 1.5 g each of m-DNB and carbon and 2.5% acrylic and tested in the dry state.

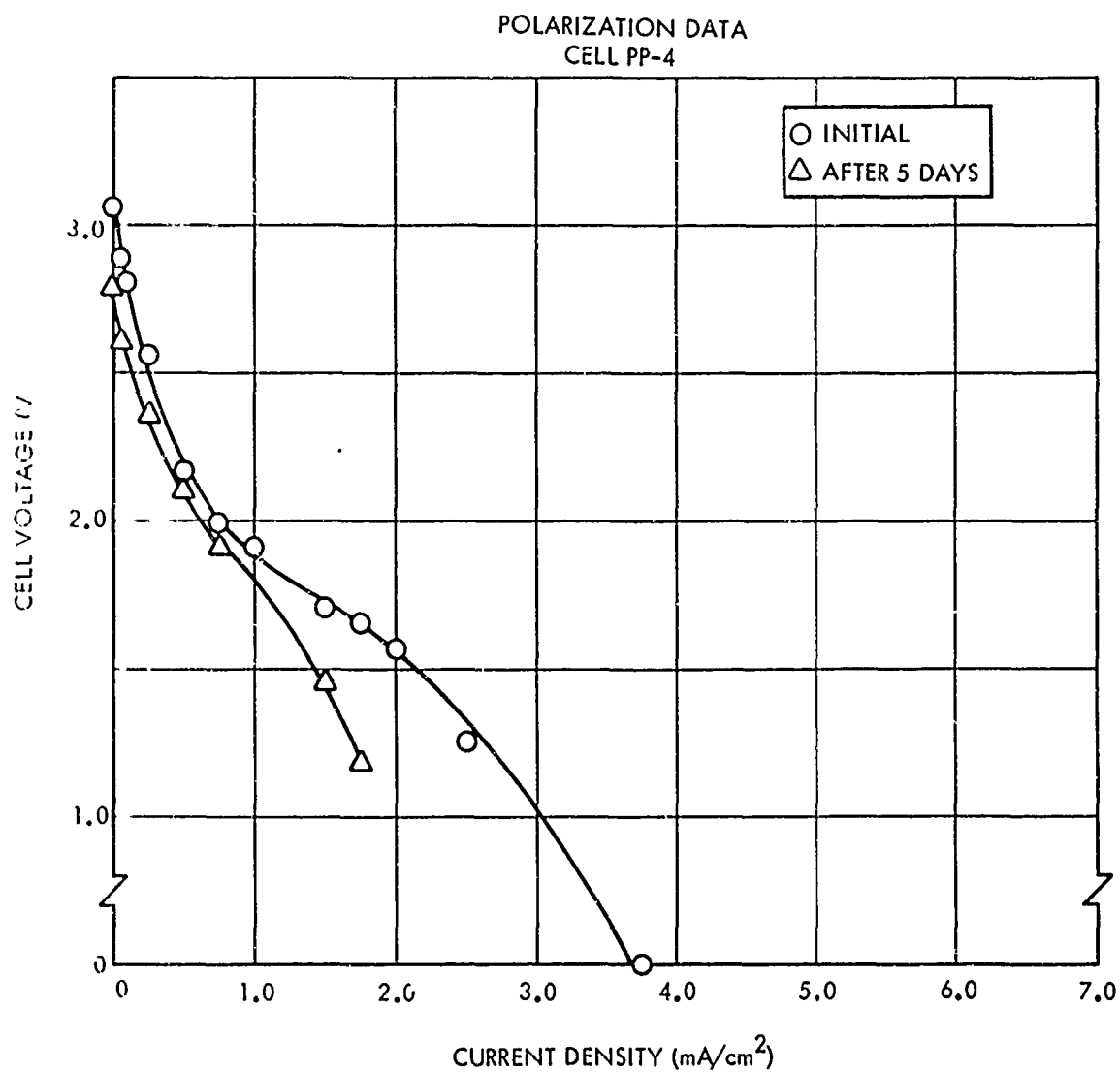


Figure 4-7. Polarization Data for Cell PP-4. Pressed cathode (10,000 psi) containing 1 g each m-DNB and carbon and 5% acrylic and tested in the dry state.

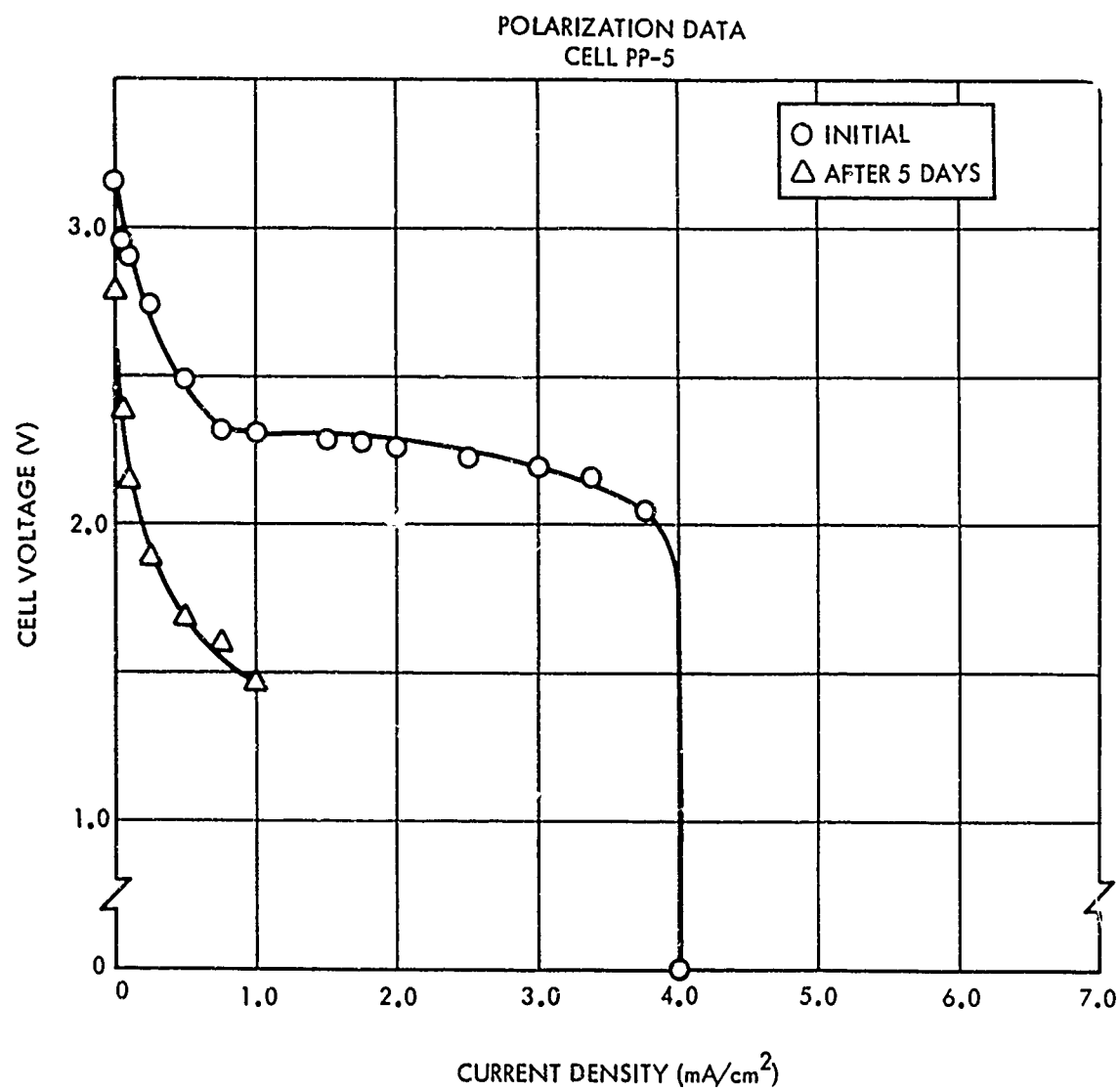


Figure 4-8. Polarization Data for Cell PP-5. Pressed cathode (10,000 psi) containing 0.5 g each m-DNB and carbon and 5% acrylic and tested in the dry state.

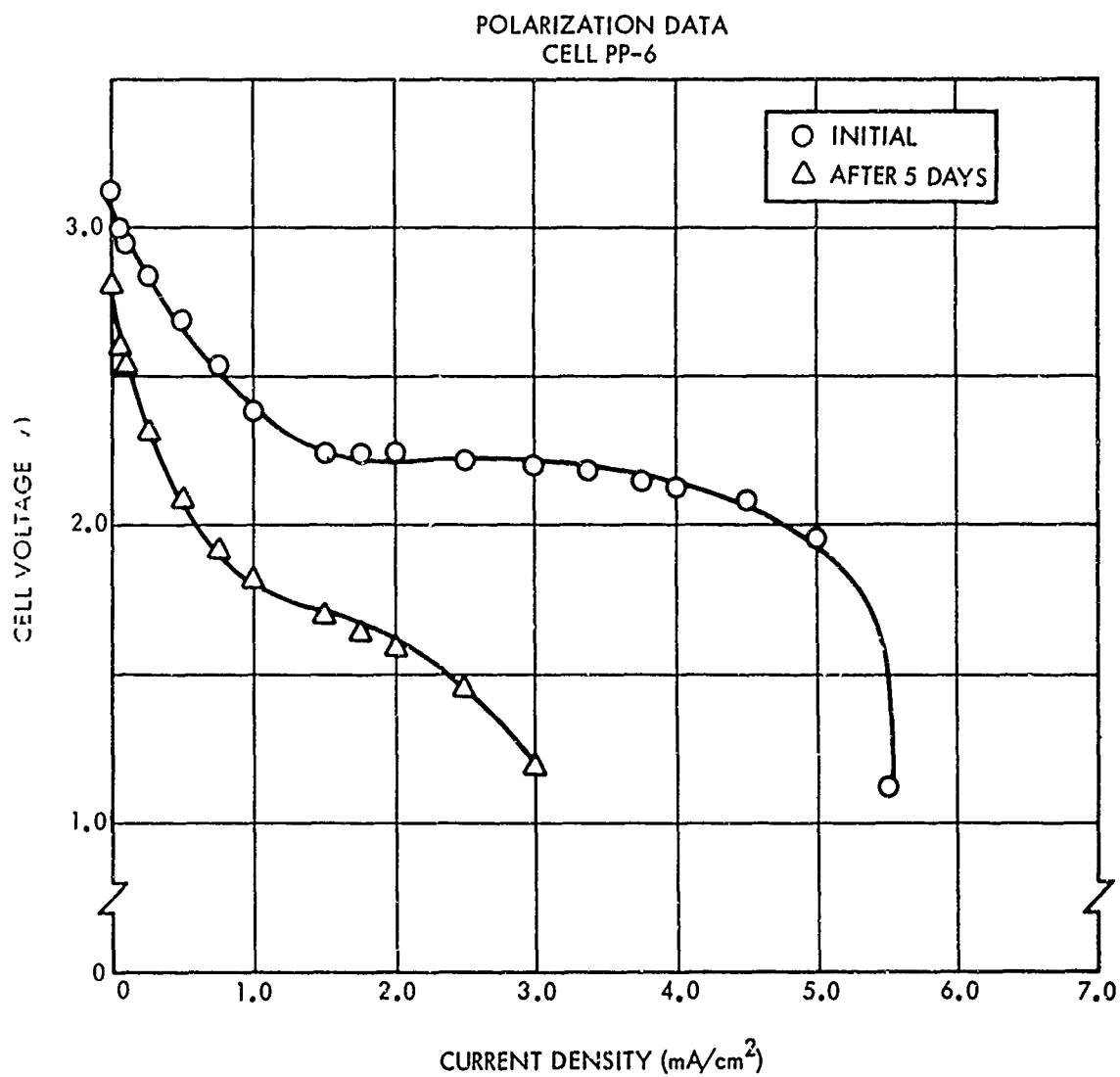


Figure 4-9. Polarization Data for Cell FP-6. Pressed cathode (10,000 psi) containing 1.5 g each m-DNB and carbon and 5% acrylic and tested in the wet state.

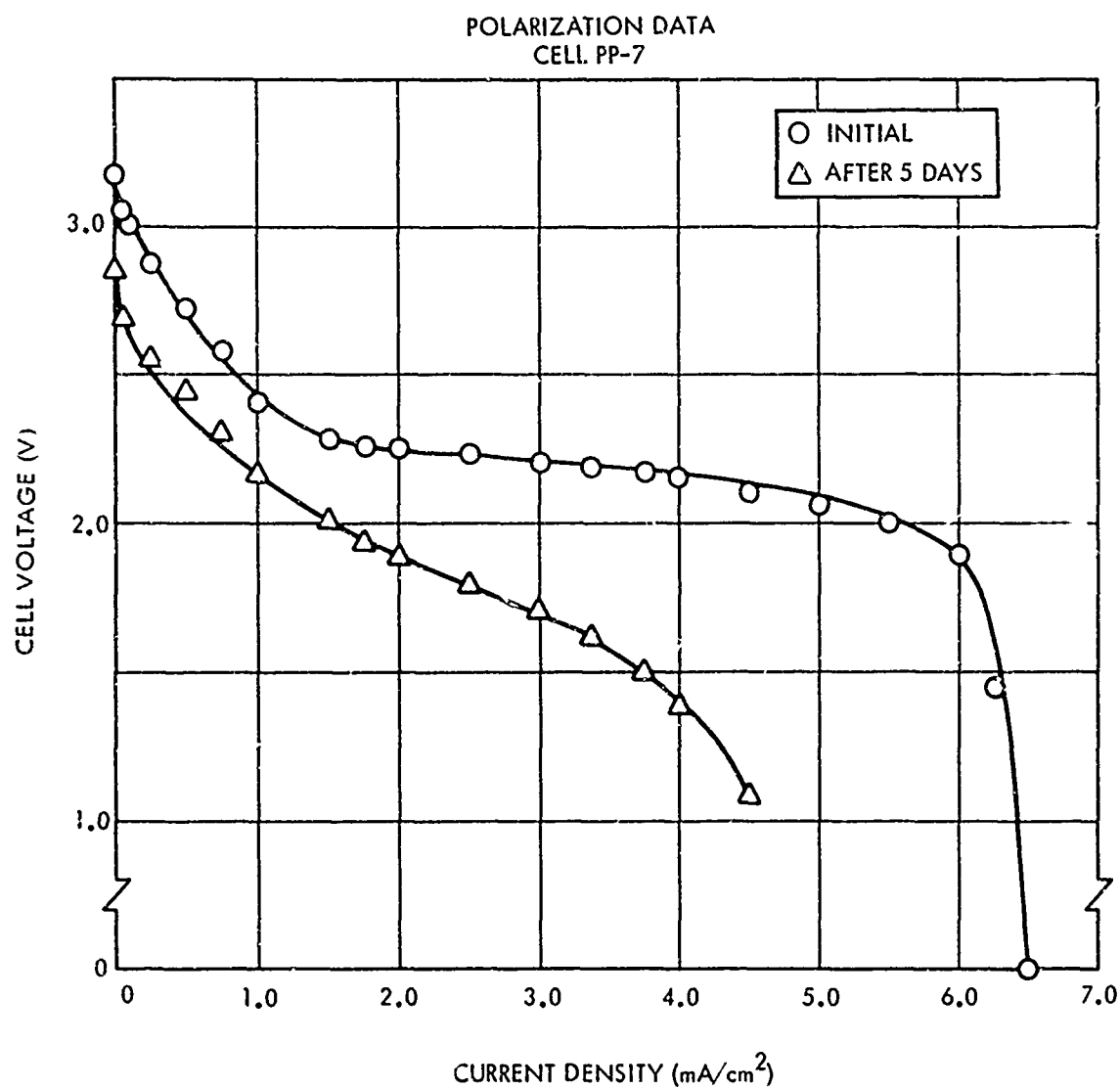


Figure 4-10. Polarization Data for Cell PP-7. Pressed cathode (10,000 psi) containing 1.5 g each *m*-DNB and carbon and 2.5% acrylic and tested in the wet state.

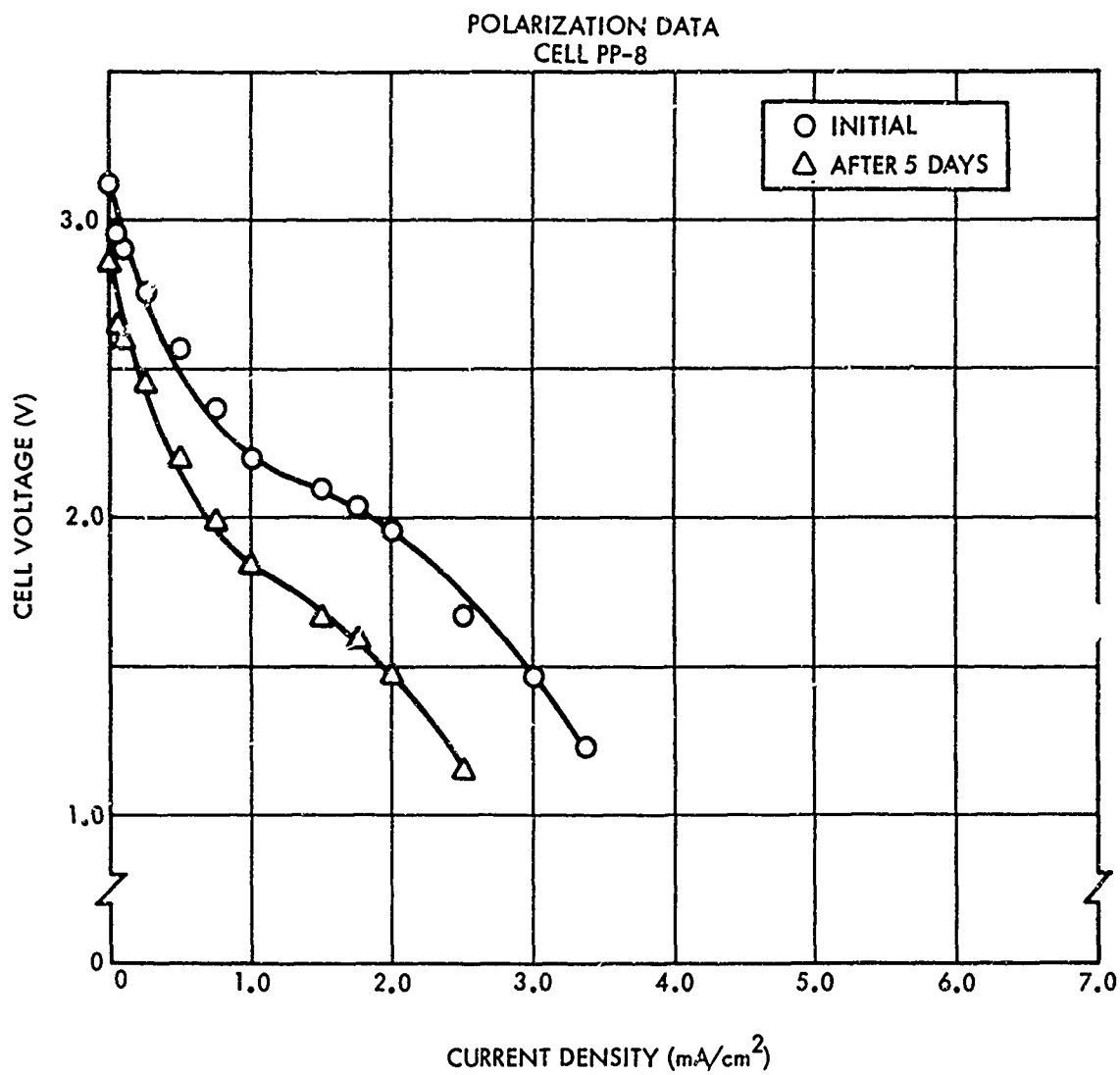


Figure 4-11. Polarization Data for Cell PP-8. Pressed cathode (10,000 psi) containing 1.5 g each m-DNB and carbon and 5% acrylic and tested in the wet state.

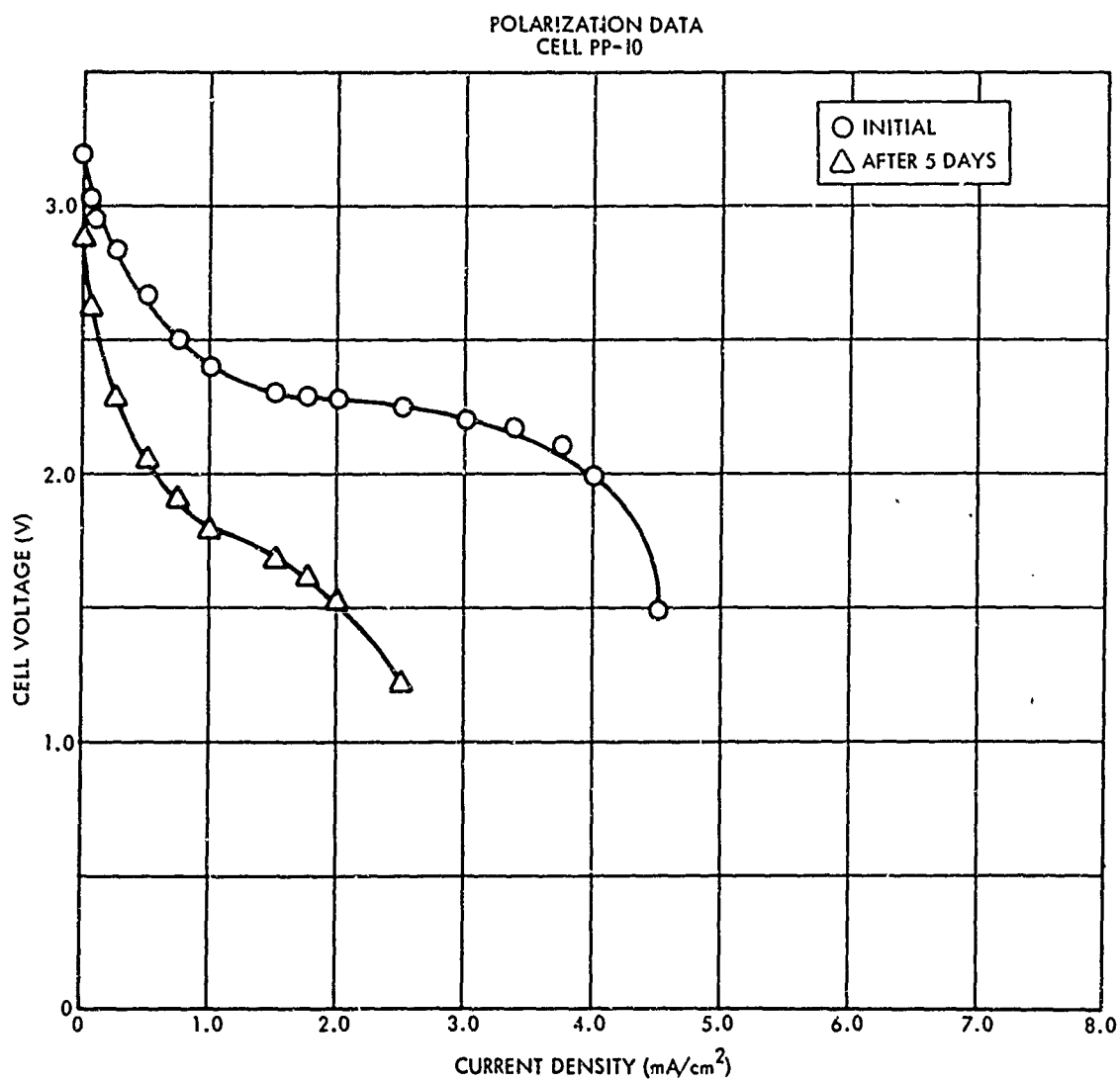


Figure 4-12. Polarization Data for Cell PP-10. Pressed cathode (5,000 psi) containing 1.5 g each m-DNB and carbon and 5% acrylic and tested in the dry state.

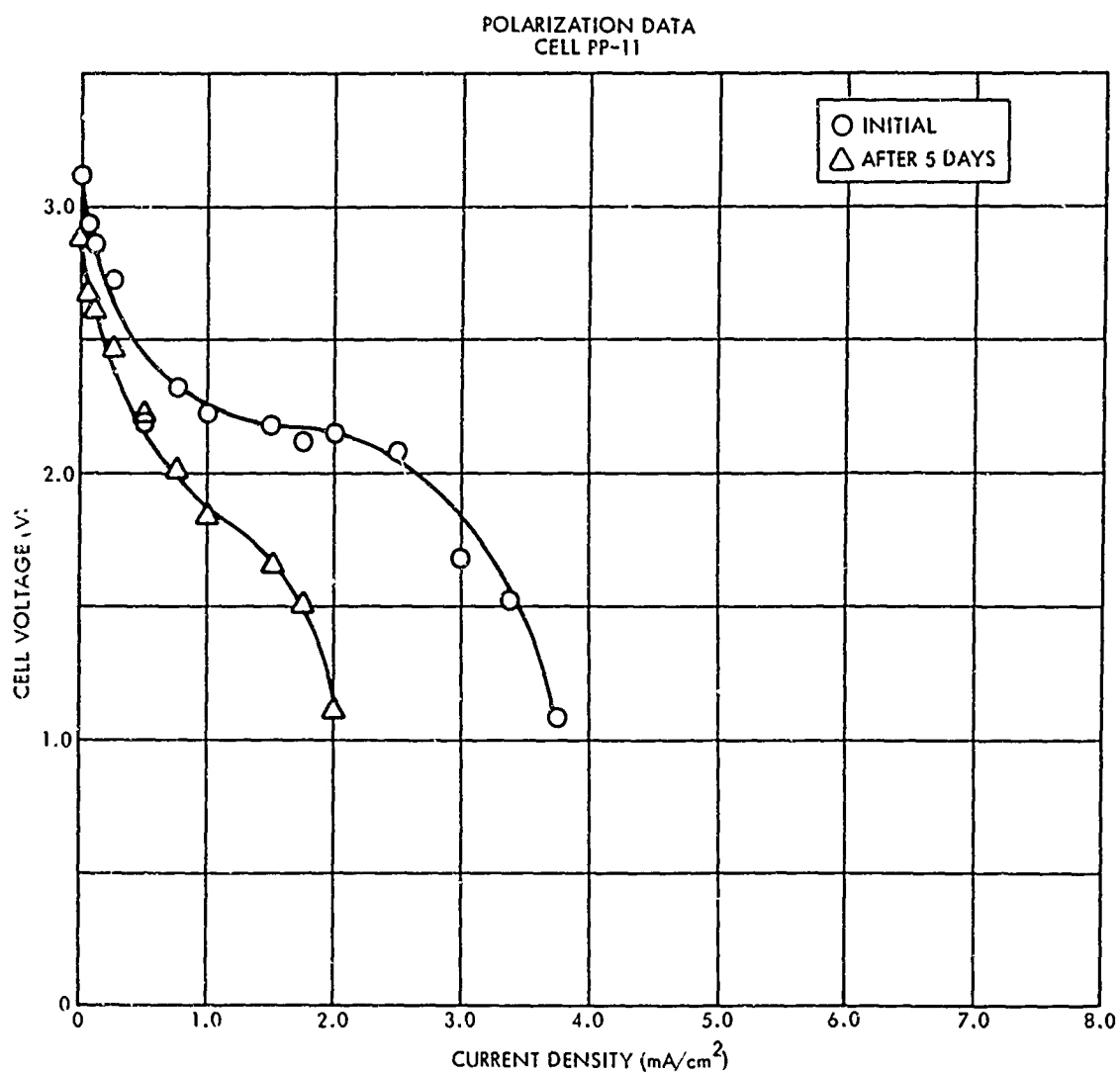


Figure 4-13. Polarization Data for Cell PP-11. Pressed cathode (15,000 psi) containing 1.5 g each m-DNB and carbon and 5% acrylic and tested in the dry state.

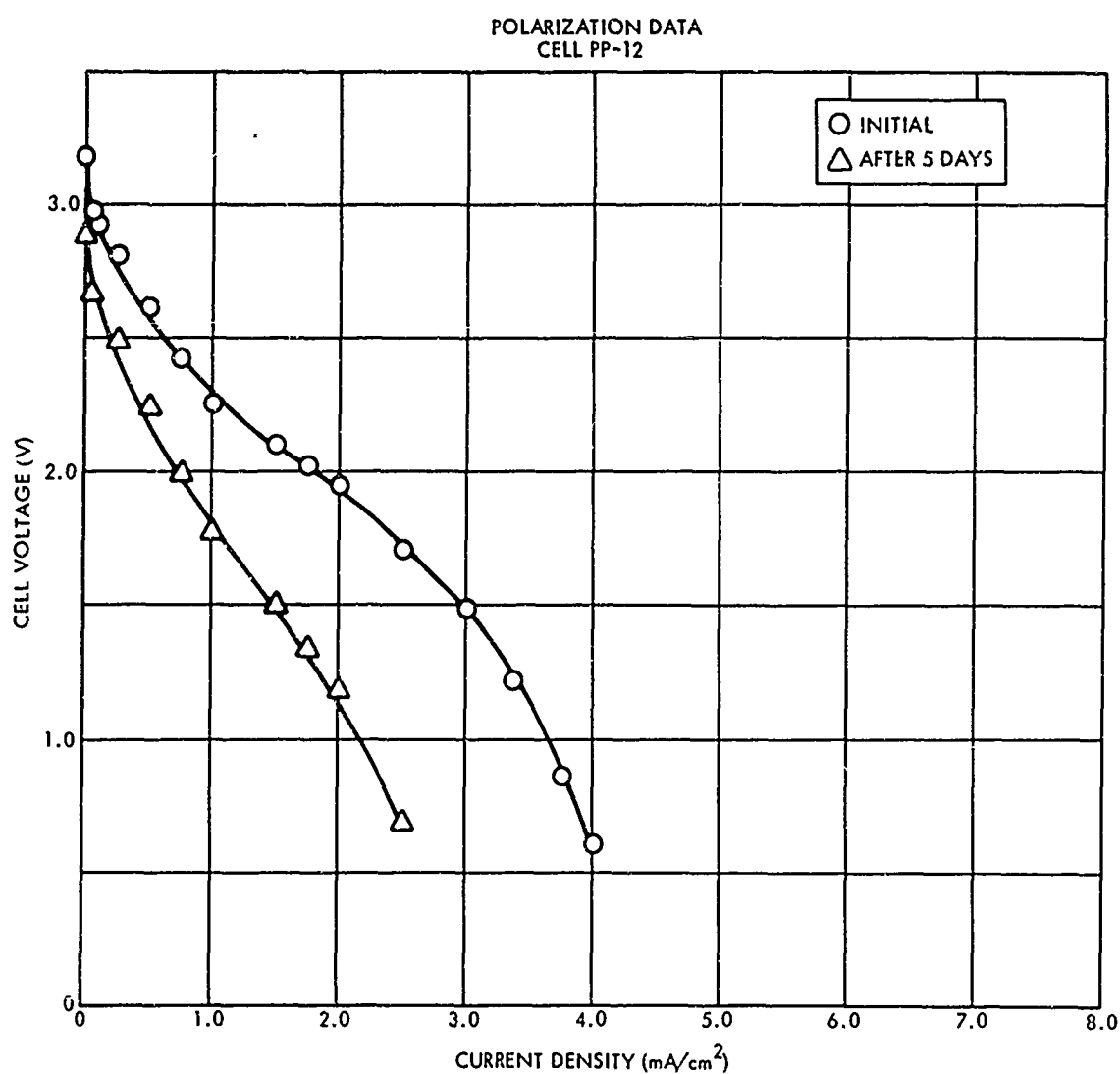


Figure 4-14. Polarization Data for Cell PP-12. Pressed cathode (5,000 psi) containing 1.5 g each m-DNB and carbon and 5% acrylic and tested in the wet state.

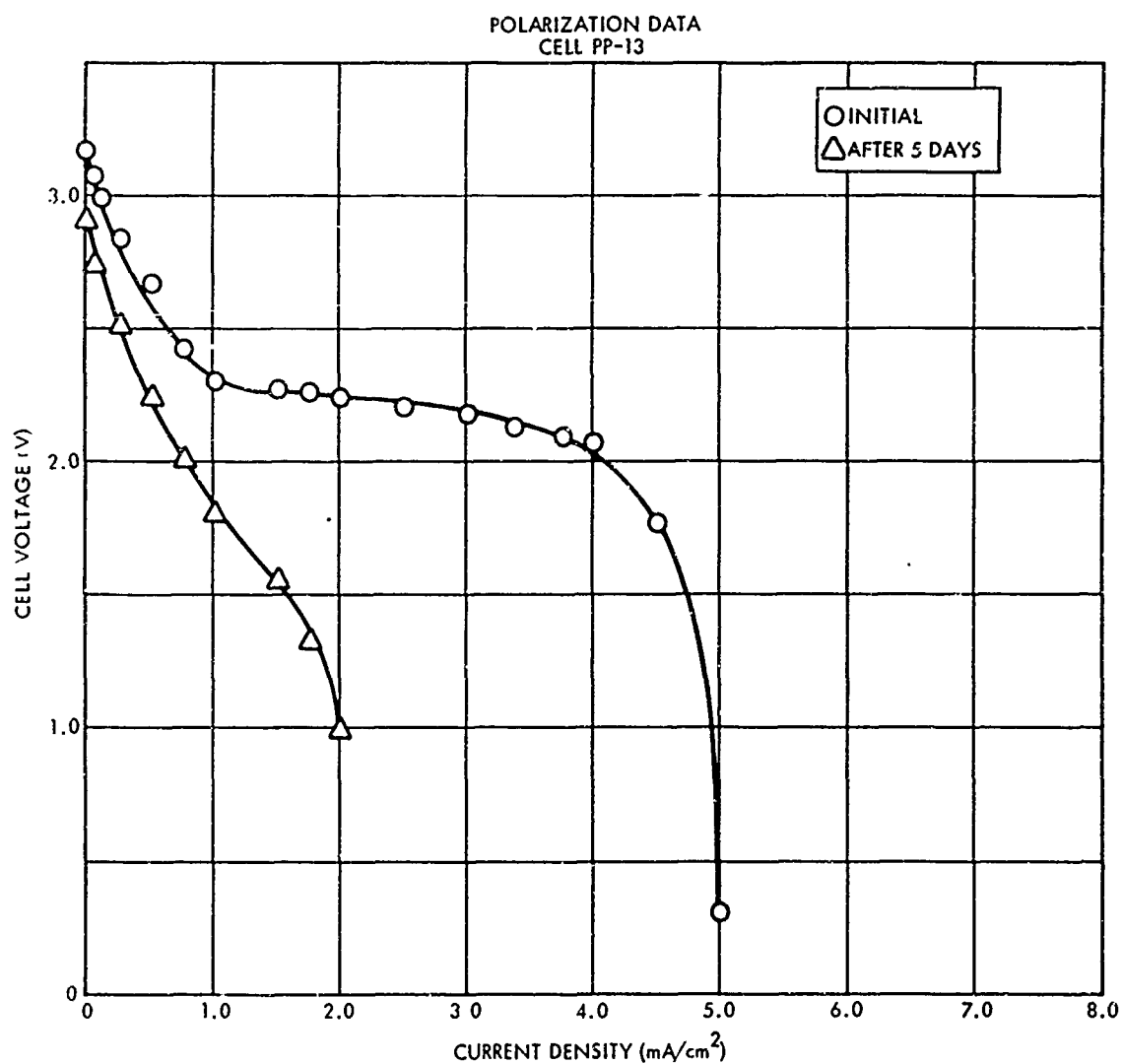


Figure 4-15. Polarization Data for Cell PP-13. Pressed cathode (15,000 psi) containing 1.5 g each m-DNB and carbon and 5% acrylic and tested in the wet state.

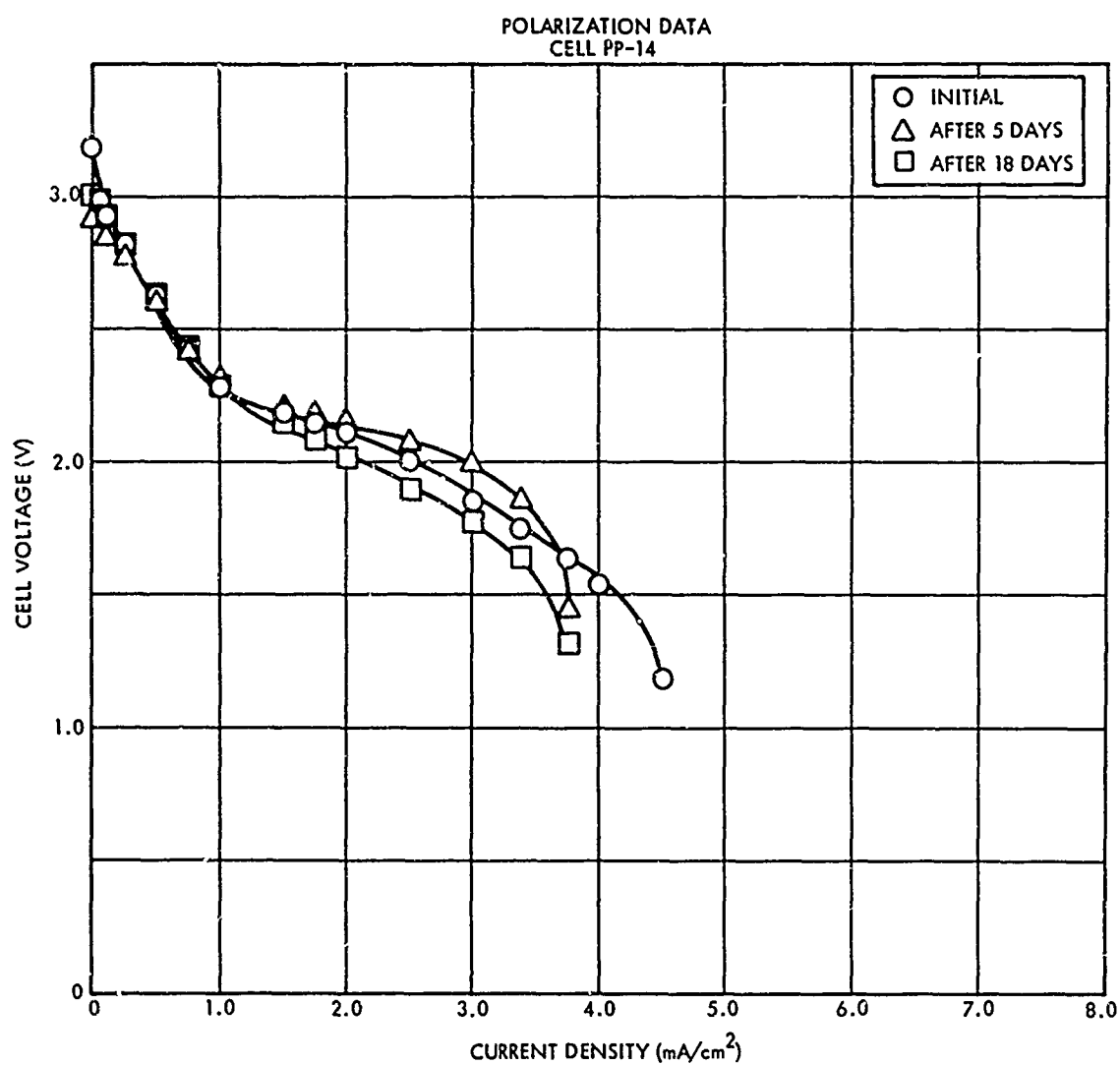


Figure 4-16. Polarization Data for Cell PP-14. Pressed cathode (10,000 psi) containing 1.5 g each m-DNB and carbon and 5% acrylic and tested in the wet state.

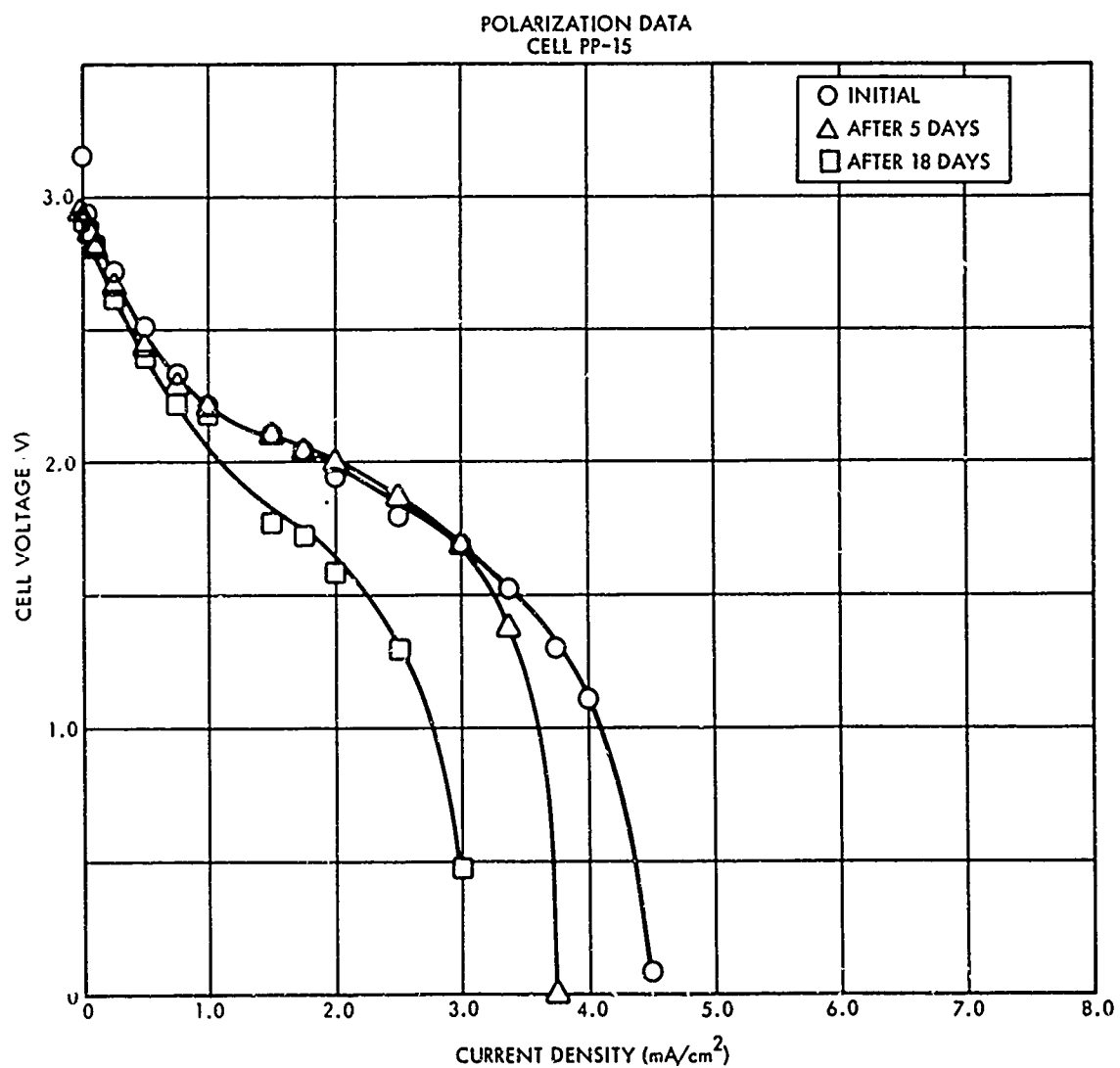


Figure 4-17. Polarization Data for Cell PP-15. Pressed cathode (20,000 psi) containing 1.5 g each m-DNB and carbon and 5% acrylic and tested in the wet state.

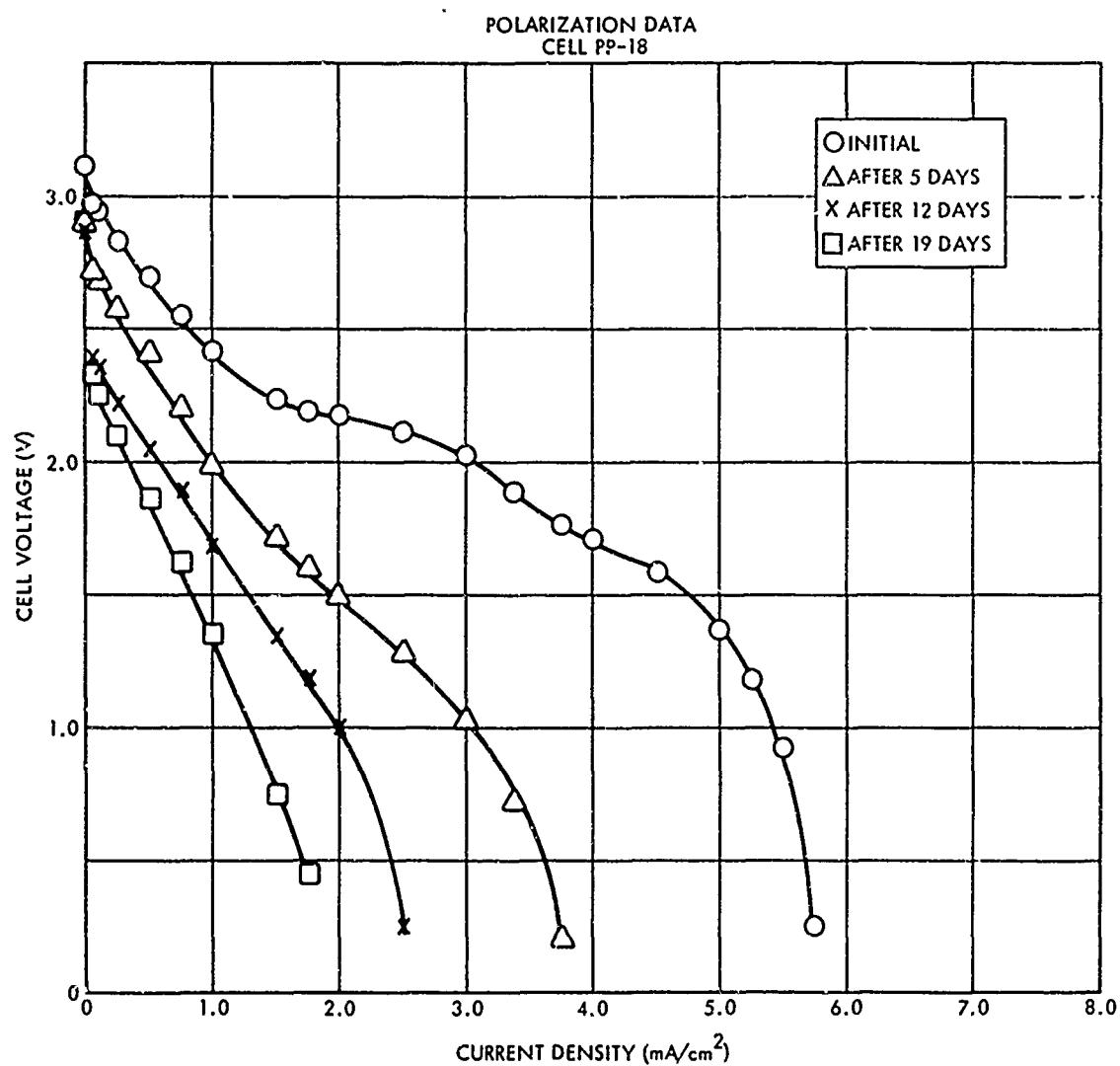


Figure 4-18. Polarization Data for Cell PP-18. Pressed cathode (10,000 psi) containing 1.5 g each m-DNB and carbon and 5% acrylic and tested in the wet state.

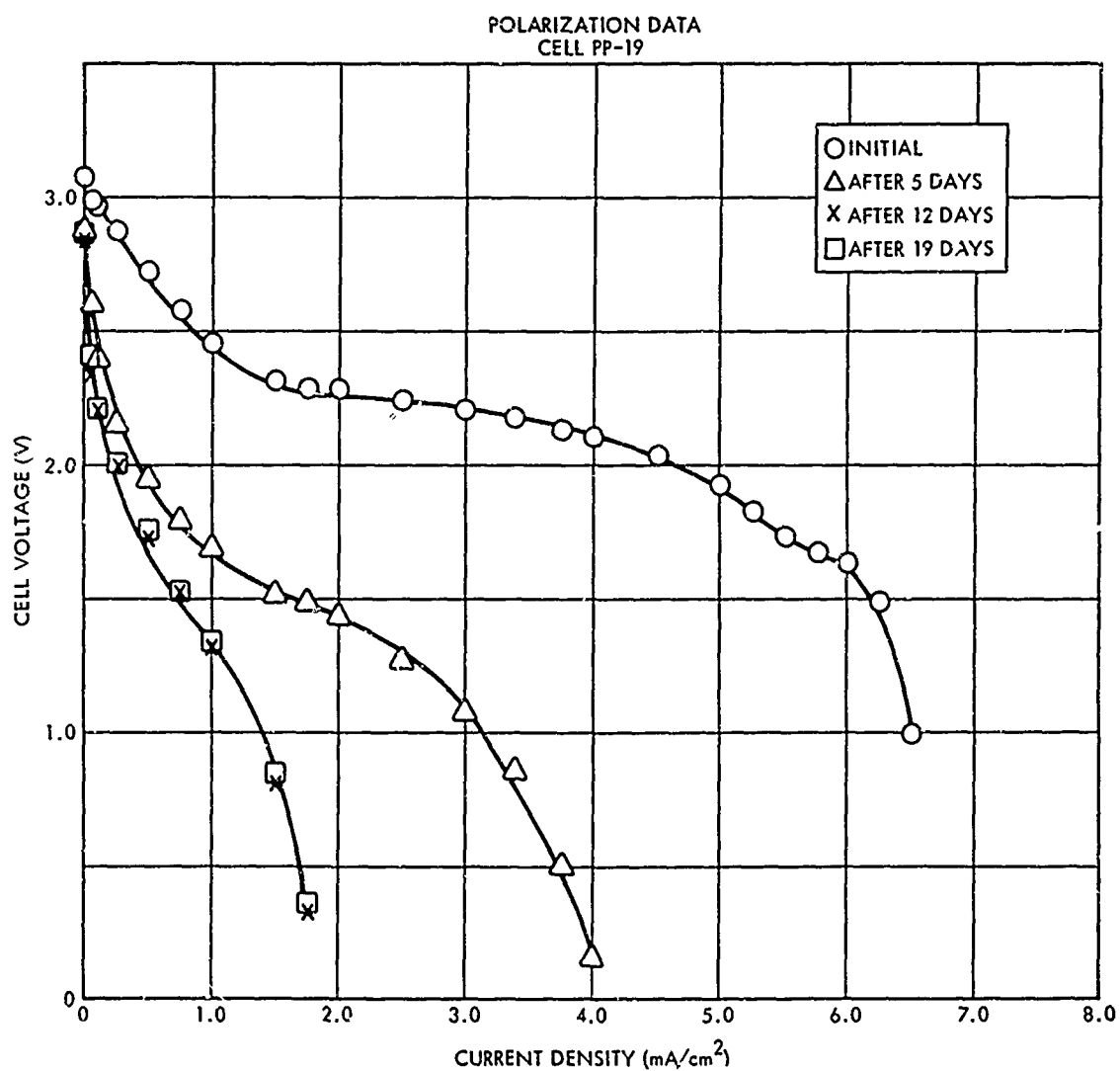


Figure 4-19. Polarization Data for Cell PP-19. Pressed cathode (10,000 psi) containing 1.5 g each m-DNB and carbon and 5% acrylic and tested in the wet state.

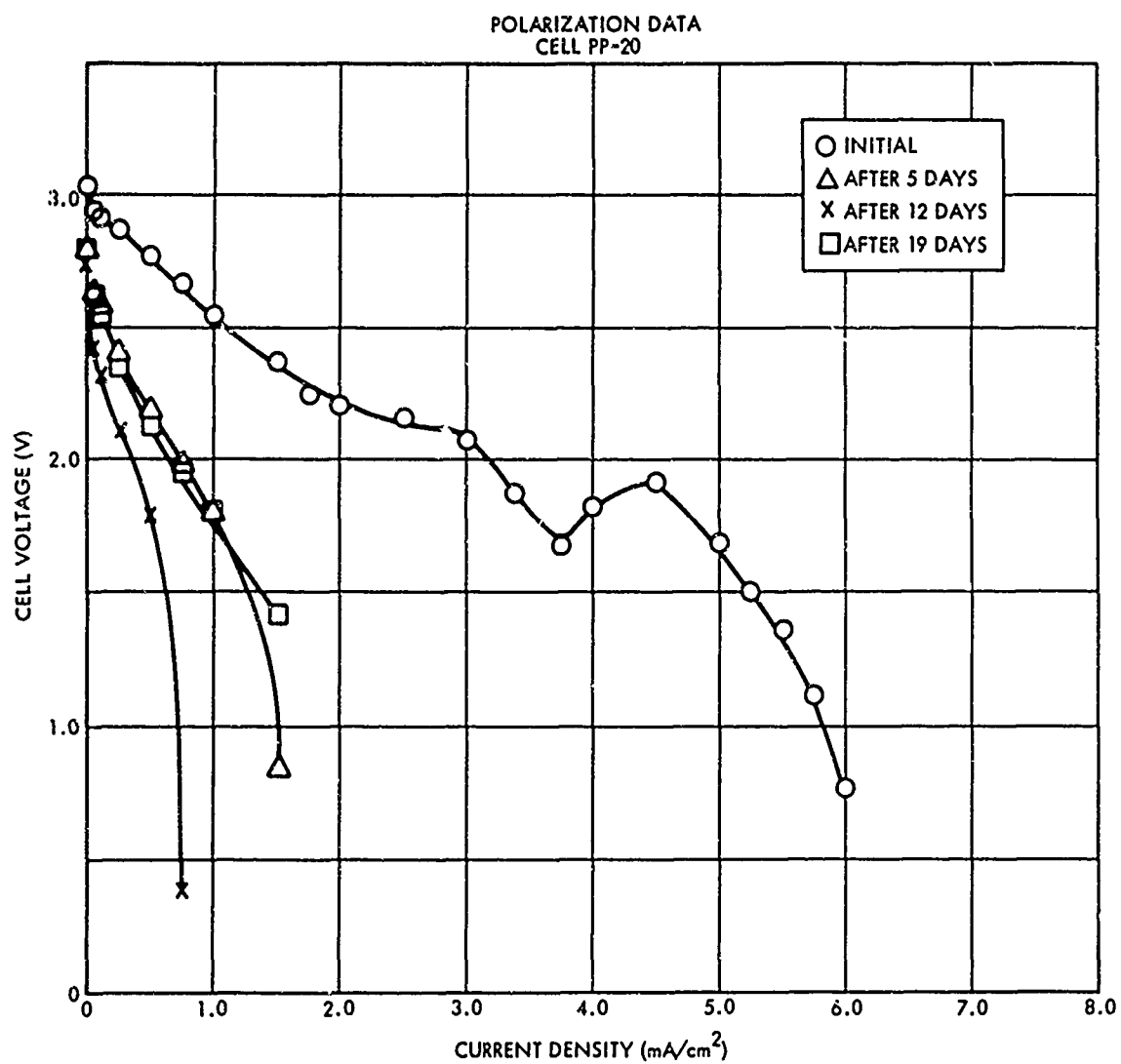


Figure 4-20. Polarization Data for Cell PP-20. Pressed cathode (10,000 psi) containing 1.5 g each m-DNB and carbon and 2.5% acrylic and tested in the wet state.

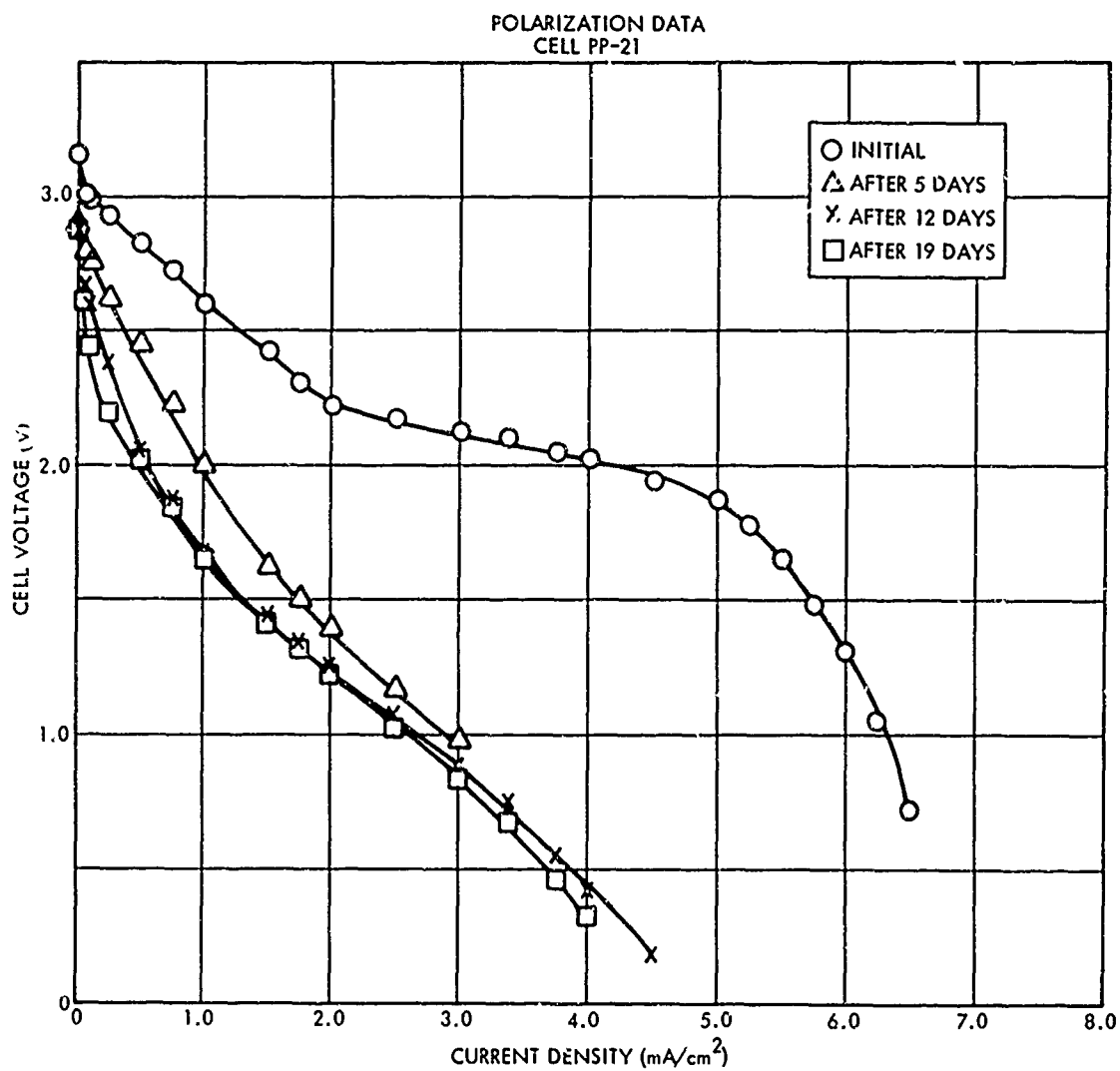


Figure 4-21. Polarization Data for Cell PP-21. Pressed cathode (10,000 psi) containing 1.5 g each m-DNB and carbon and 2.5% acrylic and tested in the wet state.

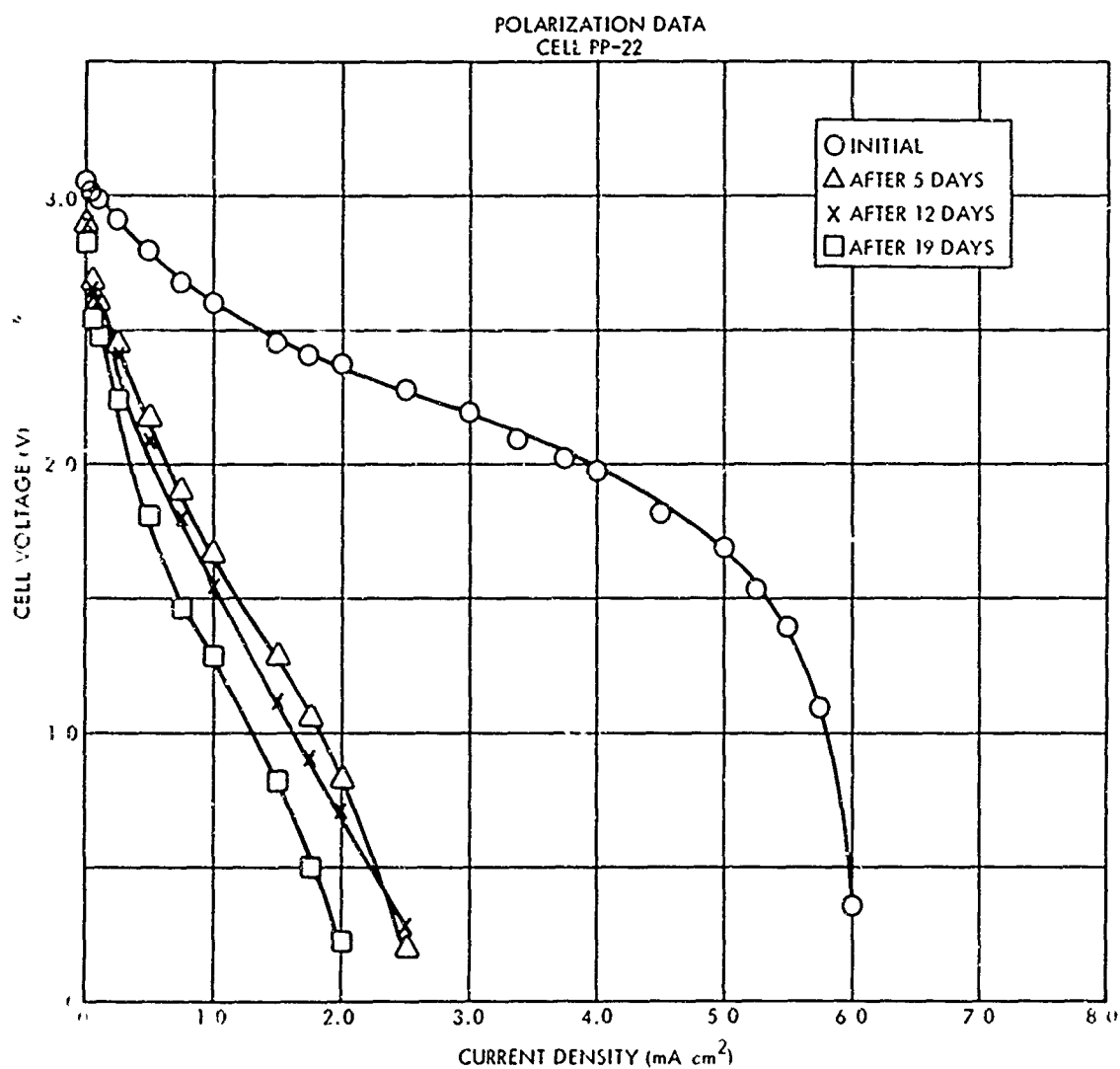


Figure 4-22. Polarization Data for Cell PP-22. Pressed cathode (10,000 psi) containing 1.5 g each m-DNB and carbon and 5% rosin and tested in the wet state.

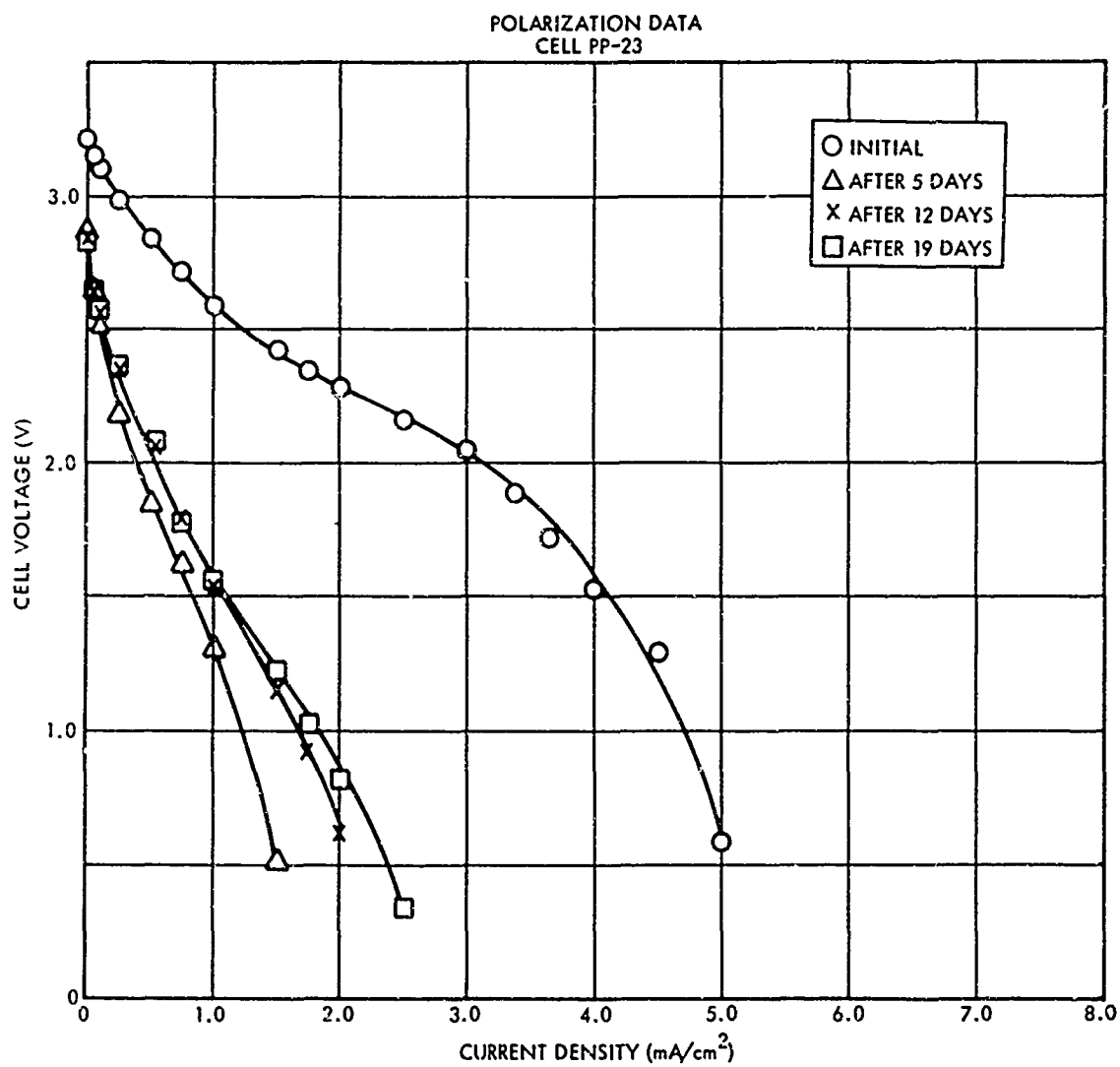


Figure 4-23. Polarization Data for Cell PP-23. Pressed cathode (10,000 psi) containing 1.5 g each m-DNB and carbon and 5% mastic gum and tested in the wet state.

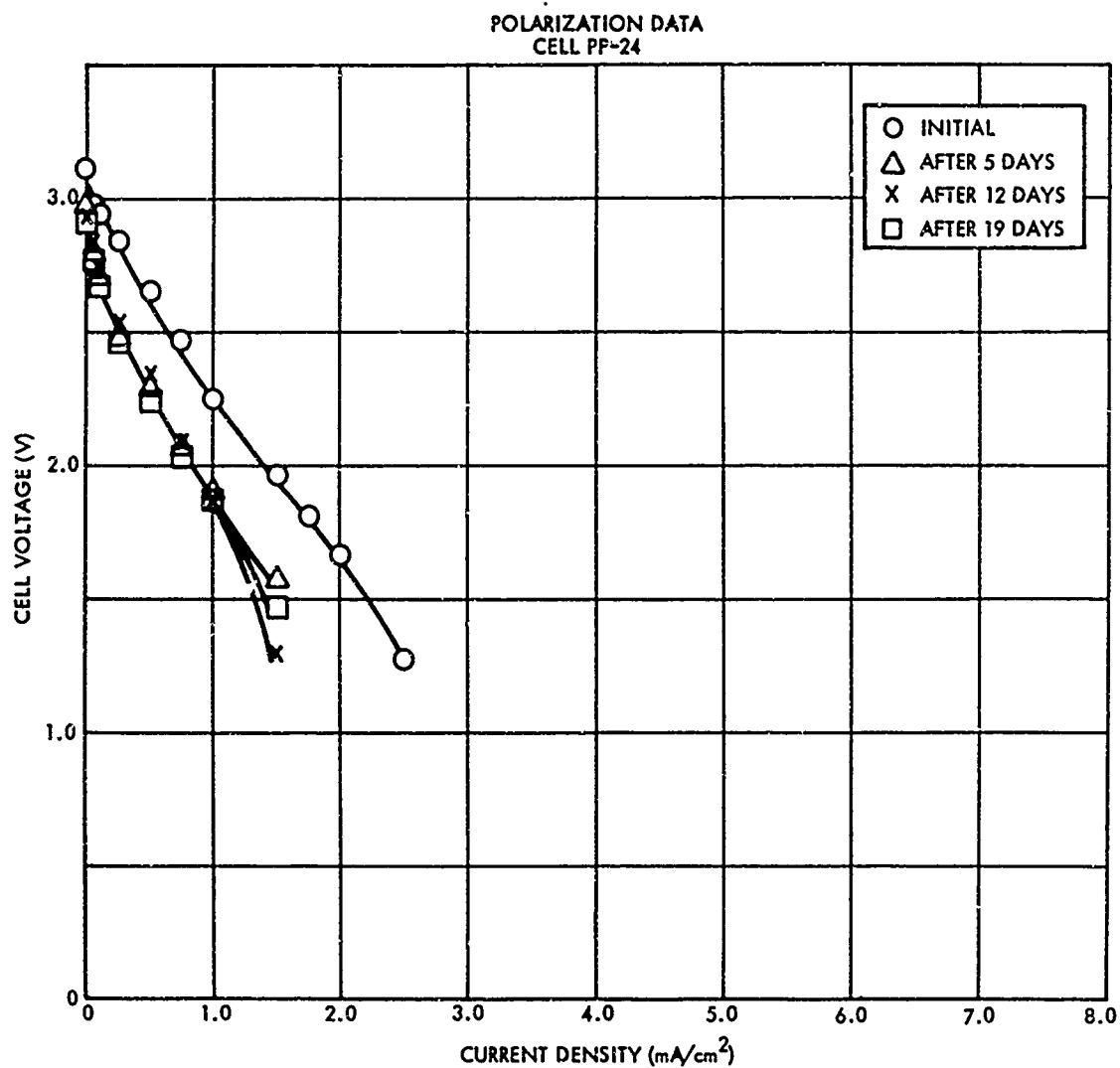


Figure 4-24. Polarization Data for Cell PP-24. Pressed cathode (10,000 psi) containing 1.5 g each m-DNB and carbon and 5% benzoin gum and tested in the wet state.

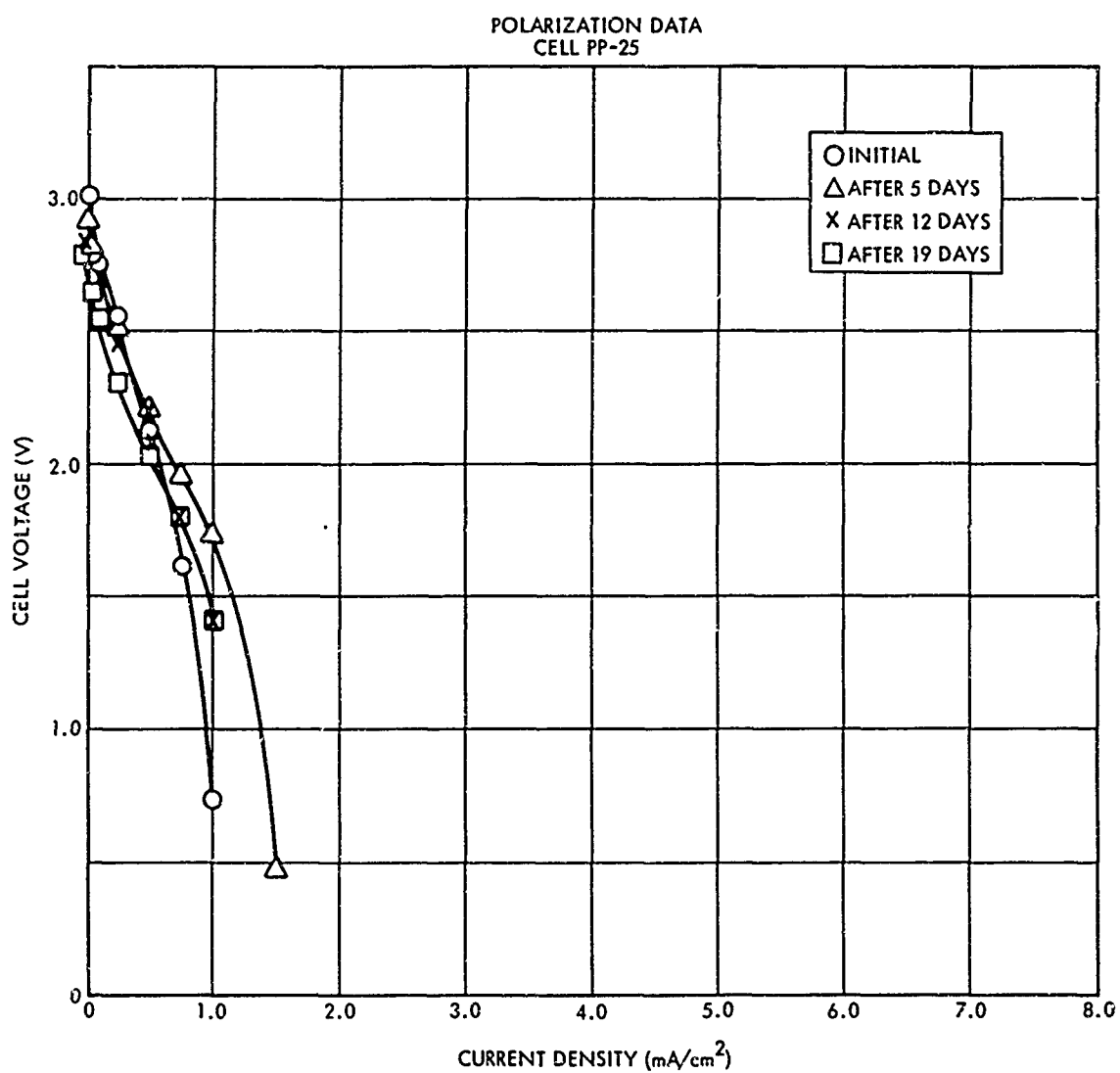


Figure 4-25. Polarization Data for Cell PP-25. Pressed cathode (10,000 psi) containing 1.5 g each m-DNB and carbon and 5% dammar gum and tested in the wet state.

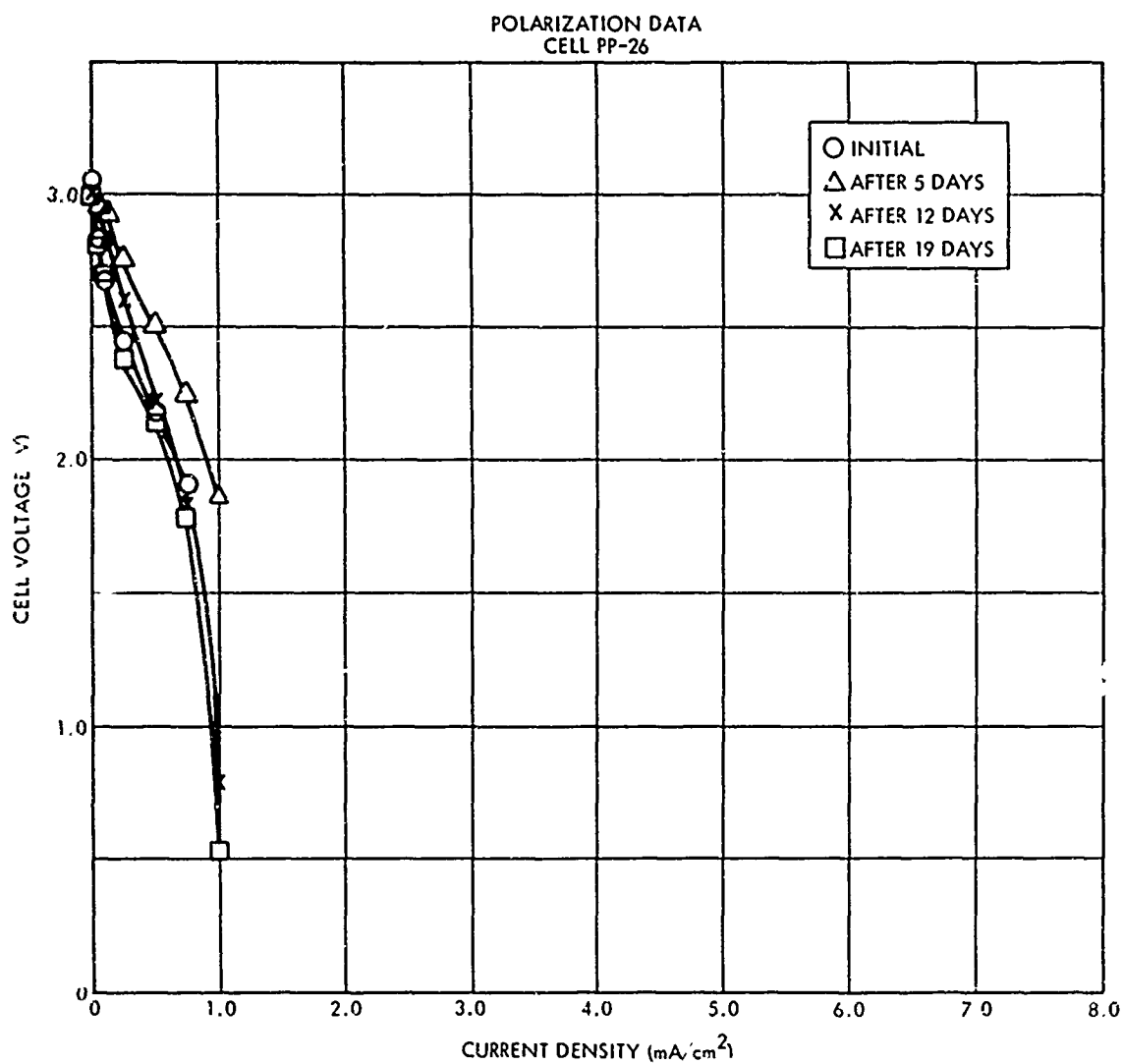


Figure 4-26. Polarization Data for Cell PP-26. Pressed cathode (10,000 psi) containing 1.5 g each m-DNB and carbon and 5% guaiac gum and tested in the wet state.

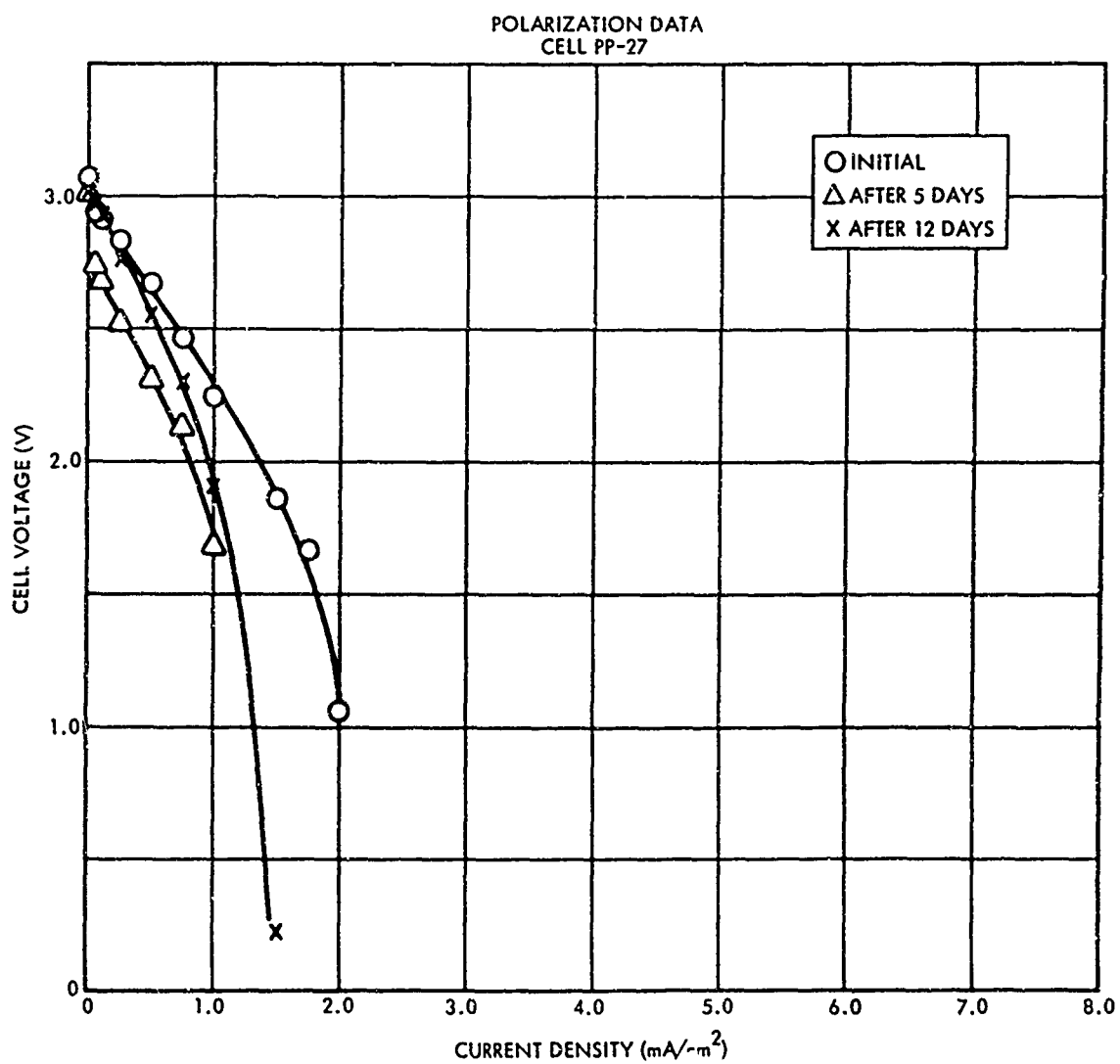


Figure 4-27. Polarization Data for Cell PP-27. Pressed cathode (10,000 psi) containing 1.5 g each m-DNB and carbon and 5% gum arabic and tested in the wet state.

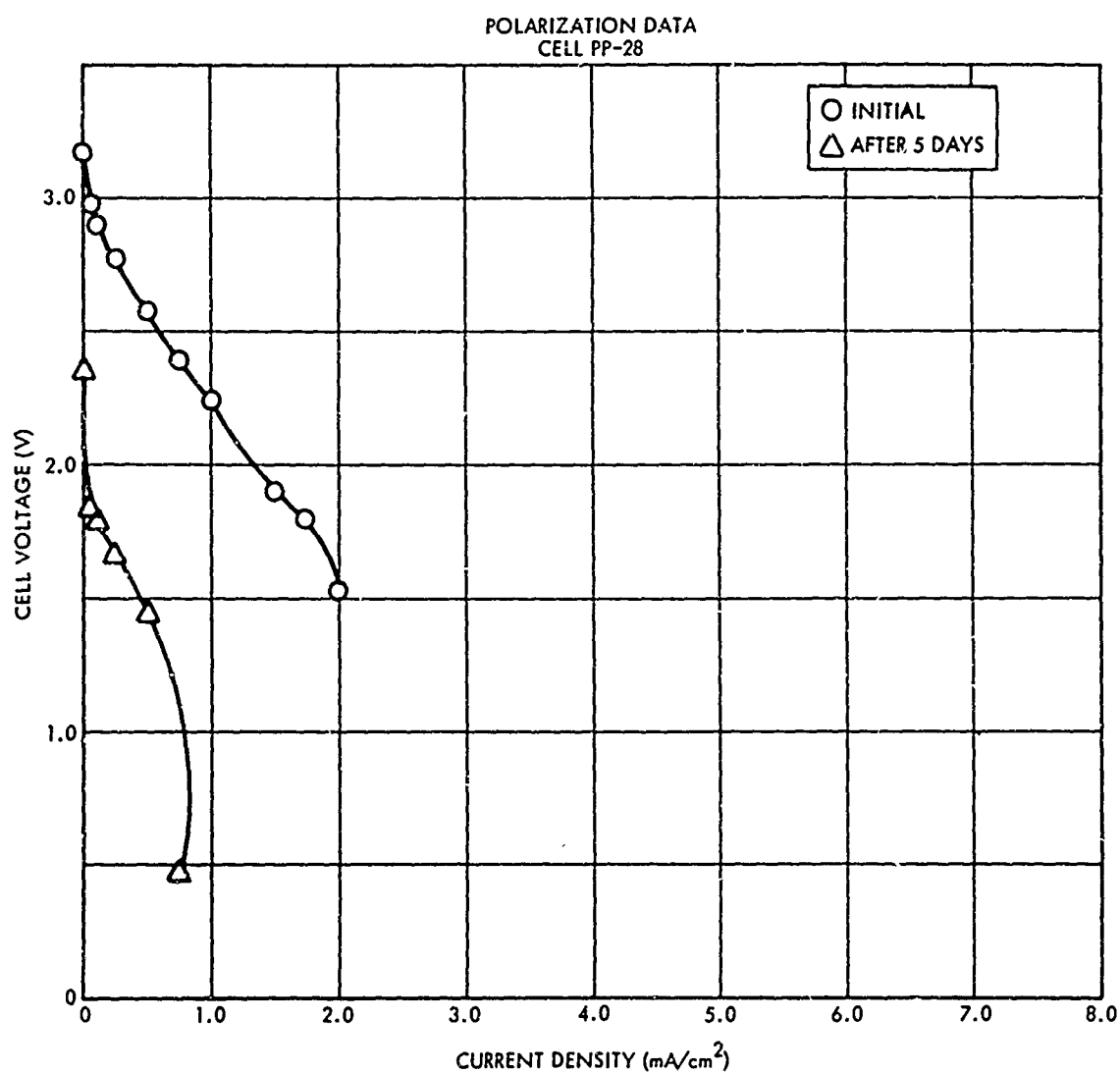


Figure 4-28. Polarization Data for Cell PP-28. Pressed cathode (10,000 psi) containing 1.5 g each m-DNB and carbon and 5% acrylic and tested in the wet state.

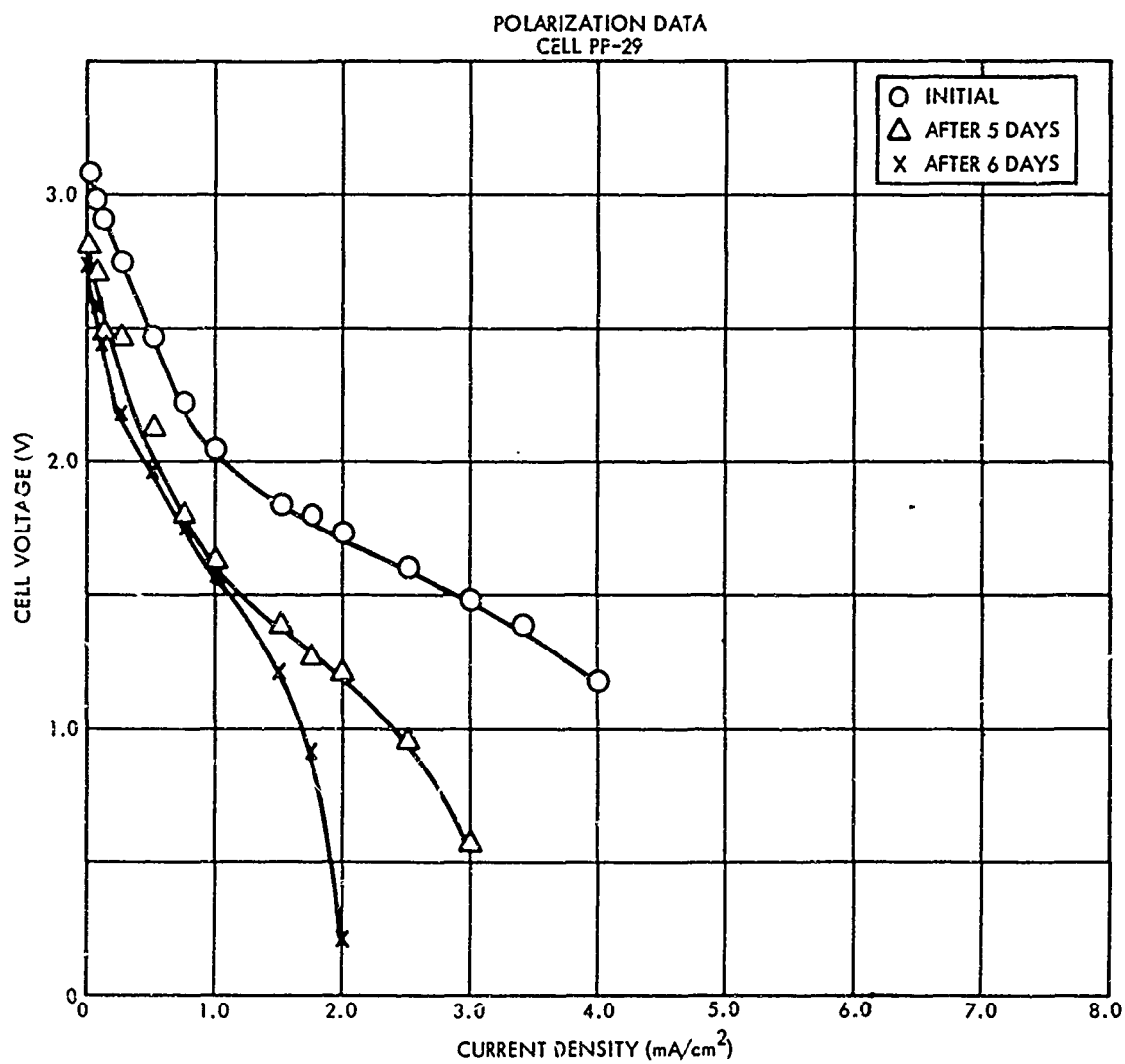


Figure 4-29. Polarization Data for Cell PF-29. Pressed cathode (10,000 psi) containing 1.5 g each m-DNE and carbon and 5% acrylic and tested in the wet state.

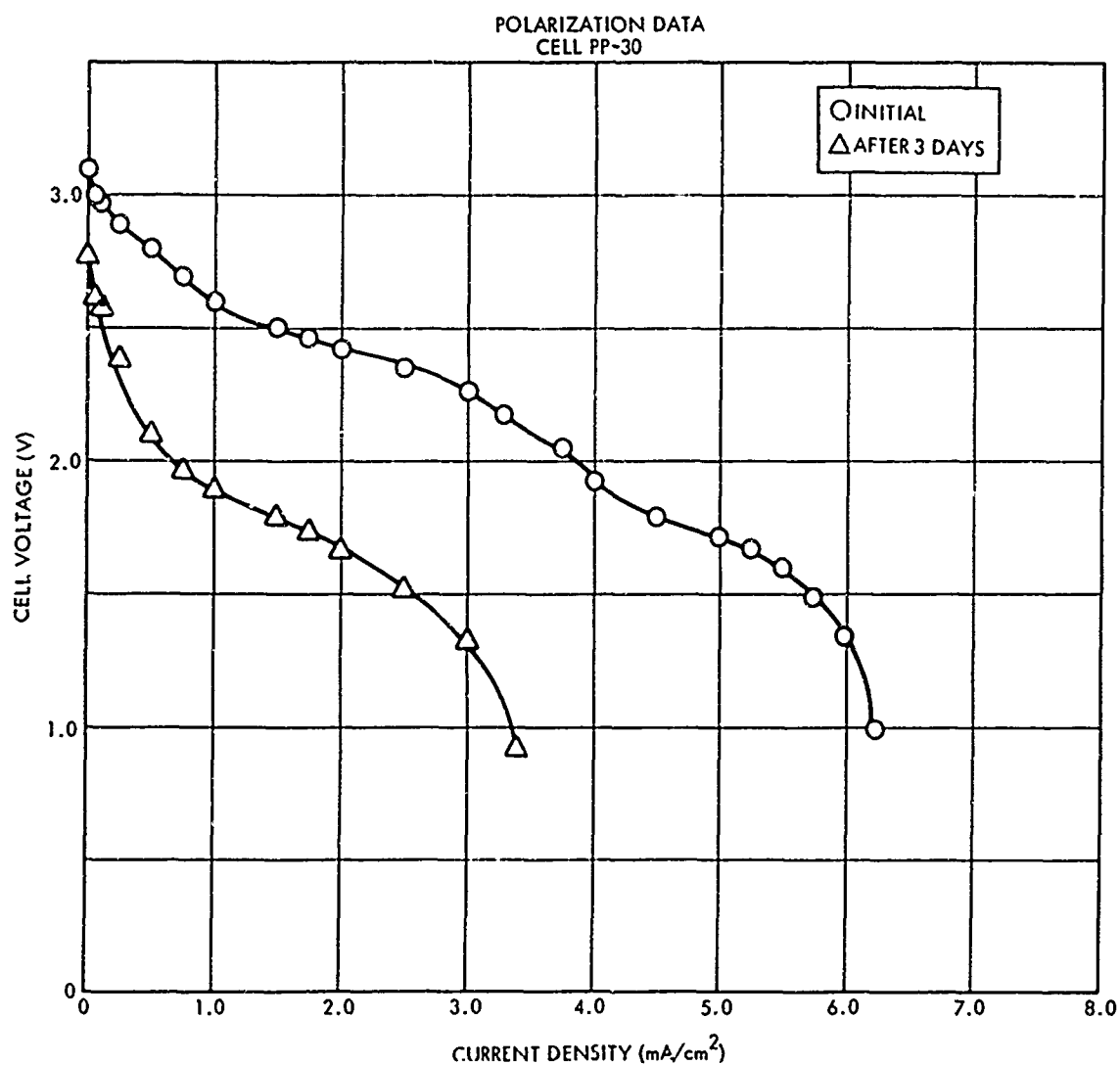


Figure 4-30. Polarization Data for Cell PP-30. Pressed cathode (10,000 psi) containing 1.5 g each m-DNB and carbon and 5% Canada balsam and tested in the wet state.

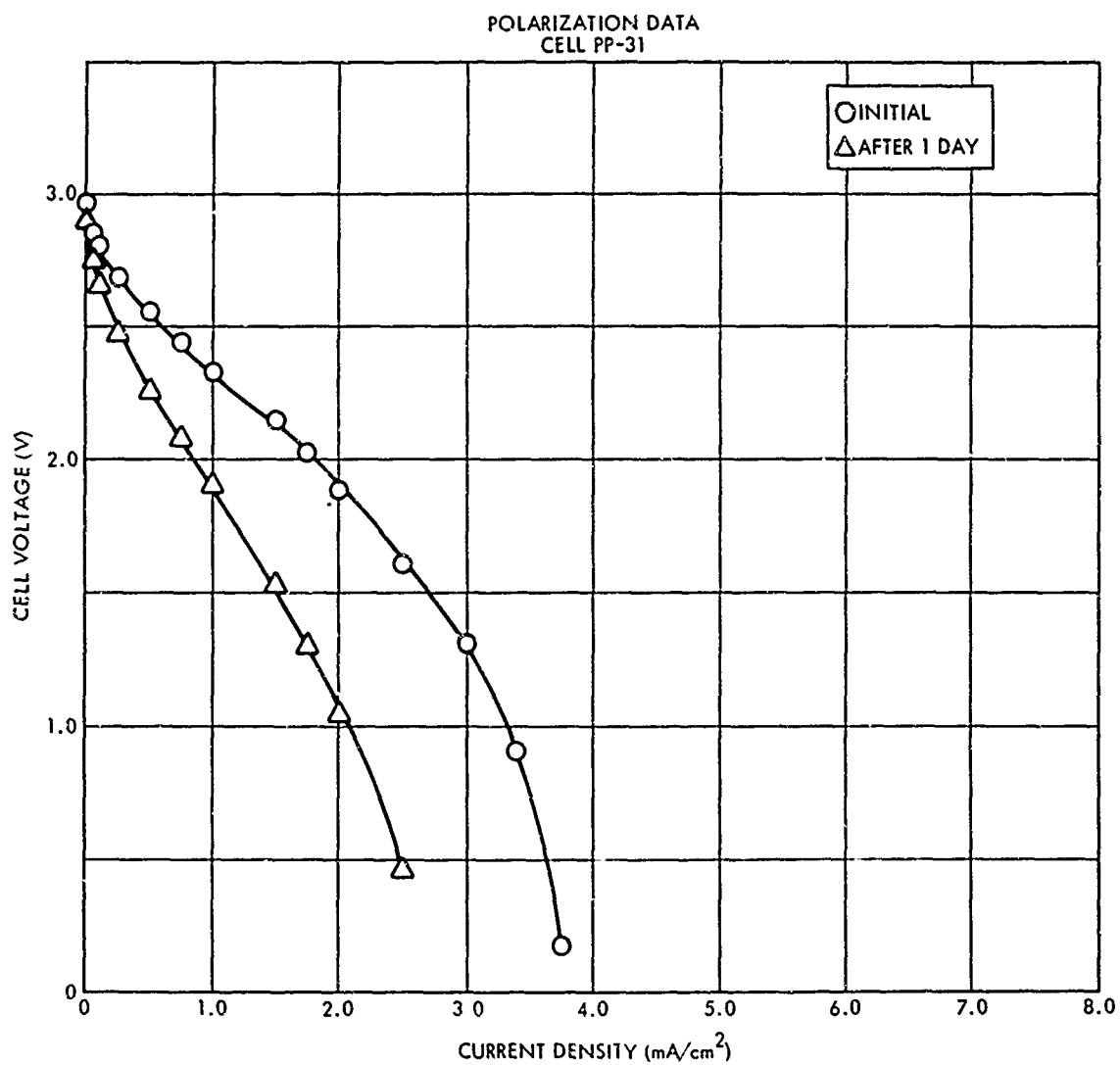


Figure 4-31. Polarization Data for Cell PP-31. Pressed cathode (10,000 psi) containing 1.5 g each hexachloromelamine and carbon and 5% acrylic and tested in the wet state.

The data of Table 4-2 show that, in general, over the range of cathode thicknesses tested, cell performance decreases with decreasing thickness. This may be in part due to a decrease in physical integrity of the cathodes as the thickness decreases.

The data also show that for pressing pressures of 5,000, 10,000, and 15,000 psi, better performance was obtained at 10,000 psi. This is probably a result of lower physical integrity of cathodes pressed at 5,000 psi, while cathodes pressed at 15,000 psi are too dense to absorb sufficient electrolyte to give good performance. In an attempt to fabricate a cathode at 20,000 psi, the die used for cathode fabrication was deformed, and a new die was made and used in fabrication of cathodes starting with cathode PP-14. To determine if the new die had any effect on performance, cell PP-14 was prepared as a duplicate of PP-6. PP-6 performed better initially, PP-14 showed better performance after five days. Cell PP-15 was fabricated at 20,000 with the new die, and comparison of the performance of the cell with PP-14 indicates that the relationship between fabrication pressure and cell performance with the new die was the same as that observed with the old die.

A number of naturally-occurring organic resins was evaluated as possible binder material for cathode fabrication. Polarization data for these cathodes are presented in Table 4-2 (PP-21 through PP-27 and PP-30) and depicted graphically in Figures 4-22 through 4-28. For comparative purposes, two paste cathodes (P-10 and P-11), two cathodes using 5% acrylic binder (PP-18 and PP-19), and two cathodes using 2.5% acrylic (PP-20) were also included in this test series. All the cathodes except the paste cathodes were pressed at 10,000 psi, and were soaked in the electrolyte prior to incorporation into the cell assembly. All the resin binders were composed of 5% by weight of binder in appropriate solvents, with the solvent being removed prior to cathode fabrication. Polarization data for all of these cells were obtained immediately after fabrication and after five days, except cell PP-30 (Canada balsam) for which data was obtained initially and after three days. In addition, polarization data was obtained at 12 and 19 days for some of these cells. The cells using paste cathodes, and the cells using cathodes with 5% and 2.5% acrylic binder all showed comparable performance initially. However, after 19 days, the paste cathodes were superior to the 2.5% acrylic binder cathodes which, in turn, were superior to the 5% acrylic binder cathodes. The cathode showing the best performance after 19 days was the first electrode fabricated with the new die and used a 5% acrylic binder. This cell showed a voltage of 1.77 V at 3 mA/cm² after 19 days. The differences were attributed to variances in absorptive properties of the cathodes. Canada balsam was the only naturally-occurring resin that gave comparable performance to the acrylic resin.

It was noted during the fabrication and cleaning process used for the lithium anode that a dull bronze-colored film was deposited on the surface. This film occurred whenever the 1,1,1-trichloroethane

came in contact with the lithium surface. In order to avoid the formation of this film, the cleaning process was altered by immersing the lithium in the electrolyte immediately after etching in methanol instead of immersing in 1, 1, 1-trichloroethane. Since the paste cathodes in cells P-10 and P-11 were fabricated identically and the pressed cathodes in cells PP-20 and PP-21 using 2.5% acrylic binder were also fabricated identically, one anode of each set (P-11 and P-21) was cleaned by the new process. The results of this experiment, shown in Table 4-2 and Figures 4-3, 4-4, 4-21, and 4-22, demonstrate that the cells which used electrolyte rather than 1, 1, 1-trichloroethane in the cleaning process gave better performance not only initially, but also after 5, 12, and 19 days.

One cathode was fabricated using hexachloromelamine as the organic active cathode material. The cathode was fabricated using 5% acrylic as the binder material, the pressing pressure was 10,000 psi, and the cathode was soaked in the electrolyte prior to incorporation into the cell. Polarization data for this cell are presented in Table 4-2 and Figure 4-31. Comparison with a similar cell using m-dinitrobenzene shows a lower output performance for the hexachloromelamine. Time did not permit a polarization measurement after five days, but a measurement made after one day shows a considerable decrease in performance. However, previous experience indicates that hexachloromelamine cells with lithium anodes in γ -butyrolactone can have open circuit voltages up to 4.1 V and cell voltages of about 2.5 V at current densities of 6 mA/cm².

The data in Table 4-2 show some rather high impedances before and after each polarization test. The high impedance is partly attributable to the increase in cell resistance from drying of the separator, but it could also be caused by the formation of a passive film on one or both electrodes. According to the data, very little current is required to break down the passive layer if indeed it is present, and there was no correlation between the measured impedances and cell performance.

Visual inspection of all the cells tested during this program revealed a yellow-brown discoloration on the surface of the anode facing the cathode, and a yellow liquid on the reverse side of the anode. All cathodes were physically intact and could easily be removed from the collector and, although their physical integrity had been somewhat reduced, the cathodes could be handled without breaking. Also, there was some discoloration, ranging from blue to grey, on the cathode side of the current collector in contact with the cathode. Table 4-3 gives a summary of the visual inspection of the cathodes.

4.3 Studies Monitoring Individual Electrode Potentials.
Electrode potential studies were made on cells PP-28 and PP-29 using the apparatus shown in Figure 2-4. The cell voltage data are

presented in Table 4-2 and Figures 4-28 and 4-29 while the potentials between anode and reference and between the cathode and reference are shown in Figures 4-32 and 4-33. Both cells were tested using the silver-silver-perchlorate reference electrode. However, even though the reference electrode was protected from light, the silver perchlorate appeared to decompose as evidenced by the formation of a grey to black deposit which appeared to be metallic silver. Because of the possible decomposition of the silver perchlorate, one polarization study was made on cell PP-29 six days after fabrication using an aqueous saturated calomel electrode as the reference. The data in Figures 4-32 and 4-33 show that the lithium anode is the limiting electrode for each cell. The cathode potential with respect to the reference electrode for each cell has a sharp drop as the current density is increased to 1 mA/cm^2 , then levels off as the current density is increased beyond 1 mA/cm^2 , and maintains a relatively constant value as the anode becomes limiting. The performance of these cells (PP-28 and PP-29) is not as good as comparable cells using 5% acrylic binder. This difference could be attributed to the fact that these cells were flooded with respect to electrolyte solution while comparable cells were in a starved state with respect to electrolyte solution.

4.4 Discharge Capacity Studies. Table 4-4 gives the capacity data for those cells discharged through fixed resistor (67 ohms), and the discharge voltage-time and current-time curves are shown in Figures 4-34 through 4-39.

Discharge capacity was determined for four cells immediately after fabrication using a fixed load of 67 ohms. Two cells (P-8 and P-9) were fabricated using paste cathodes, and two cells had 2.5% acrylic binder cathodes. Table 4-4 gives a summary of the capacity data, and Figures 4-34 through 4-37 show the current-time and voltage-time curves for the discharge. Table 4-5 shows the breakdown of the weights and percentage of the total weight for each of the cell components. The discharge capacity was calculated by integrating the area under the curve. The efficiencies and the energy density in watt-hours per pound of Table 4-4 are based on the active cathode material only. Two efficiencies are given, one efficiency is based on a two-electron reduction and the other efficiency (in parentheses) is based on a three-electron reduction. Cyclic voltammetric data indicate a two-electron reduction in the absence of lithium ions in aprotic solvents. With lithium ions, the reduction involves three, possibly four electrons. Also, two calculated capacities are given, one based on a two-electron reduction and the other (in parentheses) based on a three-electron reduction. In the following discussion concerning efficiencies, the values are for two-electron reductions, the values in parentheses are for three-electron reductions.

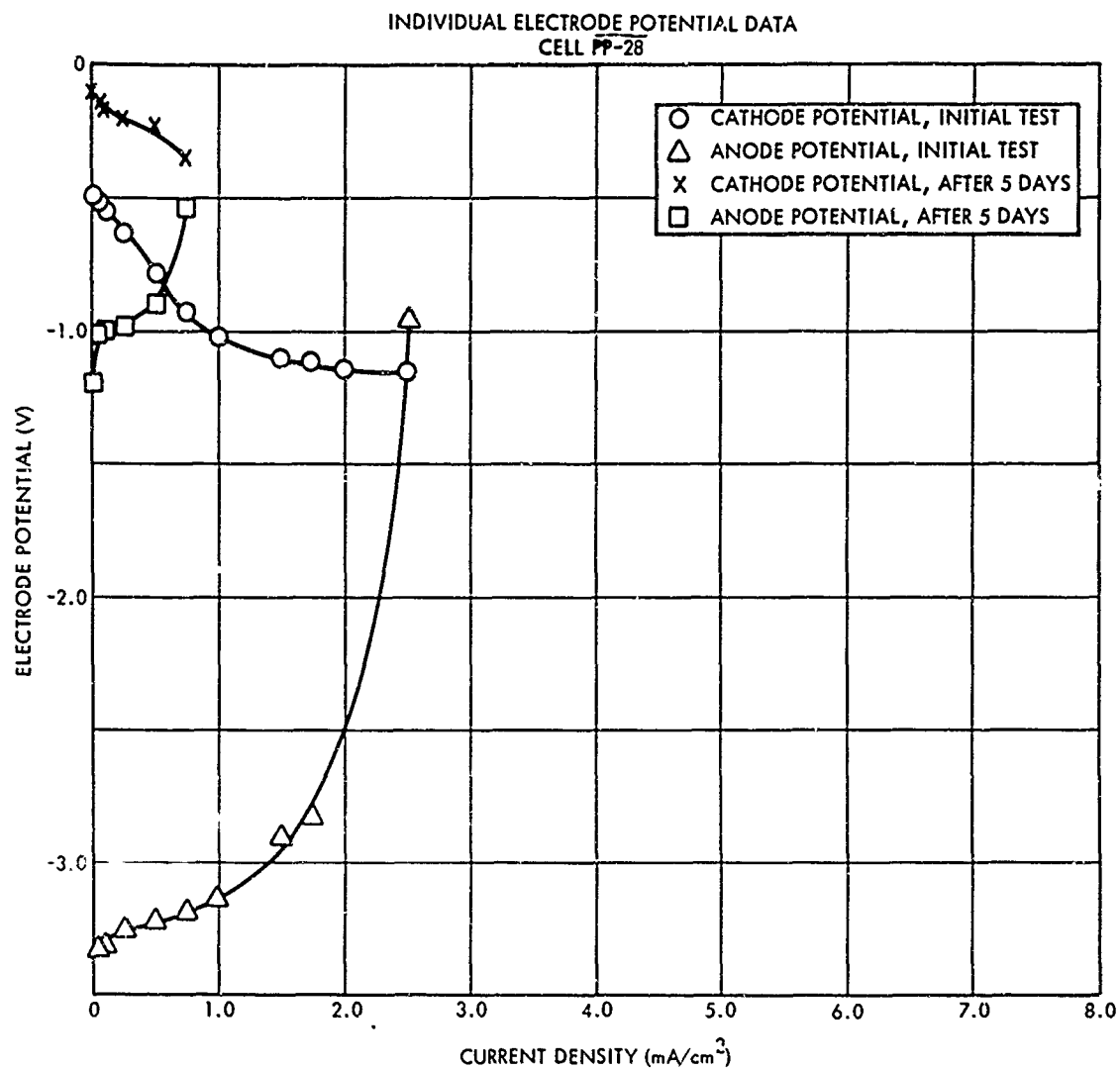


Figure 4-32. Individual Electrode Polarization Curves—Cell PP-28. Electrode potential measured against a silver/silver perchlorate electrode.

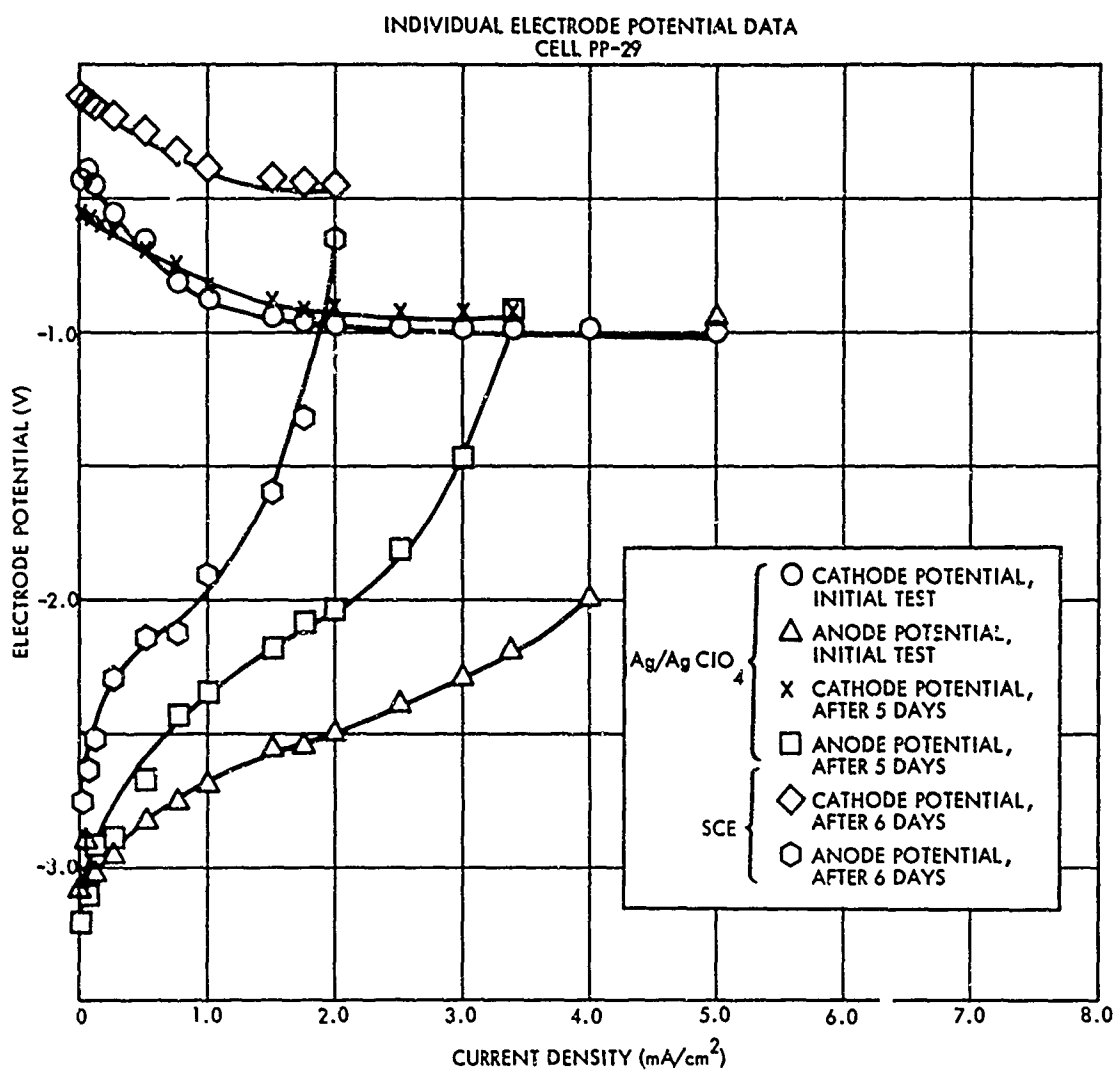


Figure 4-33. Individual Electrode Polarization Curves—Cell PP-29.

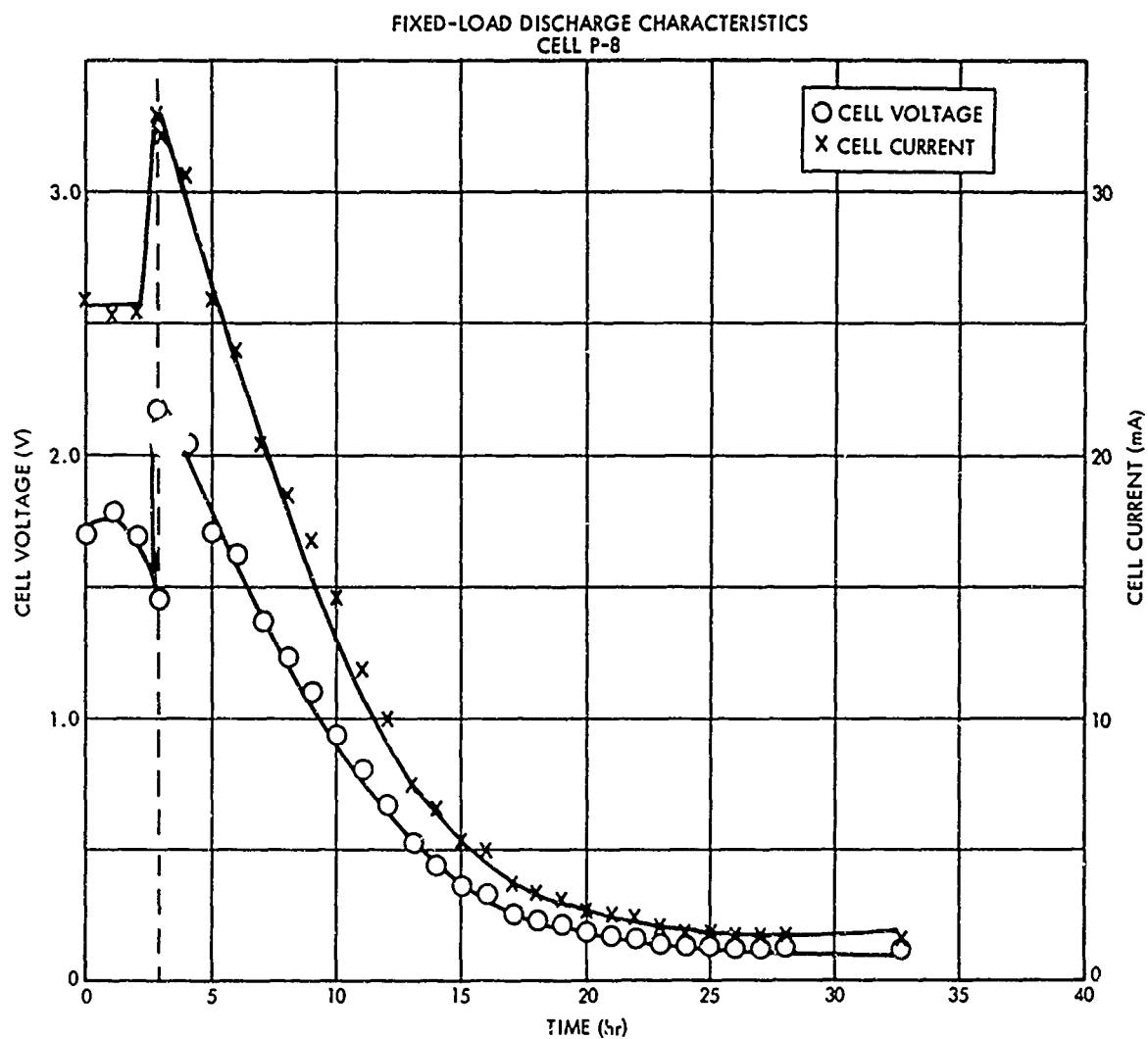


Figure 4-34. Fixed-Load Discharge Curves—Cell P-8. Discharge initiated immediately after cell assembly. Load, 67 ohms; cathode area, 15.5 cm². Dashed-line indicates 12-hour interruption.

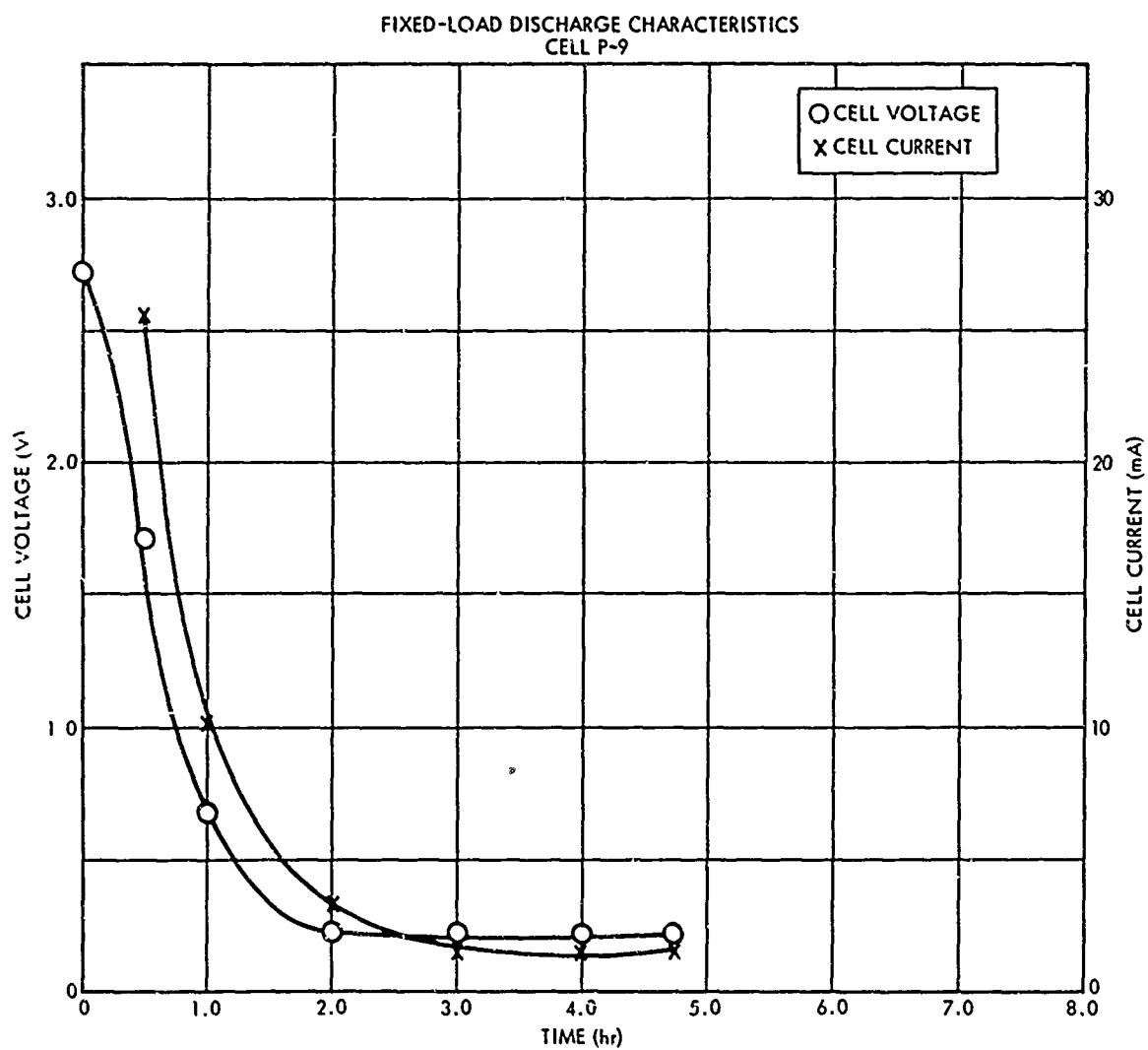


Figure 4-35. Fixed-Load Discharge Curves—Cell P-9. Discharge initiated immediately after cell assembly. Load, 67 ohms; cathode area, 15.5 cm².

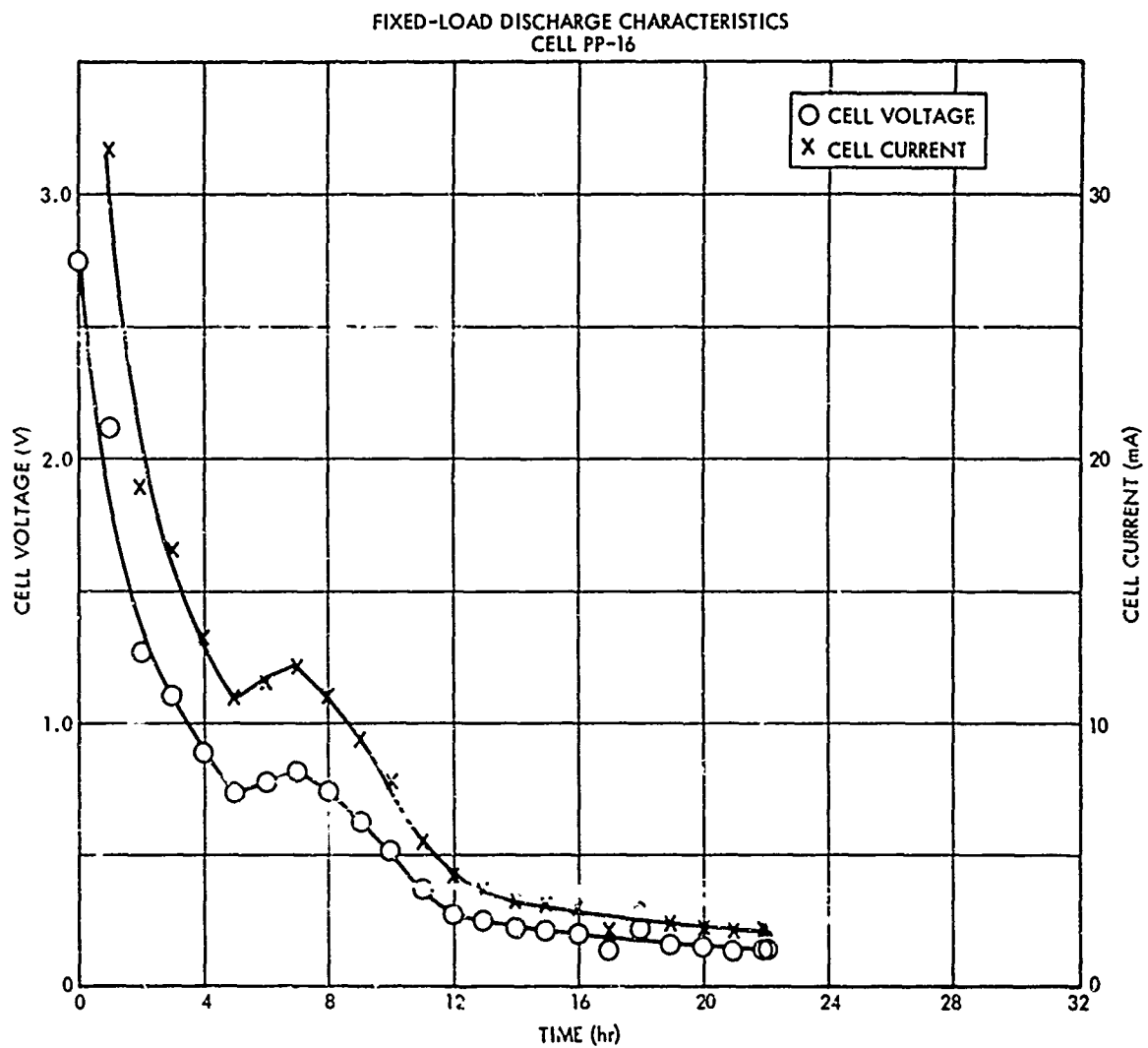


Figure 4-36. Fixed-Load Discharge Curves—Cell PP-16. Discharge initiated immediately after cell assembly. Load, 67 ohms; cathode area, 15.5 cm².

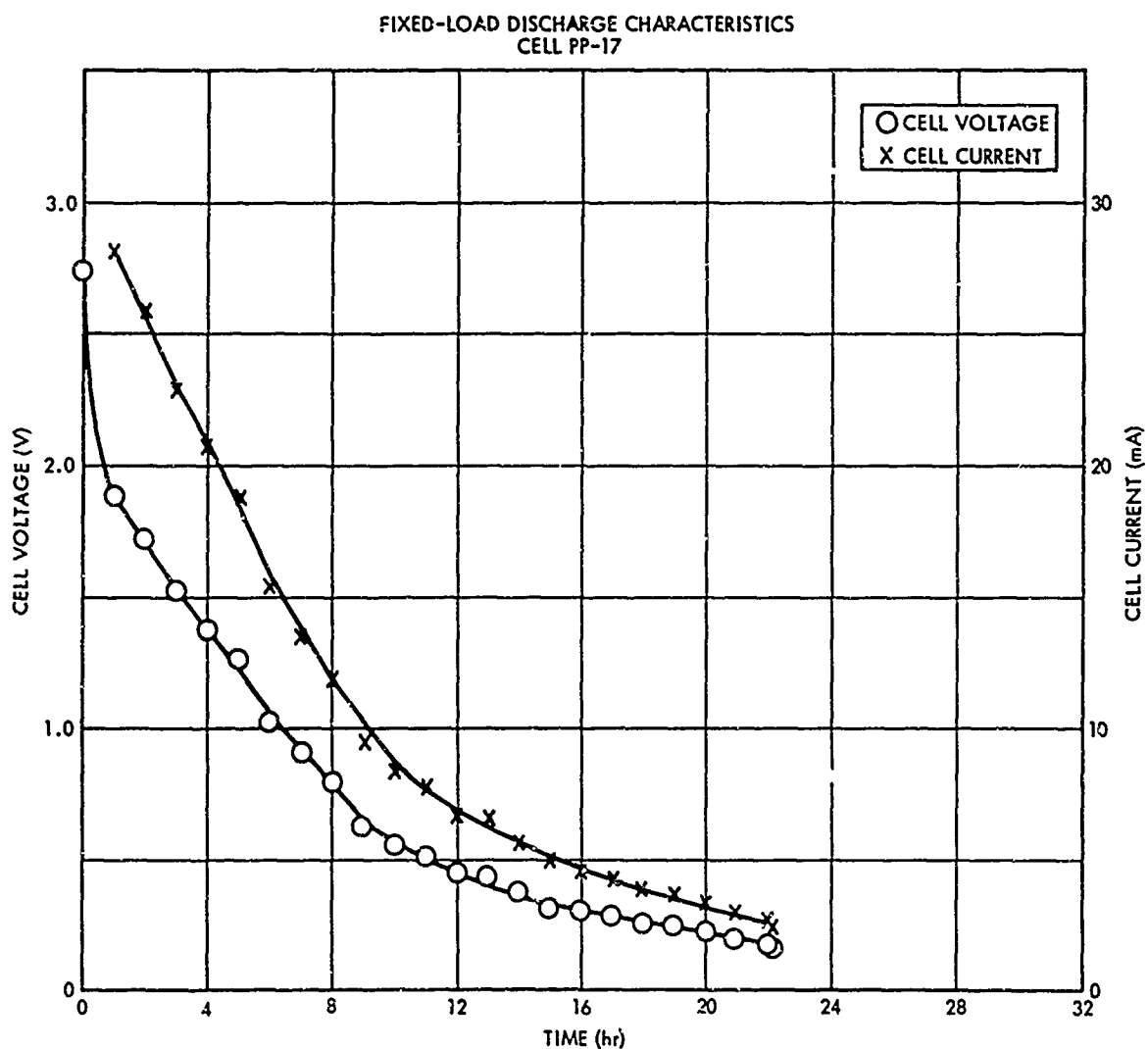


Figure 4-37. Fixed-Load Discharge Curves—Cell PP-17. Discharge initiated immediately after cell assembly. Load, 67 ohms; cathode area, 15.5 cm².

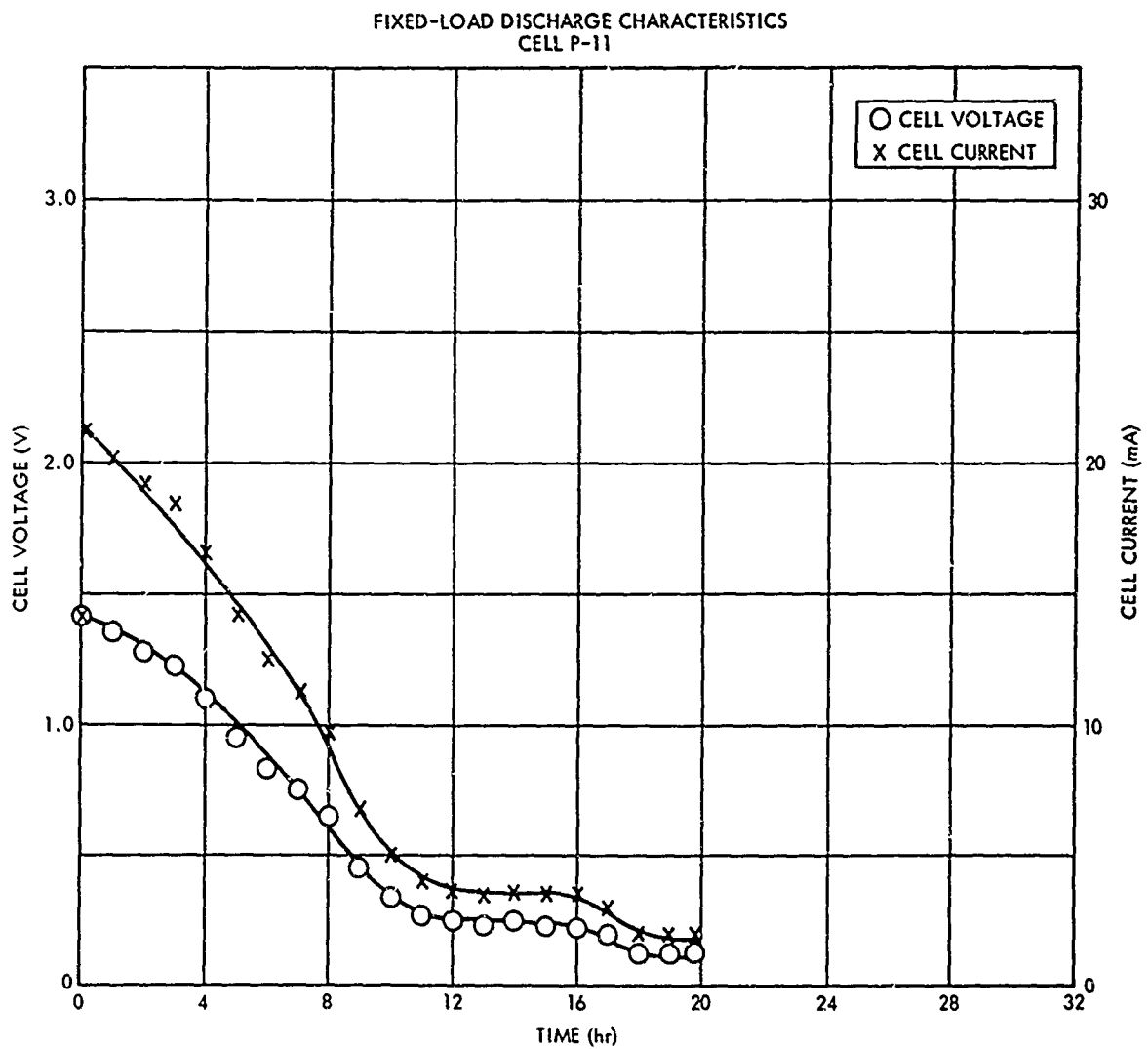


Figure 4-38. Fixed-Load Discharge Curves—Cell P-11. Discharge initiated 31 days after cell assembly. Cell subjected to polarization tests prior to fixed-load discharge. Load, 67 ohms; cathode area, 15.5 cm²

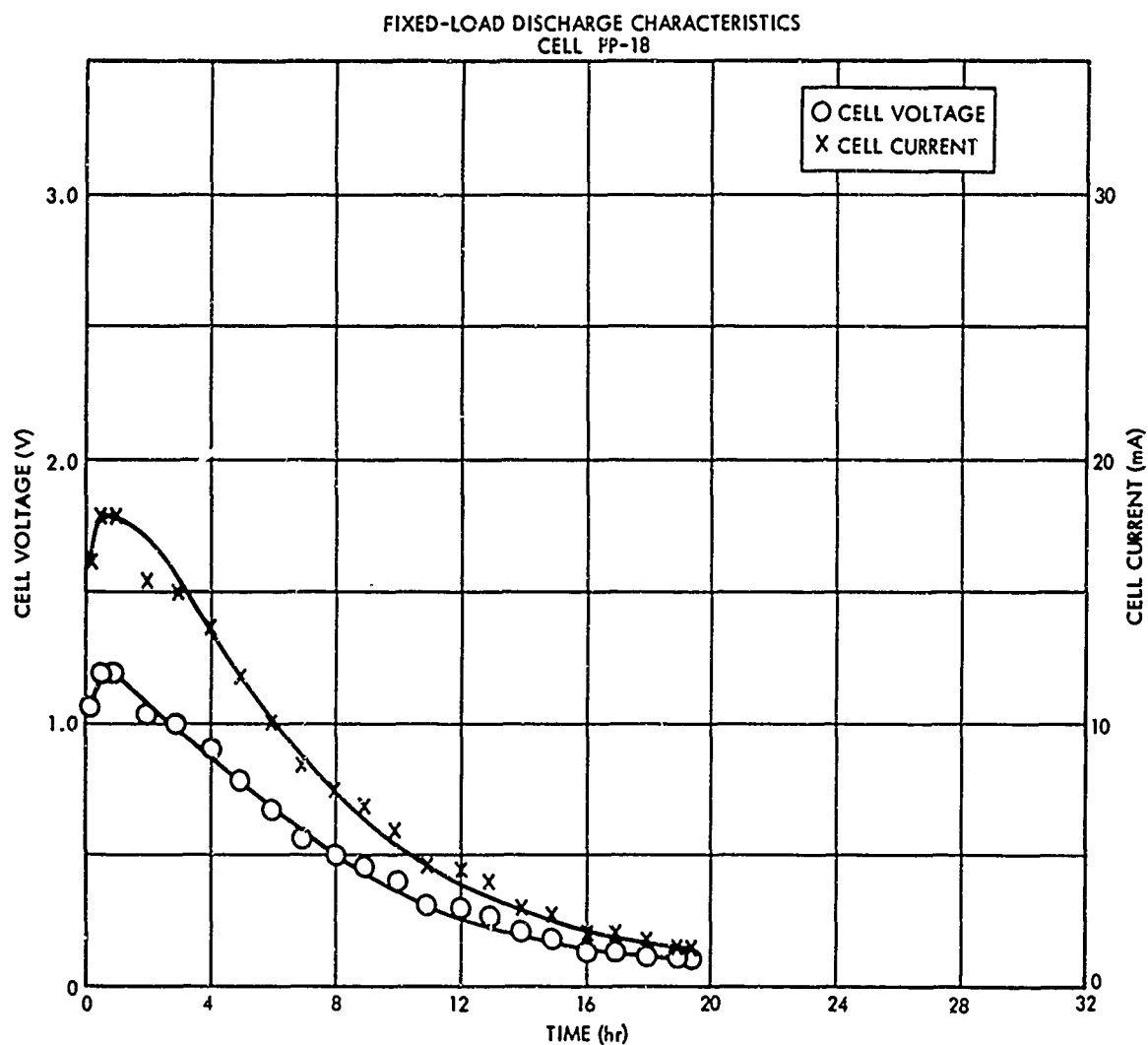


Figure 4-39. Fixed-Load Discharge Curves—Cell PP-18. Discharge initiated 19 days after cell assembly. Cell subjected to polarization tests prior to fixed-load discharge. Load, 67 ohms; cathode area, 15.5 cm²

TABLE 4-4
DISCHARGE-CAPACITY DATA^(b)

Cell No.	Measured Capacity (mA-min)	Efficiency ^(a) (%)	End of Discharge Voltage(V)	Energy Density ^(c) (W-hr/lb)	Discharge Duration (hr)	Stand Time (days)
P-8	19.6×10^3	73.0 (45.5)	0.11	133.7	32.6	0
P-9	2.0	7.6 (4.7)	0.10	16.5	4.7	0
P-11	10.3	38.6	0.13	47.1	19.7	31
PP-16	11.9	44.7 (27.8)	0.14	69.9	22.1	0
PP-17	14.9	56 (34.7)	0.17	90.4	22.2	0
PP-18	9.0	33 (20.8)	0.11	32.4	19.5	19

(a) The calculated capacity was 26.7×10^3 and 43.0×10^3 mA-min based on two- and three-electron reductions respectively. The percent efficiency values in parentheses represent three-electron reductions.

(b) Energy density based on the active cathode material.

TABLE 4-5
CELL COMPONENT WEIGHTS

<u>Pressed Cathodes</u>				<u>Paste Cathodes</u>			
Component	Weight (g)	% (a)	% (b)	Component	Weight (g)	% (a)	% (b)
Cathode				Cathode			
Silver Foil	2.3	14.4	2.0	Silver Foil	2.3	8.3	1.8
<u>m</u> -DNB	1.5	9.4	1.3	<u>m</u> -DNB	1.5	5.4	1.2
Carbon	1.5	9.4	1.3	Carbon	1.5	5.4	1.2
Acrylic Binder	0.7	4.3	0.6	Electrolyte Solution	12.5	44.9	10.0
Anode				Anode			
Silver Mesh	0.5	4.4	0.1	Silver Mesh	0.5	1.8	0.4
Lithium	1.5	3.1	1.5	Lithium	1.5	5.4	1.2

TABLE 4-5
CELL COMPONENT WEIGHTS (Continued)

<u>Pressed Cathodes</u>				<u>Paste Cathodes</u>			
Component	Weight (g)	% ^(a)	% ^(b)	Component	Weight (g)	% ^(a)	% ^(b)
Electrolyte Solution	7.5	46.8	6.6	Electrolyte Solution	7.5	27.0	6.0
Separators	0.5	3.1	0.4	Separators	0.5	1.8	0.4
Sub Total	16.0	100		Sub Total	27.8	100	
Case	97.4		85.9	Case	97.9		77.8
Total	113.4		100	Total	125.2		100

(a) Percentage calculated on all components excluding the polypropylene case.

(b) Percentage calculated on the total weight including the polypropylene case.

The discharge data for the paste cathode cells show a wide variation in capacity. Cell P-8 showed a capacity of 19,600 mA-min which was 73% (45.5) of the calculated value. Cell P-9 had a capacity of 2,000 mA-min which was only 7.6% (4.7) of the calculated value. The wide variation in data for this cell could have resulted from uneven distribution of the electrolyte in the separator or passivating film formation on one or both of the electrodes. Both electrodes showed a discoloration indicating the occurrence of some surface phenomenon and that the center separator was partially dry. Also, the discharge of cell P-8 was interrupted after approximately 3 hr of discharge for 12 hr; then the discharge was resumed. The discharge of cell P-9 was not interrupted. Cells PP-16 and PP-17 which had 2.5% acrylic cathodes showed comparable discharge data. Cell PP-16 had a capacity of 11,900 mA-min which was 45% (27.8) of the calculated value. Cell PP-17 had a 14,900 mA-min capacity which was 56% (34.7) of the calculated value. All discharge capacities were calculated on the basis of the cut-off (end-of-discharge) voltage indicated in Table 4-4. Neglecting the low capacity of Cell P-9, the data show that the paste cathode cells to be more efficient. Two cells, one with a paste cathode and one with a 5% acrylic were discharged through a fix load (67 ohms) after standing varying lengths of time. The paste cathode (P-11) cell was discharged 31 days after

fabrication and the 5% acrylic cathode (PP-18) was discharged 19 days after fabrication. Both cells had been subjected to polarization test at 5, 12, and 19 days, but the capacity withdrawn from the cell during the polarization testing was not considered in the calculation of the discharge capacity. Discharge data for these cells is presented in Table 4-4 and the current-voltage curves are shown in Figures 4-38 and 4-39. The paste cathode cell showed a capacity of 10,300 mA-min which was 38.6% (24.0) of the calculated value, while the 2.5% acrylic cathode showed a 9,000 mA-min capacity which was 33% (20.8) of the calculated value. Again the paste cathode showed better performance than the 2.5% acrylic cathode. Comparison of the discharge capacities of these two cells with those discharges immediately after fabrication shows an approximate 50% loss of capacity on standing for one month.

4.5 Conclusions. Several materials were evaluated as binders for cathode fabrication. Of the binder materials evaluated, an acrylic molding compound and Canada balsam were found to impart the desired structural stability to the cathode and also demonstrated a reasonable shelf life. The fabrication parameters of the amount of binder, pressure applied to fabricate the cathode, and thickness of cathode were evaluated. The results of this evaluation established 10,000 psi as the fabrication pressure, 0.080 in. cathode thickness, and 10 ml. of a 2.5% to 5% by weight of binder solution as the most desirable for good cell performance. Cathodes formulated and fabricated according to the established parameters demonstrated good physical integrity and shelf life and were comparable in performance to paste cathodes.

The polarization studies using the reference electrode to evaluate the performance of the individual electrodes showed that the anode (lithium) was the limiting electrode.

Discharge capacity data showed that the paste cathodes were more efficient than the cathodes fabricated with 2.5% acrylic binder. This held true whether the cells were discharged immediately after fabrication or at varying lengths of time after discharge. A stand time of 31 days reduced the capacity of the paste cathode cells from approximately 70% to 20% of the calculated capacity. A stand time of 19 days reduced the capacity of the acrylic binder cathodes from approximately 50% to 25% of the calculated value.

The data showed some rather high impedance values, both before and after polarization testing. These high values could be attributed to drying of the separator or to formation of passivating films on one or both of the electrodes.

The physical integrity of the fabricated cathodes was degraded during testing, but the cathodes remained intact.

All the data collected and the visual observations made during the test program seem to indicate that the lithium anode contributed heavily to the operating performance of the cells. The individual electrode study showed that the lithium anode was limiting. Also, the surfaces of the lithium anodes removed from the cells were discolored, indicating a possible surface passivation. The cleaning process used in the latter portion of this study tended to reduce the discoloration of the lithium surface. A study pertaining to the cleaning and protection of lithium anode surfaces prior to incorporation of an anode in a cell seems to be warranted. The results also indicate that drying out of the separators was a factor contributing to cell performance.

5. REFERENCES

1. K.H.M. Braeuer and J. A. Harvey, "Status Report on Organic Electrolyte High Energy Density Batteries," Technical Report ECOM-2844, U.S. Army Electronics Command, Fort Monmouth, New Jersey, May 1967.
2. G. Lauer, Ph.D. Dissertation, California Institute of Technology, 1966.
3. A.H. Maki and D.H. Geske, J. Chem. Phys. 33, 825 (1960).
4. R.D. Allendoerfer and P.H. Rieger, J. Am. Chem. Soc. 88, 3711 (1966).
5. L. Holleck and M. Schmidt, Z. Elektrochem. 54, 1039 (1956).
6. J.Q. Chambers, III, and R.N. Adams, J. Electroanal. Chem. 9, 400 (1956).
7. P.H. Rieger, I. Bernal, W. H. Reinmuth and G.K. Fraenkel, J. Am. Chem. Soc. 85, 683 (1963).
8. T. Kitagawa, T.P. Layloff and R.N. Adams, Anal. Chem. 35, 1086 (1963).
9. T. Fujinaga, T. Arai and C. Kitazawa, Nippon Kagaku Zasshi 85, 811 (1964).
10. T. Fujinaga, Y. Deguchi and K. Umemoto, Bull. Chem. Soc. (Japan) 37, 822 (1964).
11. W. Kemula and R. Sioda, Bull. Acad. Polon. Sci., Ser. Sci., Chim. 10, 107 (1962).
12. D.H. Geske and A.H. Maki, J. Am. Chem. Soc. 82, 2671 (1960).
13. G.W.C. Milner, "Principles and Applications of Polarography," Longsman Green and Co., New York, 1957, p. 44.
14. R.S. Nicholson and I. Shain, Anal. Chem. 37, 190 (1965).
15. D.S. Polcyn and I. Shain, Anal. Chem. 38, 376 (1966).
16. G.W. Jackson and J.S. Dereska, J. Electrochem. Soc. 112, 1218 (1965).
17. W. Kemula and R. Sioda, J. Electroanal. Chem. 6, 183 (1963).
18. G.A. Russell and E.J. Geels, J. Am. Chem. Soc. 87, 122 (1965).
19. D.H. Geske, J.L. Ragle, M.A. Bambenek and A.L. Balch, J. Am. Chem. Soc. 86, 987 (1964).
20. I. Bernal and G.K. Fraenkel, J. Am. Chem. Soc. 86, 1671 (1964).
21. G.S. Alberts and I. Shain, Anal. Chem. 35, 1859 (1963).

Unclassified
Security Classification

DOCUMENT CONTROL DATA - R&D		
(Security classification of title, body of abstract and indexing annotation must be entered when the overall report is classified)		
1 ORIGINATING ACTIVITY (Corporate author) TRW Systems Group One Space Park Redondo Beach, California 90278		2a REPORT SECURITY CLASSIFICATION Unclassified
		2b GROUP
3 REPORT TITLE VOLTAMMETRIC STUDIES OF NON-AQUEOUS SYSTEMS		
4 DESCRIPTIVE NOTES (Type of report and inclusive dates) Final		
5 AUTHOR(S) (Last name, first name, initial) Fogle, R. F., Seo, E. T., Silverman, H. P.		
6 REPORT DATE December 1967	7a. TOTAL NO. OF PAGES 124	7b NO OF REFS 21
8a CONTRACT OR GRANT NO DA-28-043-AMC-02464(E)	9a ORIGINATOR'S REPORT NUMBER(S) Report No. 2	
b PROJECT NO. 1C014501A34A-00-09		
c	9b OTHER REPORT NO(S) (Any other numbers that may be assigned this report)	
d	ECOM-02464-F	
10 AVAILABILITY/LIMITATION NOTICES Distribution of this document is unlimited		
11 SUPPLEMENTARY NOTES	12. SPONSORING MILITARY ACTIVITY U.S. Army Electronics Command Fort Monmouth, N. J. 07703 ATTN: AMSEL-KL-PB	
13 ABSTRACT Voltammetric studies of the reduction of organic compounds in organic solvents were undertaken as part of a program to develop high-energy density organic electrolyte batteries. Cyclic voltammetry has been used as a major diagnostic tool for evaluating organic oxidizing agents as possible high-energy density cathode materials, and to elucidate the mechanisms of a heterogeneous electron transfer and any homogeneous follow-up chemical reactions. This report covers the study of various nitroaromatic compounds; cyclic voltammetric current-potential curves and their interpretation have been presented for a number of selected nitroaromatic compounds. The effects of methyl-, halo-, and hydroxy-groups on the electroreduction process have been demonstrated. Compounds studied included m- and p-dinitrobenzene, 2,5-dinitrophenol, m-dinitrotoluene, 1-chloro-2,6-dinitrobenzene and nitroalkanes. The addition of lithium ions has been shown to have a beneficial effect on organic reductions under selected conditions. Polarization and capacity data were obtained at the plate level through constant-current and fixed-load discharge of cells comprising m-dinitrobenzene as the electroactive cathode material, a lithium anode, and a lithium perchlorate-propylene carbonate electrolyte solution. Cathodes were prepared in both pressed and paste forms. Various cathode compositions and fabrication procedures were evaluated. (continued)		

DD FORM 1473 0101-807-6800
1 JAN 64

Unclassified
Security Classification

13. Abstract (Continued)

Polarization studies showed that among the several binder materials tested, Canada balsam and an acrylic molding compound imparted the desired structural integrity to the cathode and provided a reasonable shelf life for the cell. Capacity data indicated that paste cathodes were superior to pressed cathodes. Energy densities ranged from 16 to 133 W-hr/lb. Results showed that the lithium anode limited cell performance.

Unclassified
Security Classification

14 KEY WORDS	LINK A		LINK B		LINK C	
	ROLE	WT	ROLE	WT	ROLE	WT
High-Energy Battery Systems Non-Aqueous Solvent Systems Organic Cathode Materials Dinitrobenzenes Electroreduction Lithium Ion Complexes Non-Aqueous Organic Batteries Cyclic Voltammetry Lithium Anodes						

INSTRUCTIONS

1. **ORIGINATING ACTIVITY.** Enter the name and address of the contractor, subcontractor, grantee, Department of Defense activity or other organization (*corporate author*) issuing the report.

2a. **REPORT SECURITY CLASSIFICATION:** Enter the overall security classification of the report. Indicate whether "Restricted Data" is included. Marking is to be in accordance with appropriate security regulations.

2b. **GROUP:** Automatic downgrading is specified in DoD Directive 5200.10 and Armed Forces Industrial Manual. Enter the group number. Also, when applicable, show that optional markings have been used for Group 3 and Group 4 as authorized.

3. **REPORT TITLE:** Enter the complete report title in all capital letters. Titles in all cases should be unclassified. If a meaningful title cannot be selected without classification, show title classification in all capitals in parenthesis immediately following the title.

4. **DESCRIPTIVE NOTES:** If appropriate, enter the type of report, e.g., interim, progress, summary, annual, or final. Give the inclusive dates when a specific reporting period is covered.

5. **AUTHOR(S):** Enter the name(s) of author(s) as shown on or in the report. Enter last name, first name, middle initial. If military, show rank and branch of service. The name of the principal author is an absolute minimum requirement.

6. **REPORT DATE:** Enter the date of the report as day, month, year, or month, year. If more than one date appears on the report, use date of publication.

7a. **TOTAL NUMBER OF PAGES:** The total page count should follow normal pagination procedures, i.e., enter the number of pages containing information.

7b. **NUMBER OF REFERENCES:** Enter the total number of references cited in the report.

8a. **CONTRACT OR GRANT NUMBER.** If appropriate, enter the applicable number of the contract or grant under which the report was written.

8b, 8c, & 8d. **PROJECT NUMBER:** Enter the appropriate military department identification, such as project number, subproject number, system numbers, task number, etc.

9a. **ORIGINATOR'S REPORT NUMBER(S):** Enter the official report number by which the document will be identified and controlled by the originating activity. This number must be unique to this report.

9b. **OTHER REPORT NUMBER(S):** If the report has been assigned any other report numbers (*either by the originator or by the sponsor*), also enter this number(s).

10. **AVAILABILITY/LIMITATION NOTICES:** Enter any limitations on further dissemination of the report, other than those imposed by security classification, using standard statements such as:

(1) "Qualified requesters may obtain copies of this report from DDC."

(2) "Foreign announcement and dissemination of this report by DDC is not authorized."

(3) "U. S. Government agencies may obtain copies of this report directly from DDC. Other qualified DDC users shall request through _____."

(4) "U. S. military agencies may obtain copies of this report directly from DDC. Other qualified users shall request through _____."

(5) "All distribution of this report is controlled. Qualified DDC users shall request through _____."

If the report has been furnished to the Office of Technical Services, Department of Commerce, for sale to the public, indicate this fact and enter the price, if known.

11. **SUPPLEMENTARY NOTES:** Use for additional explanatory notes.

12. **SPONSORING MILITARY ACTIVITY.** Enter the name of the departmental project office or laboratory sponsoring (*paying for*) the research and development. Include address.

13. **ABSTRACT:** Enter an abstract giving a brief and factual summary of the document indicative of the report, even though it may also appear elsewhere in the body of the technical report. If additional space is required, a continuation sheet shall be attached.

It is highly desirable that the abstract of classified reports be unclassified. Each paragraph of the abstract shall end with an indication of the military security classification of the information in the paragraph, represented as (TS) (S) (C) or (U).

There is no limitation on the length of the abstract. However, the suggested length is from 150 to 225 words.

14. **KEY WORDS:** Key words are technically meaningful terms or short phrases that characterize a report and may be used as index entries for cataloging the report. Key words must be selected so that no security classification is required. Identifiers, such as equipment model designation, trade name, military project code name, geographic location, may be used as key words but will be followed by an indication of technical context. The assignment of links, roles, and weights is optional.

Unclassified
Security Classification